



EDITORIAL BOARD

Editor-in-Chief

B.E. Paton

Scientists of PWI, Kyiv

S.I. Kuchuk-Yatsenko (*vice-chief ed.*),

V.N. Lipodaev (*vice-chief ed.*),

Yu.S. Borisov, G.M. Grigorenko,

A.T. Zelnichenko, V.V. Knysh,

I.V. Krivtsun, Yu.N. Lankin,

L.M. Lobanov, V.D. Poznyakov,

I.A. Ryabtsev, K.A. Yushchenko

Scientists of Ukrainian Universities

V.V. Dmitrik, NTU «KPI», Kharkov

V.V. Kvasnitsky, NTUU «KPI», Kyiv

E.P. Chvertko, NTUU «KPI», Kyiv

Foreign Scientists

N.P. Alyoshin

N.E. Bauman MSTU, Moscow, Russia

Guan Qiao

Beijing Aeronautical Institute, China

M. Zinigrad

Ariel University, Israel

V.I. Lysak

Volgograd STU, Russia

Ya. Pilarczyk

Welding Institute, Gliwice, Poland

U. Reisgen

Welding and Joining Institute, Aachen, Germany

G.A. Turichin

St. Petersburg SPU, Russia

Founders

E.O. Paton Electric Welding Institute, NASU

International Association «Welding»

Publisher

International Association «Welding»

Translators

A.A. Fomin, O.S. Kurochko, I.N. Kutianova

Editor

N.G. Khomenko

Electron galley

D.I. Sereda, T.Yu. Snegiryova

Address

E.O. Paton Electric Welding Institute,

International Association «Welding»

11 Kazimir Malevich Str. (former Bozhenko Str.),

03150, Kyiv, Ukraine

Tel.: (38044) 200 60 16, 200 82 77

Fax: (38044) 200 82 77, 200 81 45

E-mail: journal@paton.kiev.ua

www.patonpublishinghouse.com

State Registration Certificate

KV 4790 of 09.01.2001

ISSN 0957-798X

DOI: <http://dx.doi.org/10.15407/tpwj>

Subscriptions

\$384, 12 issues per year,

air postage and packaging included.

Back issues available.

All rights reserved.

This publication and each of the articles contained

herein are protected by copyright.

Permission to reproduce material contained in this
journal must be obtained in writing from the Publisher.

CONTENTS

60 Years of the First in the World Mobile Machine for Flash-Butt Welding
of Rails in the Field Conditions 2

SCIENTIFIC AND TECHNICAL

Lychko I.I., Yushchenko K.A., Suprun S.A. and Kozulin S.M. Peculiarities
of electrode and base metal melting in electroslog welding 6

*Skulsky V.Yu., Moravetsky S.I., Nimko M.A., Pashchenko Yu.G.,
Kantor A.G. and Dmytryk V.V.* Effect of reheating in multipass
submerged-arc welding on delayed fracture resistance of rotor steel
welded joints 11

Ryabtsev I.A., Babinets A.A., Lentyugov I.P. and Turyk E.V. Influence of
electrode wire feed speed on base metal penetration in arc surfacing 15

*Polishko A.A., Medovar L.B., Stovpchenko A.P., Antipin E.V.,
Didkovsky A.V. and Tunik A.Yu.* Weldability of electroslog remelted
high-carbon steel at flash-butt welding 20

INDUSTRIAL

Kuskov Yu.M. Application of flux-cored wires at surfacing, remelting
and in metallurgy 27

Kolenic F., Kovac L., Sekerka R. and Faragula P. Modular design of high
productivity electron beam welding machines 34

Tkach P.N., Moltasov A.V., Tkach I.G. and Prokopchuk S.N. Methods for
determination of local stresses in welded pipe joints (Review) 42

*Lobanov L.M., Makhlin N.M., Vodolazsky V.E., Popov V.E. and
Mutsenko L.P.* New equipment for preparation of position butts of NPP
pipelines for welding 49

CALENDAR OF MARCH 53

60 Years of the First in the World Mobile Machine for Flash-Butt Welding of Rails in the Field Conditions

In the post-war years the tens of thousands of kilometers of railway tracks, damaged by war and quite unsuitable for any traffic on them, were available at the most part of the former USSR territory. The situation was redoubled also by the absence of production of new rails at that period. The way out of the situation was the only one: to start the restoration of railway tracks by using the remained undamaged rails to recommence the delivery of necessary cargoes along them. Moreover, even at this stage of reconstruction the task was to pass to the most progressive technology, namely to provide the continuous track (without double-sided cover plates), which will allow developing high speeds of traffic and being more reliable in maintenance.

The primary task was the searching for a reliable permanent joining of rail ends. Methods of welding, thermit and electric arc ones, known at those years, were characterized by a very low efficiency (1–2 butt joints per hour), and required to use a large amount of welding consumables and highly-qualified operators. At the same time the noted methods of welding did not provide the mechanical properties of joints, meeting high requirements to the continuous track joints (close to properties of the rail base metal).

Such requirements were satisfied by the flash-butt welding of rails, which was used at the factories abroad, equipped by stationary rail-welding machines. Using these machines the rail sections of 200–400 m length were welded in them and transported to the laying sites by special trains. Such machines consumed power of 400–500 kV·A, and their mass exceeded 200 tons. This circumstance allowed their application only in specialized rail welding shops, having the sufficient power supply (600–800 kV·A). The construction of similar enterprises at the USSR territory at that time was not possible.

In the middle of the 1950s the governmental task was put forward to the Electric Welding Institute: to design equipment for flash-butt welding of rails directly in operating track at its reconstruction and repair. Moreover, the welding process should be realized completely in the automatic mode and with account for minimized requirements to accuracy of cutting the rail ends as compared to the requirements under the factory shop conditions. The latter was specified by the fact that it is difficult to use the equipment for high-accuracy treatment of rail ends in the field conditions.

The development of the new technology and equipment for rail welding in the field conditions was carried out at the Electric Welding Institute integrally. Together with searching for welding technology, providing the required quality



Mobile complex K355 during tests at Kiev rail road tracks (1960)



Mobile rail welding complex on railway platform

of joints at a minimum power consumption, the control systems, providing its stable reproduction, independently of changing the service conditions, as well as equipment, having much less weight and dimensions, were developed. It was assumed to apply the equipment being designed as a tool, mounted on the rails being welded. It was found, that the significant decrease in welding process power, consumed in flash-butt welding of rails, can be achieved when using the power for welding with a continuous flashing for basic heating instead of used heating by resistance in stationary machines of the shops. Exciting by the continuous flashing at low specific powers became possible due to applying the controllers of flashing rate and high reduction (by 2–3 times) in resistance of welding circuit of the machines.

To produce the required heating in welding, a programmed reduction of voltage during flashing was suggested for the first time. Such technology, named as the continuous flashing with a programmed reduction in voltage, was used as a basis for the development of modes for welding of different rail types. For all the mentioned innovations, the International patents were obtained in the leading countries of the world. With their application, the first in the world mobile welding machine K355 was designed for continuous flash-butt welding of rails in the field conditions. It was characterized by a low weight (2.3 tons), allowed its application for mounting on rails using standard hoisting mechanisms. The welding machine power was 150 kW, it was enough to use the standard diesel-generating electric stations of 200 kV·A for its power supply. The first rail welding machines were mounted on all-terrain vehicles of a high trafficability, equipped with the hydraulic jacks and used in excavators. The electric supply of two welding machines, operating simultaneously, was realized from





generator, connected with a shaft of power take-off of all-terrain vehicle. Several tens of such mobile welding complexes were successfully used for restoration of railway tracks in hard-to-reach regions of the former USSR railroads.

During restoration of the railroads the main volume of welding works was connected with their reconstruction and laying of new sections of rails with sleepers. For these purposes, the mobile complexes were developed on the base of self-propelled railway platforms (PRSM) with a gantry hoisting devices. To increase the efficiency, the simultaneous welding of two butt welds by separate machines was provided.

In 1960, in accordance with documentation, worked out at the PWI, the Kakhovka plant of electric welding equipment (KPEWE) started production of the machine K355. By the middle of the 1960s about hundreds of such machines were in service in the USSR. Their design was continuously improved with account for needs of consumers. Since the middle of the 1970s the export of such machines to different countries of world started. They were bought by the USA, Great Britain, Austria, China and other countries. In total, from the data of KPEWE, 80 % of the world park of mobile welding machines is the machines, manufactured in Ukraine.

At the modern stage, the development of the new types of welding machines at PWI is continued. This is caused by the tendency of applying the high-strength rails of a new generation at the railway tracks.

In the recent decade the developments in the direction of updating the equipment for welding rails in the field conditions are continued. Here, the real tasks are taken into consideration for applying these machines in different regions of the world.

The application of the new technology of welding of high-strength rails, combined with their tension, required the creation of new generations of rail welding machines, characterized by much higher upsetting forces, equipped with built-in mechanisms for removal of weld reinforcement in a hot state. The above-given peculiarities of the new technology of welding of high-strength rails and systems of multifactorial control were used as a basis for the design of a new generation of mobile rail welding machines. Modern systems of computing technology, quick-response hydraulic drives and powerful systems of electron control of welding parameters are used in them. Such machines allow performing welding of long-length rail sections, combined with their tension.

The first machine K921 for welding rails by a pulsating flashing with tension was designed at the PWI in 2001 and manufactured by KPEWE in cooperation with the Norfolk Southern Company (USA). Its implementation and final testing of the technology of rail welding were carried out with the PWI participation on rail roads, which belong to this Company. For the first time in the world practice the flash-butt welding of rail sections of an infinite length, being up to several hundreds of kilometers without bolted joints, was performed. From the available data the total length of continuous tracks of infinite length, welded by the Company, exceeds 10 thou km.

In 2001–2005 the machines of K920 and K922 types of two modifications were designed. The parameters of these machines (forces of upsetting and clamping, machine dimensions) were optimized with account for applied technologies of repair and construction and available mobile rail welding complexes. In particular, it was possible to decrease greatly (by 1.5 times) the weight and dimensions of the machines as compared to the first experimental-industrial model K921.

In 2010–2012, according to the license agreement with Holland Company (USA) the PWI designed machines K930 and K945, which have an enlarged travel of movable clamp of up to 450 m at upsetting force of 120 tons. This allows welding of long rail sections of large length in reconstruction of railway tracks. The mobile complexes for operation with such machines were designed, respectively. Ten such complexes are operating since 2014 at the rail roads of Great Britain. They use the machines K945, designed at the PWI and manufactured at KPEWE.

The modern mobile rail welding complexes, manufactured by KPEWE, represent self-propelled units, which are provided with a rail travel or a combined travel, allowing moving both on rails, and also on high-way and earthen roads.

A qualitatively new level of mobile rail welding equipment was achieved as a result of the cooperation of PWI with the Progress Rail Services Corporation Company (USA). In 2014–2018, in accordance with the license agreement, the machines K960 and K1045 were designed and manufactured, which made it possible to significantly expand the fields of FBW application.

The machine K960 (upsetting force of 200 tons) is the most powerful among the production line of mobile machines for welding rails with tension, created by PWI and in present it is successfully operated in the reconstruction and repair of railways in the USA.

A unique arrangement of the suspended single-rod rail welding machine K1045 provided the ability to perform works in hard-to-reach places (in the underground, in welding rail endings of crossing pieces), which is a significant competitive advantage as compared to the known rail welding complexes.

On the mobile complexes, except the rail welding machines, the diesel-generator units of 200–300 kW capacity, hydraulic jacks, auxiliary equipment for rail preparation for welding, system of nondestructive testing are mounted. Mobile complexes of similar type, where machines K920, K922, K930, K950 are applied, are used at the rail roads of Europe, by Holland Company in the USA, Network Rail Company in Great Britain, in China, Australia, Taiwan, Malaysia, India, Turkey, Saudi Arabia and Thailand.

Prof. S.I. Kuchuk-Yatsenko

PECULIARITIES OF ELECTRODE AND BASE METAL MELTING IN ELECTROSLAG WELDING

I.I. LYCHKO, K.A. YUSHCHENKO, S.A. SUPRUN and S.M. KOZULIN

E.O. Paton Electric Welding Institute of the NAS of Ukraine

11 Kazimir Malevich Str., 03150, Kyiv, Ukraine. E-mail: office@paton.kiev.ua

Results of experimental studies of the connection between the processes proceeding in the electrode wire melting zone and electric parameters of the electroslag welding mode are described. The experimental procedure envisaged electroslag welding of specimens from 60 mm thick steel 09G2S in the modes identical to those, used earlier for photographing and filming the welding zone through an optically transparent medium. Hall sensor, ADC module E-140 and «Power Graph» software were applied for high-speed recording of electric parameters of mode (10 thousand records per second). Measurements of slag pool temperature near the electrode wire melting zone were taken simultaneously. Analysis and comparison of visual observations of the welding zone through an optically transparent medium with the characteristics of electroslag welding mode (U_w , I_w , $V_{w,t}$) were performed, confirming the cyclic existence of some nucleus in the molten slag between the electrode wire and liquid metal, formed under the effect of electric potential between the base and electrode metal. 9 Ref., 4 Figures.

Keywords: *electroslag welding, slag pool, interelectrode gap, high-speed recoding of electric parameters of mode, active zone, energetic nucleus, «discharge», melting and transfer of liquid metal, high-speed photographing and filming*

Electroslag welding (ESW) is one of the types of fusion welding and is based on use of heat energy released during electric current passing through the molten flux. This process has a number of specific characteristics which determine the priority and scope of its application in different branches of the national economy in welding metal of 40 mm thickness and larger in one pass [1].

Studying the physical nature of ESW will not only allow improving the efficiency of the welding process control to optimize sizes of the weld and penetration depth of the base metal, but also finding the ways to reduce heat input in welding zone for decreasing the volume of subsequent heat treatment of welded joint metal necessary for recovery of high service characteristics of a welded structure.

Therefore, the studying of processes, proceeding in interelectrode gap when performing ESW, was always relevant. However, often, due to the present demands in the welding industry, the mentioned study was inferior to solving practical problems in the development of welding technologies for specific metal structures of heavy machine building, hydropower engineering and other industries.

From the beginning of the electroslag welding process development, researchers were striving to look into the welding zone. The primary ideas about the processes occurring in the slag pool were obtained using the methods of indirect observation and described in the works [2–6]. The first information about the

shape of melting electrode and interelectrode gap was obtained by G.Z. Voloshkevich [2, 3]. However, due to a number of technical reasons, the obtained results did not allow studying the dynamics of processes proceeding in the interelectrode gap.

Later, the authors of works [7, 8] managed to carry out a more successful direct observation of the ESW process and its high-speed filming by conducting the specially prepared experiments using heat-resistant glass, which was installed instead of a copper water-cooled shoe.

It is known that the phenomena, observed in the welding zone, arise in the process of conversion of electric energy into heat one (electric parameters of the welding mode). Their character also depends on the physicochemical properties of the slag pool and electrode material.

According to the literature data [1–3, 9], the heating and melting of the wire electrode occurs in the area of an active contact of its surface, which is moistened with slag. The area of this surface is variable and depends on the welding mode parameters (values of voltage on slag pool, welding current, diameter and electrode feed speed, slag pool depth, etc.). For the established ESW processes used in practice, the contact surface area can vary in the wide ranges, for example, for wire with a diameter of 3 mm it is 14–110 mm² [9]. The molten electrode metal of the wire flows along its side surface into the gap between the electrode end and metal pool. As a result of computer processing

of filming frames of the slag pool, its typical regions were distinguished: the zone of the highest temperatures, which has a direct contact with the electrode end, and the zone, whose temperature is lower than that of the mentioned one, but higher than that in the volume of a slag pool [9].

The results of investigation of the process of electrosag welding with a wire electrode through the optically transparent medium confirmed the known basic definitions of the physical principle of this process [1], and also allowed developing the ideas about the phenomena occurring in the active zone of the slag pool, on which melting of base metal and weld formation depend [9].

On the basis of direct visual observations of the welding zone, the existence of some energetic nucleus was shown, formed under the action of electric potential between the base and electrode metal in the welding zone, in the molten slag between the end of the electrode wire and the metal pool.

During investigation and analysis of the welding mode characteristics, the following regularities were recorded:

- cyclic (with a duration of 0.3–0.6 s) nature of variation in sizes of this nucleus;
- increase in the critical state of energy characteristics of the nucleus before the end of the cycle;

• it is shown that the concept of the metal pool depth, usually defined by macrosections, does not correspond to its actual instantaneous parameters.

At the same time, it was suggested that the «explosive» change in the energy characteristics of the region between the electrode wire end and the metal pool before finishing the cycle occurs during the formation of slag vapors. During the transition of a slag from a liquid to a vapor-gas state, this region grows in volume in a very short time with the rise in conductivity and slag vapor temperature, reaching the maximum degree of ionization of the interelectrode gap, increasing the pressure, which together leads to explosive completion of the cycle.

With a decrease in the interelectrode gap due to slag evaporation, a «discharge»* occurs, in the volume of which the pressure and evolution of heat energy increase. The pressure of the «discharge» is transmitted to the metal pool and the entire volume of slag in a pulsed mode by means of electrohydrodynamic shocks, causing intensive heat flows in the metal and slag pools. Under the action of these flows, the edges being welded are fused and the slag pool is heated [9]. The given results of the investigations were obtained by studying the visual phenomena in the slag pool without a corresponding recording of the welding mode electric parameters.

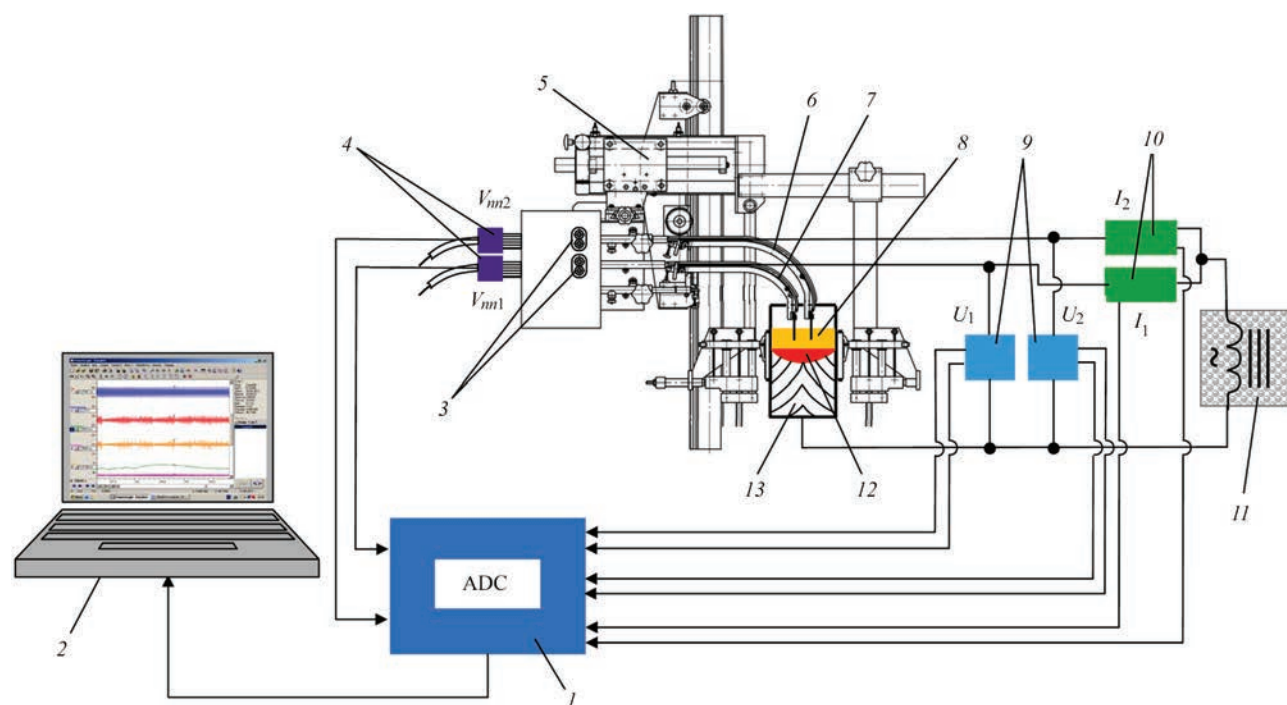


Figure 1. Scheme of high-speed recording of electric parameters of ESW mode: 1 — ADC module E-140; 2 — personal computer; 3 — feed rollers; 4 — sensors of electrode wires feed speed; 5 — welding device A-535 UKhL4; 6, 7 — upper and lower nozzles; 8 — slag pool; 9 — sensors of voltage on nozzles; 10 — welding current sensors; 11 — power source; 12 — metal pool; 13 — weld

*To specify the physical nature of the term «discharge», additional investigations will be conducted.

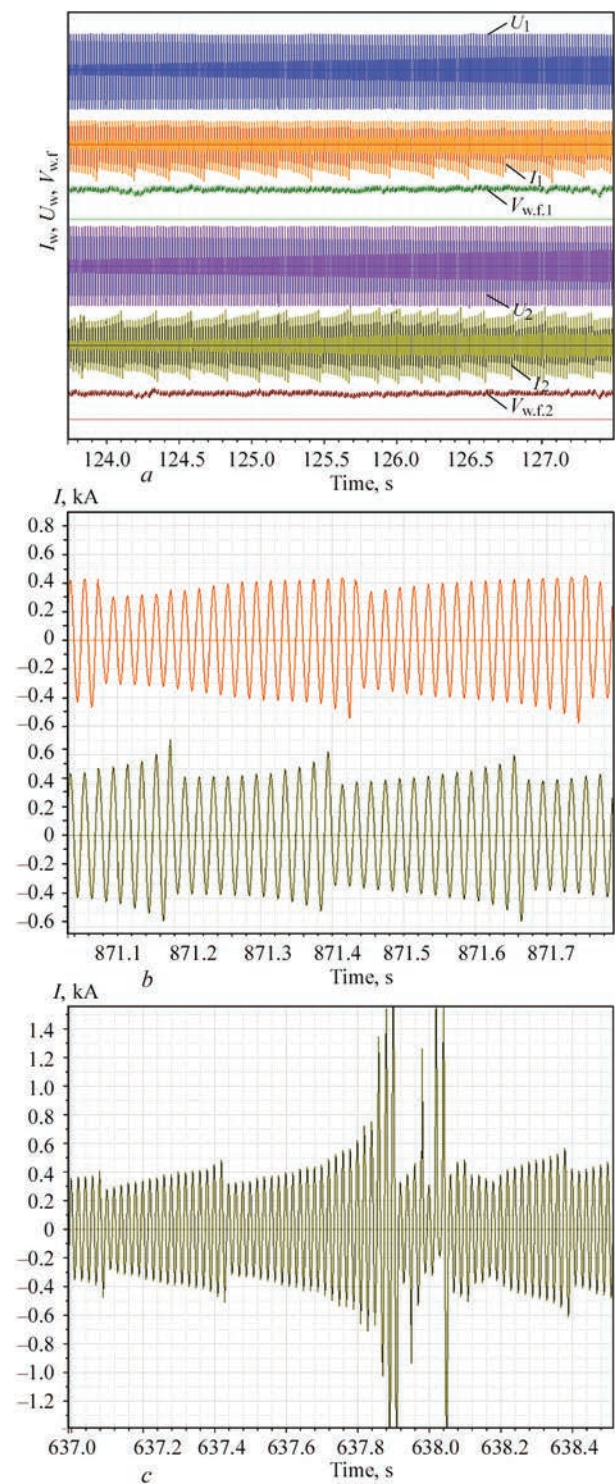


Figure 2. Fragments of recording oscillograms of parameters of the mode of ESW (I_w , U_w , $V_{w.f}$) with two electrodes: *a* — general view of the process with duration of 3.8 s; *b* — fragment of I_w recording in the interval of 871.0–871.7 s; *c* — oscillogram of I_w on the second electrode in the interval of 637.0–638.4 s

The aim of this work was to study the relationship between the phenomena visually observed in the welding zone and the basic electric parameters of the welding process mode.

The methods of performing experimental works are the following:

1. Using the device A-535UKhL4 and the AC power source TShS 3000-3, ESW of specimens of a low-alloyed steel 09G2S of 60 mm thickness was performed in the modes identical to those used in the work [8] ($n = 2$, $d_e = 3$ mm, $h_w = 45$ mm, $V_{w.f} = 112$ and 158 m/h, $B = 27$ mm, flux AN 8)*;
2. In the process of welding, a high-speed recording of electrical parameters of the mode (I_w , U_w , $V_{w.f}$) was performed using the Hall sensors, ADC module E-140 and the software «Power Graph»;
3. The numerical values of electric parameters of the welding process (I_w , U_w , $V_{w.f}$) were recorded at a frequency of 10 thou records per second (filming frequency was 100 frames per second);
4. Simultaneously with the recording of mode parameters, measurements of the slag pool temperature were performed with a digital recording of results. The thermocouple VR 5/20, installed in a protective heat-resistant case, the working end of which (immersed in a slag pool) was lined with a self-sintering graphite mass, was immersed into a slag pool to the 30 mm depth. Indications and recording of thermocouple potentials in the continuous mode were performed using the digital voltmeter VTs 7-21 and a video camera. Since the well-known temperature recording devices are very inertial, the proposed method allowed recording changes in temperature with time at the higher resolution.

The diagram of electrical connections during experiments on recording the basic electric parameters of the mode is shown in Figure 1.

The general view of the obtained oscillograms of the basic electric parameters of the welding mode with two electrode wires is shown in Figure 2. Here, a fragment of the high-speed recording of welding current, voltage on the slag pool and feed speed of the electrode wires in both nozzles are presented (Figure 2, *a*).

As a result of the analysis and comparison of visual effects of filming and recorded oscillograms of electric parameters of the mode at a qualitative level, the following regularities were established.

On the oscillograms of the set ESW mode, as well as on the frames of filming, the cyclic nature of welding process was clearly recorded, which is characteristic of each of the two wire electrodes and is determined by the dynamics of melting of each electrode. In this case, some shift in the peak values of welding current

*In the work, B.V. Tsibulenko, V.G. Yarmak, G.S. Shulzhenko and N.O. Chervyakov took part.

is observed, despite the fact that both electrodes are supplied from the same source (Figure 2, *a, b*).

It is shown that dimensions of energetic nucleus, values of welding current and shape of metallic pool have a common pattern of cyclic nature. In this case, throughout the whole ESW process, in the interelectrode gap, two types of cycles of different duration are observed, ending in «discharges», differing in their intensity (Figure 2). Each cycle is completed in the formation of «discharge» in the metal pool. After every 10–13 cycles with a duration of 0.3–0.4 s, ending in «discharges» of a comparatively low power in the area of the metal pool mirror, the cycles with a duration of 0.5–0.7 s are observed ending in «discharges» of high power, at which the nucleus mass reaches the bottom of the metal pool, causing a splash of superheated metal of the pool to the edges of base metal at a high rate (1.1–1.5 m/s).

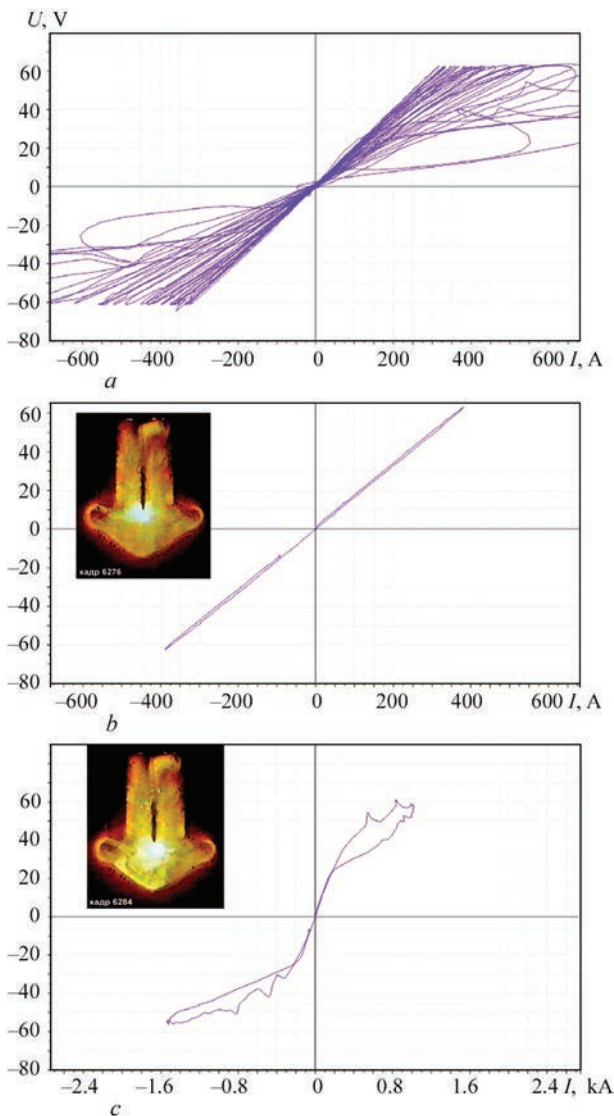


Figure 3. Voltampere characteristics of a cycle with a duration of 0.5 s on one electrode and the corresponding photos of welding zone: *a* — full cycle (see Figure 2, *c*); *b* — beginning of the cycle (0.04 s); *c* — «discharge» at the end of the cycle (0.04 s)

Thus, in the region of 3.5 s, 15–17 «discharges» of comparatively low power are noted (Figure 2, *a*). The beginning of a cycle with a duration of 0.4 s, ending in a low-power discharge (Figure 2, *b*), is characterized by a low value of welding current, equal to 312 A, and the minimum size of energetic nucleus. By the time of ending the «discharge», the welding current is gradually increased to 622 A. Simultaneously, with the increase in current, the size of the energetic nucleus increased, which shifted to the metal pool mirror. The voltage at the slag pool was changed slightly: in the range of 1.0–1.5 V.

Figure 2, *c* shows a fragment of the oscillogram, where the intensity of the current increment had a different nature. Here, a cycle with a duration of 0.5 s, ending in a «discharge» of high power, begins with a welding current value equal to 412 A, and ends in a value of 1580 A. At the same time, simultaneously with the increase in welding current, the region of energetic nucleus increases from 25 to 200 mm². In the

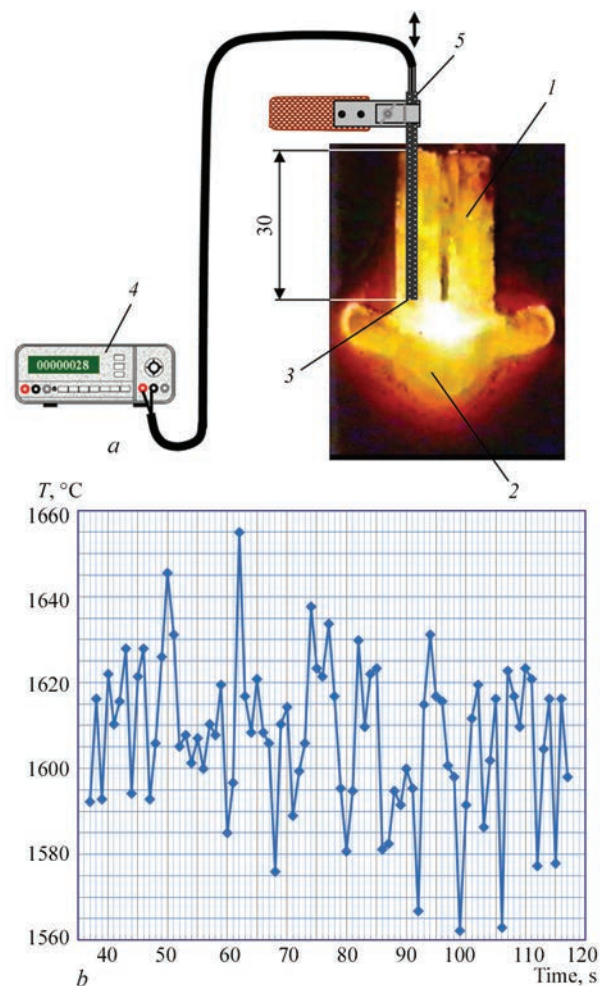


Figure 4. Scheme of measurements of temperature of the slag pool (*a*) (1 — slag pool; 2 — metal pool; 3 — place for deepening of thermocouple; 4 — digital voltmeter; 5 — probe with thermocouple in a special protective case) and fragment of variation of its temperature (*b*)

region of sharp current peaks, the voltage at the slag pool decreases by 3.0–4.0 V.

The resolution of the used methods for measuring electric parameters of the mode allowed recording changes in welding current and voltage starting from 0.001 s. The comparison of oscillograms of the welding current with the video frames of filming in the limits of one cycle allowed studying the dynamics of «discharge» formation from the beginning to the end of its existence (Figure 3). It is shown that the end of existence of a «discharge» and the transition of its mass in the form of electrohydrodynamic impact into a metal pool is characterized by a sharp increase in welding current (Figure 2, *c*) and thermal energy in the interelectrode gap.

Comparison of the dynamics of variation in the shape of metal pool with electric parameters of the mode showed that at the end of a high power «discharge», the mass of metal pool instantly moves down and, reaching its bottom, it moves upward the welded edges by fusion of the base metal grain boundaries.

The measurements of temperature of the slag pool near the electrode melting zone showed that its change is also cyclical in nature, however, a direct correlation with cyclic changes in welding current and sizes of the nucleus was not established (Figure 4). In this case, the peaks of the maximum temperature of the slag pool are observed after the completion of 3–7 high-power «discharges». Despite the fact that insufficient resolution of the used instruments did not allow establishing the correct relationship between the results of measurements of temperature of the slag pool and frequency of the formation of «discharges», it can be assumed that the general tendency of cyclical changes in temperature is observed.

Conclusions

1. Based on the analysis of the results of direct visual investigations of the welding zone through an optically transparent medium and oscillograms of parameters of the steady state of ESW mode (I_w , U_w , $V_{w,f}$), the existence of some kind of energetic nucleus in the molten slag between electrode wire and the mirror of metal pool was confirmed, formed under the action

of electric potential between the base and electrode metal in the welding zone.

2. Comparative analysis at the qualitative level of dynamics of changes in the geometrical parameters of the welding zone and the basic electric parameters of welding process showed that the sizes of energetic nucleus in the molten slag, the value of welding current, the number of discharges and the nature of shape of the change of metal pool have a common cyclical pattern. Moreover, each cycle ends in a «discharge» into the metal pool.

3. For further expansion of ideas about the processes occurring in the interelectrode gap at ESW using wire electrode and the development of methods for controlling heat input to the base metal by controlling the shape and intensity of «discharges», as well as conditions for existence of energetic nucleus, it is necessary to conduct additional experimental investigations providing a correct synchronization of the fixed video effects of welding zone with the results of recording the electric parameters of the mode.

1. (1980) *Electroslag welding and surfacing*. Ed. by B.E. Paton. Moscow, Mashinostroenie [in Russian].
2. Voloshkevich, G.Z. (1955) X-ray investigation of electrode melting and metal transfer. In: *Problems of electric arc and resistance welding*. Moscow, Mashgiz, 292–300 [in Russian].
3. Voloshkevich, G.Z. (1958) Electrode melting and metal transfer in electroslag welding. *Avtomatch. Svarka*, **10**, 14–21 [in Russian].
4. Ando, A., Nakata, S., Wada, H. (1970) Studies on the electroslag welding (Report 111). *J. Jap. Weld. Soc.*, **40**(11), 1104–1110.
5. Kaluc, E., Taban, E., Dhooze, A. (2006) *Electroslag welding process and industrial applications*. Metal Dnyasi, Ocak 2006 Sayi: 152, Yil: 13, Sayfa, 100–104 [in Turkish].
6. Brandi, S.D., Liu, S., Thomas, R.D. (2012) Electroslag and electrogas welding. *AWS Welding Handbook*, **6A**, 365–379.
7. Konigsmark, J. (1970) Direct observation of electroslag process at welding with wire electrode with diameter of 3.15 mm. *Zvaranie*, **19**(9–10), 265–269 [in Slovak].
8. Dudko, D.A., Voloshkevich, G.Z., Sushchuk-Slyusarenko, I.I., Lychko, I.I. (1971) Study of electroslag process using filming and photography through transparent medium. *Avtomatch. Svarka*, **2**, 15–17 [in Russian].
9. Paton, B.E., Lychko, I.I., Yushchenko, K.A. et al. (2013) Melting of electrode and base metal in electroslag welding. *The Paton Welding J.*, **7**, 31–38.

Received 15.11.2018

EFFECT OF REHEATING IN MULTIPASS SUBMERGED-ARC WELDING ON DELAYED FRACTURE RESISTANCE OF ROTOR STEEL WELDED JOINTS

**V.Yu. SKULSKY¹, S.I. MORAVETSKY¹, M.A. NIMKO¹, Yu.G. PASHCHENKO²,
A.G. KANTOR² and V.V. DMYTRYK³**

¹E.O. Paton Electric Welding Institute of the NAS of Ukraine
11 Kazimir Malevich Str., 03150, Kyiv, Ukraine. E-mail: office@paton.kiev.ua

²JSC «Turboatom»

199 Moscow Ave., 61037, Kharkov, Ukraine. E-mail: office@turboatom.com.ua

³NTU «Kharkov Polytechnic Institute»

2 Kirpicheva Str., 61002, Kharkov, Ukraine

The change in relayed fracture resistance, depending on preheating temperature and thermal effect during deposition of new beads was experimentally studied, using the Implant method, in the case of 0.25C–2CrNiMoV rotor steel joints, produced by submerged-arc welding. The nature of the change in hardness in the cross-section of quenching steel with a deposited bead was investigated, which illustrates formation of quenching and tempering areas under the influence of reheating in welding. Using critical stresses as a quantitative index, causing delayed fracture, it was shown that after reheating in welding, the cracking resistance can increase by about 1.5–2.5 times or more. Under the conditions of welding without preheating, one-time and two-time cycles of heating in welding increase the cracking resistance up to the level obtained during welding with preheating up to 150–200 °C. 9 Ref., 4 Figures.

Keywords: *heat-resistant rotor steel, submerged-arc welding, quenching, reheating in welding, Implant, delayed fracture resistance*

One of the advantages of automatic submerged-arc welding is its high efficiency, which allows producing metal joints of larger cross-section at smaller number of passes. Higher efficiency is achieved due to greater thermal power of the welding arc. However, welding in the modes with a higher heat input leads to higher welding stresses [1] that can have a negative effect on welded joint performance. Moreover, welding stresses are a factor, provoking development of delayed fracture in quenching steel welded joints. In its turn, excess heating leads to undesirable structural changes, increase of grain size in the HAZ that also adversely affects the service properties, increases the probability of delayed fracture and reheating cracks [2–5]. In order to lower the level of residual stresses, the heat input into the joint zone should be limited, as well as the preheating temperature [1, 2]. For the case of welded joints of power engineering steels of great thicknesses, including rotor structures, narrow-gap submerged-arc multipass welding is used. A rational technological scheme also envisages limitation of the heat input in order to obtain the optimum cross-section of the deposited beads that ensures sound formation of the welded joint and lowering of the level of residual stresses [5].

Thus, in many cases multipass welding with limitation of welding mode parameters is preferable that has a positive effect both on lowering of the stress-strain state, and on formation of a uniform structure and resulting properties. The cold cracking problem is solved by application of preheating and concurrent heating in welding. As shown in [6], in the case of coated-electrode multipass manual arc welding, reheating, by influencing the structural and hydrogen factors, allows a considerable increase of delayed fracture resistance of metal in earlier deposited layers. This enables a certain lowering of preheating temperature, making the welding process more cost-effective. It is of interest to check the possibility of obtaining such an effect under the conditions of automatic submerged-arc welding.

The objective of this work is evaluation of the effect of reheating in submerged-arc welding on cold cracking resistance of quenching steel.

Investigations were performed with application of rotor steel of 0.25C–2Cr–NiMoV type. Cold cracking tests were conducted by the Implant method [3], using 8 mm diameter samples with a spiral stress raiser in the test part. Minimum (critical) stress σ_{cr} , above which delayed fracture developed, was the cracking

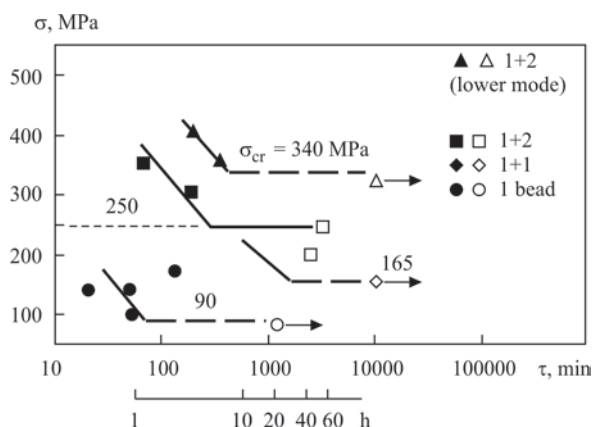


Figure 1. Influence of reheating in automatic submerged-arc welding (without preheating) on delayed fracture susceptibility of test joints of rotor steel of 0.25C–2CrNiMoV type (dark and light signs mean there is fracture or no fracture, respectively). $[H]_{\text{dif}} = 5.23 \text{ cm}^3/100 \text{ g Me}$

resistance characteristic. Automatic welding of Implant samples with a backing plate (from steel 20), and deposition of process beads were performed with wire of 0.14C–Cr–2NiMo alloying system using agglomerated flux UV422TT of basic type (basicity according to Bonishevsky of 2.5 for wt.%). Temperature measurement in the sample HAZ was conducted using a thermocouple passed through a hole in the plate end face and welded to the sample by a capacitor-type machine [6, Figure 1]. Vickers hardness was measured with 50 N load on the indenter. Alcohol method was used to determine the concentration of diffusible hydrogen $[H]_{\text{dif}}$ in the deposited metal ($5.23 \text{ cm}^3/100 \text{ g Me}$) [7]. Metal samples were obtained by bead deposition on the surface of steel with a drilled-out hole — at arc shifting to the hole zone the drooping metal fell on the detachable copper mould, in which the «pencil» sample formed for analysis. Metal reheating in the area of the earlier deposited bead was created by deposition of one new bead in the center of the first (1 + 1 scheme), or of two partially overlapping beads, deposited with wire shifting from the zenith of the first bead by approximately 1/4 of its width (1 + 2 scheme). At deposition the following mode was used as the basic one: $I_w = 320\text{--}340 \text{ A}$, $U = 35 \text{ V}$, $V_w = 19 \text{ m/h}$; where additionally specified, deposition of just the new layer beads at lower current $I_w = 250\text{--}280 \text{ A}$, was performed, voltage and speed remaining the same as in the base mode. In the experiments, deposition of each of the subsequent beads was conducted after cooling of metal with the previous deposit to the temperature of 100°C and lower; loading of the tested joints was performed after their cooling to room temperature (the joints were cooled to 100°C in calm air, after that — in accelerated mode with air blowing). Unlike the recommended by GOST 26388–84 loading temperature of $150\text{--}100^\circ\text{C}$, the selected approach is explained by

the fact that, as was experimentally established [8], in the range of $120\text{--}100^\circ\text{C}$ the joints of steels with martensitic and martensitic-bainitic structure (similar to the tested one) manifested instability as regards delayed fracture resistance, and in the $100\text{--}80^\circ\text{C}$ range, they showed a rather high fracture susceptibility. Assuming that such a high sensitivity to factors, causing delayed fracture, and unstable behaviour of the loaded welded joints at their cooling from 150 to 100°C , can influence the accuracy of the results of the conducted comparative studies, it was decided to load the joints at room temperature. At evaluation of the effect of reheating on cracking resistance, the welding operations were conducted without preheating.

The experimentally found nature of the change of delayed fracture resistance of initially quenched metal in the HAZ after repeated heating cycles (Figure 1) is in agreement with the results of similar experiments in manual arc welding [6]. From the changes of critical stresses it follows that deposition of two subsequent beads is quite efficient (1 + 2 scheme): cracking resistance, compared to one-bead welding increased by approximately 2.5 times; one-time heating yields an intermediate result — σ_{cr} increased 1.6 times. An even greater effect was achieved after reheating at deposition of the second and third beads at current lowering (scheme 1 + 2 in the graph, «decreased mode»).

Change of cracking resistance is related to a certain degree to geometry of bead cross-section, temperature distribution and degree of tempering of the quenched region in the HAZ at the initial bead. In welding in the commonly used modes, the deposited beads have a shape elongated across the width, and close to an elliptical one. As shown by the results of studying bead cross-sections in automatic submerged-arc bead deposition on the steel surface (experiments were performed with application of steel Kh10CrMoVNb91), change of the heat input due to the change of current stronger affects the increase of bead width and penetration depth, deposit height changes only slightly: for instance, at q/v increase from 14 to 20 kJ/cm , the width, depth of penetration and height of the bead increased by 6.5; 1.8 and 1.0 mm, respectively. At deposition of the second bead in an unchanged welding mode a large part of the area of quenched metal in the HAZ at the first bead is again subjected to quenching, that can be seen in the scheme in Figure 2 (in this case, the second bead is made with a small shifting from the zenith of the first one; abbreviations denote: HAZ1, HAZ2 — regions of quenched metal, formed as a result of heating when making the first and second beads, delineated by boundary lines B1 and B2; FL1, FL2 are the respective fusion lines). In the two

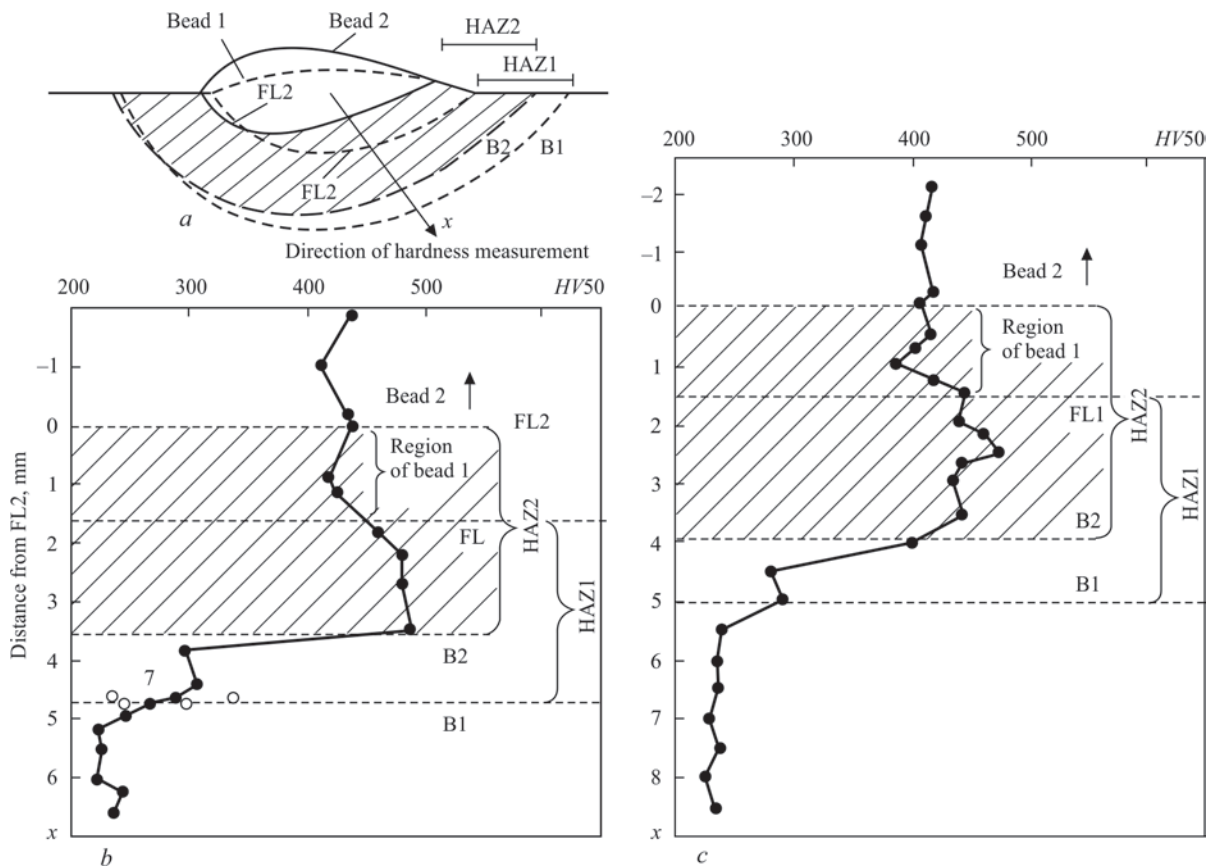


Figure 2. Change of hardness in different zones of metal cross-section with deposition of two beads: *a* — scheme of deposition of the second bead and direction of hardness measurement; *b* — distribution of hardness values corresponding to scheme (*a*) at bead deposition in the mode with heat input $q/v = 13 \text{ kJ/cm}$ ($I_w = 200 \text{ A}$, $U_a = 43 \text{ V}$, $V_w = 19 \text{ m/h}$); *c* is the hardness profile at bead deposition in higher modes — $q/v = 16.23 \text{ kJ/cm}$ ($I_w = 250 \text{ A}$, $U_a = 43 \text{ V}$, $V_w = 19 \text{ m/h}$)

schemes of hardness variation, one can see that deposition of new beads at smaller (*b*) and greater (*c*) heat input led to hardness decrease only in HAZ1 regions about 1.0 mm wide at HAZ1 total width approximately equal to 3.0 and 3.5 mm, respectively, for the considered variants. It is natural that deposition of just one bead gives a smaller tempering effect, compared to deposition of two beads, when additional metal in HAZ1 is subjected to two-time tempering heating (similar results at manual arc welding were obtained in work [6]). In its turn, deposition of two new beads at lower current creates the conditions for the impact of tempering temperatures on a larger area of initially quenched metal in HAZ1, due to lowering of penetration depth. This resulted in increase of delayed fracture resistance, compared to the variant of one-bead welding, approximately 3.5 times, and, compared to 1 + 2 scheme, performed in the basic mode — approximately 1.5 times. A similar effect should be anticipated when making new layers of deposited beads, where repeated quenching of the initial quenched metal (in HAZ1) will be eliminated when moving away from it, at the impact of just the tempering range temperatures (Figure 3).

Figure 4 gives a comparison of critical stresses, obtained in welding without preheating and with preheating up to temperature $t_{pr} 250^\circ\text{C}$. These data show that in welding without preheating, the two-time thermal impact on the quenched metal in the region of

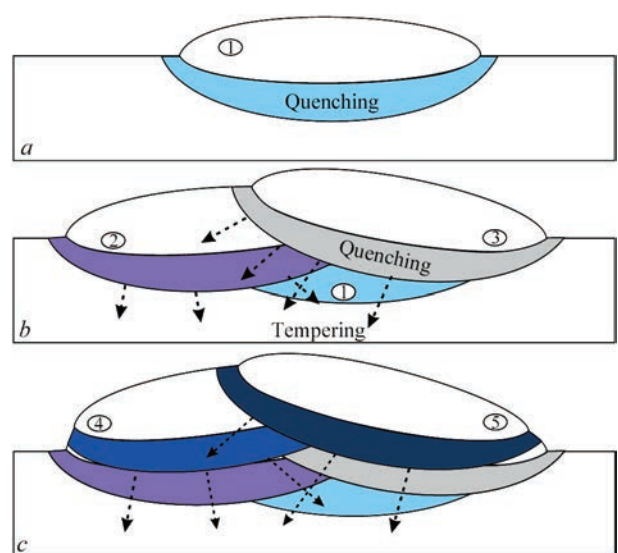


Figure 3. Schematic of bead deposition, formation of quenching regions (filled areas) and superposition of tempering range temperatures (shown by arrows); *a* — initial bead; *b*, *c* — deposition of two layers of two beads each

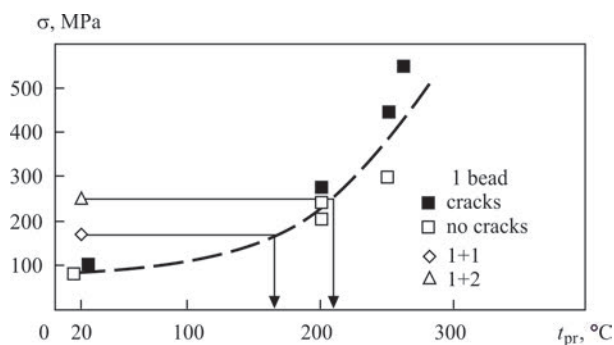


Figure 4. Influence of preheating temperature and welding conditions on delayed fracture resistance of test joints of 0.25C–2CrNi–MoV type steel (20 °C — welding without preheating)

the first pass (1 + 2 scheme) allowed achieving cracking resistance, equivalent to welding with preheating approximately to 200 °C. One-time reheating (1 + 1 scheme) also gave considerable positive effect, close to welding with preheating approximately to the level of 150 °C. The above results, as well as the data of [6], lead to the assumption that a greater number of subsequent tempering cycles in multipass submerged-arc welding without preheating should provide an even greater effect, comparable with welding with preheating up to a higher temperature. At the same time, as shown in [9], in the case of welded joints of heat-resistant steel 10CrMo9–10, preheating in submerged-arc welding promotes lowering of the concentration of diffusible hydrogen in the joint zone. In this connection, increase of delayed fracture resistance at repeated cycles of heating in welding, can be regarded as the result of the impact on the structural and, to a certain degree — on the hydrogen factors.

Thus, obtained results show that under the conditions of multipass submerged-arc welding of quench-

ing steels, reheating in welding essentially increases the delayed fracture resistance of welded joints, that was illustrated by increase of critical stresses, causing cracking, by approximately 1.5–2.5 times and more, depending on the number of heating cycles. It can be assumed that allowing for the positive effect of repeated cycles of thermal impact, multipass welding can be performed at lower preheating temperature without the risk of deterioration of technological strength of the produced joints.

1. Lobanov, L.M., Mikhoduj, L.I., Pivtorak, V.A. et al. (1995) Influence of peculiarities of submerged-arc welding technology on stress state of high-strength steel welded joints. *Avtomatich. Svarka*, **9**, 21–23 [in Russian].
2. Burashenko, I.A., Zvezdin, Yu.I., Tsukanov, V.V. (1981) Substantiation of heating temperature in welding Cr–Ni–Mo–V steels of martensitic class. *Ibid.*, **11**, 16–20 [in Russian].
3. Novikov, I.I. (1971) *Theory of heat treatment*. Moscow, Metallurgiya [in Russian].
4. Skulsky, V.Yu. (2009) *Weldability of heat-resistant steels for boiler units of high parameters*: Syn. of Thesis for Dr. of Techn. Sci. Degree. Kyiv, PWI [in Ukrainian].
5. Tsaryuk, A.K., Skulsky, V.Yu., Moravetsky, S.I. (2016) Mechanized narrow-gap submerged-arc welding of thick-walled cylindrical products. In: *Proc. of 2nd Medovar Memorium Symp. (June 7–10, 2016, Kyiv, Ukraine)*. Kyiv, Elmet-Roll.
6. Skulsky, V.Yu., Strizhius, G.N., Nimko, M.A. et al. (2019) Delayed fracture resistance of welded joints of rotor steel 25Kh2NMFA after welding reheating. *The Paton Welding J.*, **2**, 7–12. DOI: <http://dx.doi.org/10.15407/tpwj2019.02.01>
7. Kozlov, R.A. (1986) *Welding of heat-resistant steels*. Leningrad, Mashinostroenie [in Russian].
8. Skulsky, V.Yu. (2009) Thermokinetic peculiarities of formation of cold cracks in welded joints on hardening heat-resistant steels. *The Paton Welding J.*, **3**, 8–11.
9. Oring, H., Shuetz, H., Klug, P. (1996) Vorwaermen aus Sicht des Schweissgutes bei hoch- und warmfesten Schweissverbindungen. *Schweisstechnik*, **1**, 4–8 [in German].

Received 28.11.2018



FRONIUS UKRAINE LLC HOLDS THE SEMINARS

May 15, 2019 — «Automation of Welding Processes»

June 20, 2019 — «Robotization of Welding Processes»

Fronius Ukraine GmbH
 Browarskij r-n, s. Knjashitschi, ul. Slavy 24
 07455 Kievskaya obl.
 Tel.: +380 44 2772141
 Fax: +380 44 2772144
sales.ukraine@fronius.com
<http://www.fronius.ua/>

INFLUENCE OF ELECTRODE WIRE FEED SPEED ON BASE METAL PENETRATION IN ARC SURFACING

I.A. RYABTSEV¹, A.A. BABINETS¹, I.P. LENTYUGOV¹ and E.V. TURYK²

¹E.O. Paton Electric Welding Institute of the NAS of Ukraine

11 Kazimir Malevich Str., 03150, Kyiv, Ukraine. E-mail: office@paton.kiev.ua

²Institute of Welding, Gliwice, Poland; E-mail: Eugeniusz.Turyk@is.gliwice.pl

Influence of electrode wire feed speed on base metal penetration and geometrical dimensions of deposited beads at submerged-arc surfacing was studied. Four flux-cored wires of 1.2; 1.6; 1.8 and 2.0 mm diameter were used in the experiments. Feed speed adjustment was performed in the range from minimum value $V_{f,min}$, at which a stable surfacing process can be in place for these conditions, and up to maximum value $V_{f,max} = 450$ m/h, which was determined by the characteristics of the used surfacing unit. It is found that at surfacing with high wire feed speeds, there exists such an optimum ratio of feed speed and other surfacing parameters for each wire diameter, at which increase of this speed leads to reduction in penetration depth and share of base metal in the deposited metal at rising current of surfacing. Results, obtained in this work, were successfully applied at wear-resistant arc surfacing of 3 mm steel sheets, and can also be used in selection of modes of arc surfacing of other parts, which to the greatest extent meet their operating conditions, and requirements to deposited metal and base metal penetration. 10 Ref., 4 Tables, 5 Figures.

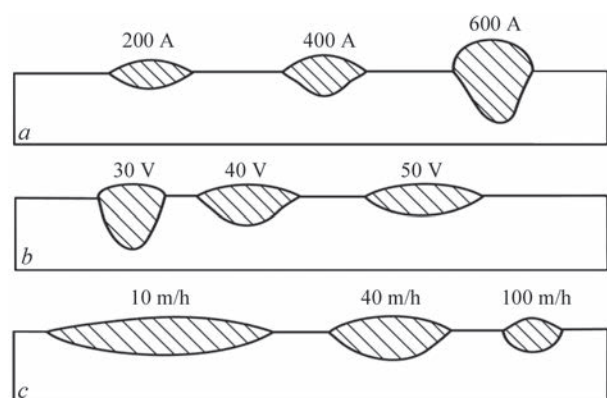
Keywords: arc surfacing, surfacing modes, electrode wire feed speed, base metal penetration, deposited metal formation, flux-cored wire, deposited metal

One of the main characteristics of different methods of surfacing is the value of penetration of base metal and, as a result, the share of base metal (SBM) in the deposited metal. As a rule, in arc surfacing with electrode wires, the share of base metal in deposited metal varies in the range of 30–50 %. As a result, in order to reach the desired chemical composition in deposited metal, it is necessary to deposit 4–5 layers. Thus, reduction in the value of penetration and SBM should improve technical and economic characteristics of the arc surfacing process, and the development of measures for their reducing remains an urgent task [1].

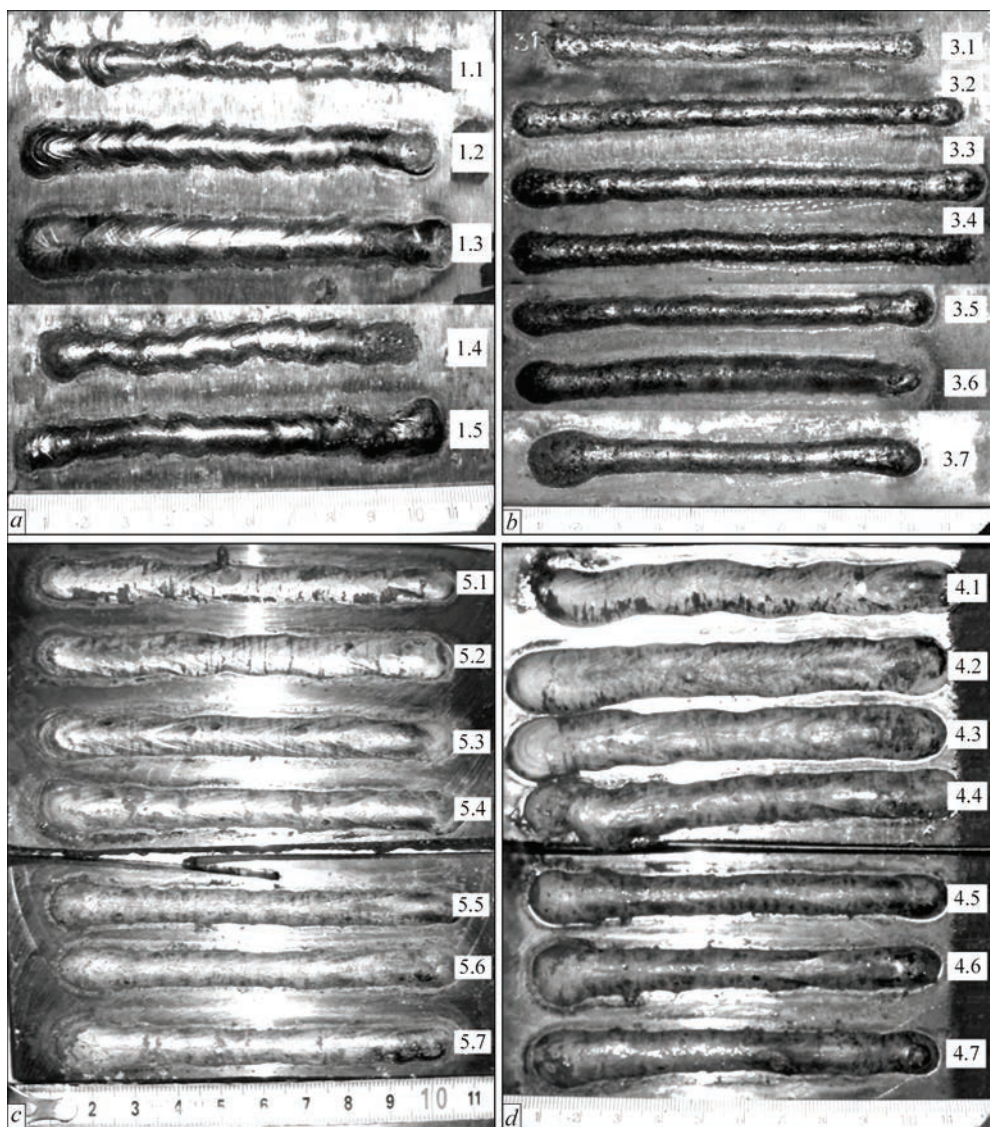
It is widely known that the quality of the deposited metal formation, its composition and structure, as well as penetration depth of base metal and SBM, depend mainly on surfacing modes [1–5]. The basic parameters of surfacing mode are current value (electrode wire feed speed); polarity and kind of current; arc voltage; surfacing speed; diameter (cross-section) of electrode material; surfacing pitch; and during surfacing of rotation bodies, displacement from the zenith or nadir. Among them, when developing the technology of arc surfacing of specific parts, the values of current and voltage, surfacing speed and diameter (cross-section) of the electrode material are usually preset [1, 5–8]. Such parameters as kind and polarity of current, the value of electrode wire stickout, etc., have a lower influence on penetration depth and SBM, shape and sizes of deposited beads [6]. At the same time, in the first place the selected mode of sur-

facing should provide a good formation of the deposited metal and a minimum, but sufficient penetration of base metal or a previously deposited layer [1].

Among the mentioned parameters of arc surfacing modes by electrode wire the current of surfacing has highest effect on the depth of penetration of base metal and SBM. A growth of current leads to a sharp increase in the penetration depth and formation of high and narrow beads (Figure 1) [3]. At the same time, it is necessary to remember about the necessary condition for surfacing, namely, maintaining a stable arc process. In order to do that, the electrode wire feed speed should be equal to the speed of its melting so, that during surfacing no short circuits or breaks of welding arc can occur [5, 7].



Figures 1. Effect of arc surfacing mode parameters on bead shape [5]: *a* — current; *b* — voltage; *c* — speed



Figures 2. Appearance of specimens after surfacing using wires with the diameter: *a* — 1.2; *b* — 1.6; *c* — 1.8; *d* — 2.0 mm

The current of surfacing is closely related to the electrode wire feed speed, and with increase in the latter, the current of surfacing increases proportionally. At a constant surfacing speed this leads to an increase in the volume of metal deposited, getting to the surface deposited in a unit of time, which should result in changing the geometric characteristics of depositing beads. In industrial practice, in arc surfacing of different parts, the electrode wire feed speed usually does not exceed 200 m/h, and the feed mechanisms of the most existing surfacing equipment and automatic devices are designed for this value, which does not exceed 450 m/h [1].

The aim of this work is to study the effect of electrode wire feed speed (current of surfacing) on penetration depth of base metal, SBM and formation of deposited beads during arc surfacing.

To study the effect of wire feed speed on penetration depth of base metal in arc surfacing, a series of experiments on surfacing of single beads with flux-

cored wires of 1.2; 1.6; 1.8 and 2.0 mm diameters under flux was conducted. The feed speed was controlled in the range from the minimum value $V_{f,min}$, at which a stable arc process was possible for these conditions, and to the maximum value $V_{f,max} = 450$ m/h, which, as was mentioned above, was determined by the characteristics of the used surfacing installation U-653 completed with the power source VDU-506.

Surfacing with all four flux-cored wires was carried out at a constant speed of surfacing $V_s = 27$ m/h. The arc voltage also remained constant during surfacing with a wire of the same diameter: for the wire with a diameter of 1.2 mm it was 22 V; for the wire with a diameter of 1.6 mm it was 24 V and for the wires with a diameter of 1.8 and 2.0 mm it was 26 V. The appearance of specimens after surfacing is shown in Figure 2.

In the process of surfacing, the values of wire feed speed and the value of current, which corresponded to the first ones, were fixed. From deposited billets,

Table 1. Effect of wire feed speed on the formation of deposited beads and penetration depth of base metal in surfacing using the wire of 1.2 mm diameter


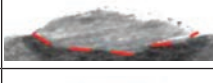




V_f , m/h	I_s , A	Dimensions of deposited beads, mm			γ_0 , %	Macrosections of cross-section of beads
		width	height	depth		
210	110	5.9	1.6	0.87	33	
260	130	7.6	1.7	0.91	34	
310	150	7.8	1.9	0.68	29	
360	160	7.9	1.9	0.92	31	
405	170	8.1	2.1	1.13	33	
450	190	8.5	2.2	1.17	31	

Table 2. Effect of wire feed speed on the formation of deposited beads and penetration depth of base metal in surfacing using the wire of 1.6 mm diameter

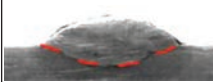


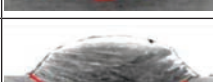

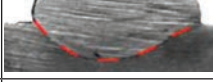

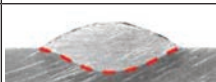
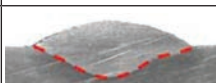


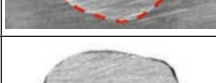
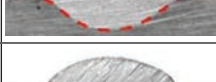
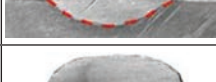
V_f , m/h	I_s , A	Dimensions of deposited beads, mm			γ_0 , %	Macrosections of cross-section of beads
		width	height	depth		
175	170	6.7	1.6	1.24	41	
210	190	7.1	2.1	1.45	38	
260	220	8.2	2.3	1.85	40	
310	260	7.8	2.5	2.49	46	
360	290	7.4	3.6	2.21	35	
405	320	9.9	3.5	3.04	40	
450	350	8.5	3.9	4.6	47	

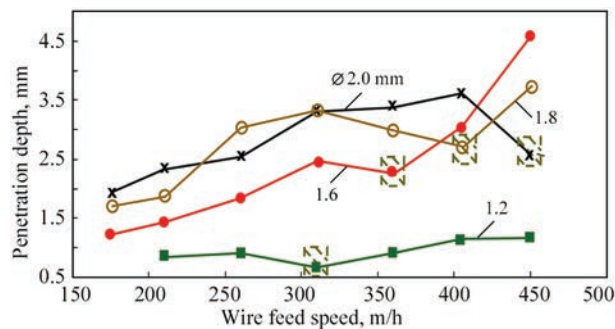
Table 3. Effect of wire feed speed on the formation of deposited beads and penetration depth of base metal in surfacing using the wire of 1.8 mm diameter

V_f , m/h	I_s , A	Dimensions of deposited beads, mm			γ_0 , %	Macrosections of cross-section of beads
		width	height	depth		
175	200	9.9	1.7	1.74	48	
210	240	10.9	1.9	1.86	45	
260	280	9.9	3.2	3.04	45	
310	310	9.7	3.3	3.35	46	
360	330	9.3	3.6	2.99	38	
405	360	9.3	3.7	2.70	38	
450	390	8.7	3.8	3.74	39	

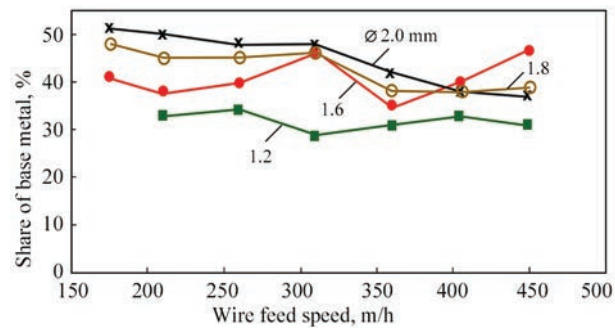
transverse macrosections were manufactured, on which the width and height of deposited beads, penetration depth were measured, as well as SBM was calculated. Macrosections of cross-sections of deposited beads and their dimensions are given in Tables 1–4.

Based on the obtained data, the dependences of the effect of electrode wire feed speed on penetration depth of base metal (Figure 3) and SBM (Figure 4) were plotted. It was established that with an increase in electrode wire feed speed, the height of deposited bead increases, penetration depth and also the width of bead varies slightly (Figure 3, Tables 1–4). At the same time, with the increase in the diameter of the applied flux-cored wire, these dependences grow. Thus, for example, for the wire with a diameter of 1.2 mm, an increase in the wire feed speed from 210 to 405 m/h leads to a growth in the height of the bead by 1.3 times, and for the wire with a diameter of 2.0 mm, the same parameter in the same range of feed speeds is increased by 2.4 times, which is associated with a proportional increase in the volume of deposited metal per a unit of the bead length.

At a gradual increase in the wire feed speed, and, consequently, in the value of welding current from the minimum possible value, at which a stable process



Figures 3. Effect of wire feed speed on penetration depth: shading indicates the area of decreasing penetration depth with increasing current



Figures 4. Effect of feed speed of electrode wire of different diameters on SBM

is observed, to the maximum value, provided by the feed mechanism of the installation, a slight decrease in SBM is noted for almost all the diameters of the tested wires (Figure 4). This is explained by the fact that with an increase in current and the wire feed



Figures 5. Appearance of 3 mm thick steel sheet prepared for surfacing (a) and a fragment of deposited sheet (b)

Table 4. Effect of wire feed speed on the formation of deposited beads and penetration depth of base metal in surfacing using the wire of 2.0 mm diameter

V_f , m/h	I_s , A	Dimensions of deposited beads, mm			γ_0 , %	Macrosections of cross-section of beads
		width	height	depth		
175	250	11.7	1.7	1.94	51	
210	290	11.9	1.9	2.34	50	
260	320	12.0	2.3	2.57	48	
310	350	10.2	2.6	3.32	48	
360	380	8.8	3.7	3.4	42	
405	410	9.2	4.4	3.6	38	
450	450	9.7	4.7	2.57	37	

speed at a constant surfacing speed, the growth rate of the area of deposited metal significantly exceeds the growth rate of the penetration area, and the deposited beads obtain a «mushroom-like» shape. This is especially peculiar during surfacing using flux-cored wires with a diameter of 1.6 mm and more.

At the same time, it was established that in surfacing using the wire of each diameter, a certain range exists, where the proportionality of wire feed speed effect on penetration depth is violated. In this range, with increase in the feed speed (at rising current), a decrease in the penetration depth occurs (Figure 3, dashed areas).

This dependence is the most significantly pronounced in surfacing with a wire of 1.2 mm diameter. In case of surfacing at the electrode wire feed speed $V_f = 310$ m/h, not only a decrease in penetration depth by 25 % is observed as compared to surfacing at a feed speed $V_f = 260$ m/h, but also the minimum value of penetration (0.68 mm) for the entire investigated range of wire feed speeds are observed. Also, for surfacing with a wire of 1.2 mm diameter at the feed speed $V_f = 310$ m/h, the SBM is characterized by a decrease from 34 to 29 %, which is also the minimum value for the whole investigated range.

It was also noted that the larger the wire diameter, then a decrease in penetration depth is observed at the

higher feed speed. Thus, for the diameter of 1.2 mm, this effect is pronounced at a feed speed of 310 m/h; for the diameter of 1.6 mm — at 360 m/h; for the diameter of 1.8 mm — at 405 m/h; and for the diameter of 2.0 mm — at a speed of 450 m/h.

However, in this case the values of current density J , at which this phenomenon is observed, are in a narrow range for all the investigated diameters of electrode wire: for the diameter of 1.2 mm the current density is $J = 136 \text{ A/mm}^2$, for the diameter of 1.6 mm $J = 144 \text{ A/mm}^2$; for the diameter of 1.8 mm $J = 142 \text{ A/mm}^2$, and for the diameter of 2.0 mm $J = 143 \text{ A/mm}^2$. The average value of current density for all the diameters is $J \approx 140 \pm 4 \text{ A/mm}^2$. Obviously, in this case, the favourable heat balance of the surfacing process is established, in which the growth in the area of deposited metal is higher than the growth in the area (depth) of penetration. The results obtained in this work are protected by the patent of Ukraine [9].

Surfacing at increased flux-cored electrode wire feed speeds was successfully applied in wear-resistant arc surfacing of 3 mm thick steel sheets. It is known [10] that one of the main problems in surfacing sheets of such a thickness is the probability of arising burn-outs in the process of surfacing.

Surfacing of sheets with the dimensions of $3 \times 200 \times 300 \text{ mm}$ was performed with a flux-cored wire of 1.2 mm diameter under the flux at the mode: $V_f = 310 \text{ m/h}$ ($I = 150 \text{ A}$), $U = 22 \text{ V}$, $V_s = 30 \text{ m/h}$, overlapping of the neighbouring beads is $\approx 50 \%$. To reduce deformation of sheets in the process of surfacing, a device with a cooled copper table was used, on which the sheets were fixed with the help of hold-down straps. The appearance of the sheet prepared for surfacing and fixed in the fixture is shown in Figure 5, *a*; and the appearance of a fragment of a deposited sheet is shown in Figure 5, *b*. The control confirmed the quality formation of deposited metal and the absence of surfacing defects in the form of burn-outs, pores, cracks and other defects.

Conclusions

1. In arc surfacing using high wire feed speeds, for each diameter of the wire such an optimal ratio of value of feed speed and other surfacing parameters exist,

at which its increase leads to a decrease in penetration depth and SBM at a rising current of surfacing.

2. The values of current density J , at which a decrease in penetration depth is observed, for all investigated diameters of electrode wire are in a narrow range: for the diameter of 1.2 mm, $J = 136 \text{ A/mm}^2$; for the diameter of 1.6 mm, $J = 144 \text{ A/mm}^2$; for the diameter of 1.8 mm $J = 142 \text{ A/mm}^2$ and for the diameter of 2.0 mm $J = 143 \text{ A/mm}^2$. The average value of the current density for all diameters is $J \approx 140 \pm 4 \text{ A/mm}^2$. In this case, a favourable heat balance of the surfacing process is established, in which the growth in the area of deposited metal is higher than the growth in the area (depth) of penetration.

3. The results of investigations were successfully used in the development of technology for wear-resistant arc surfacing and of 3 mm thick steel sheets under the flux. The control confirmed the quality formation of deposited metal and the absence of surfacing defects in the form of burn-outs, pores, cracks and other defects.

1. Ryabtsev, I.A., Senchenkov, I.K. (2013) *Theory and practice of surfacing works*. Kiev, Ekotekhnologiya [in Russian].
2. Pokhodnya, I.K., Suptel, A.M., Shlepakov, V.N. (1972) *Flux-cored wire welding*. Kiev, Naukova Dumka [in Russian].
3. Yuzvenko, Yu.A., Kirilyuk, G.A. (1973) *Flux-cored wire surfacing*. Moscow, Mashinostroenie [in Russian].
4. Babinets, A.A., Ryabtsev, I.A., Panfilov, A.I. et al. (2016) Influence of methods of arc surfacing with flux-cored wire on penetration of base metal and formation of deposited metal. *The Paton Welding J.*, **11**, 17–22. <https://doi.org/10.15407/as2016.08.01>
5. Frumin, I.I. (1961) *Automatic electric arc surfacing*. Kharkov, Metallurgizdat [in Russian].
6. Akulov, A.I., Belchuk, G.A., Demyantsevich, V.P. (1977) *Technology and equipment of fusion welding*. Moscow, Mashinostroenie [in Russian].
7. Panteleenko, F.I., Lyalyakin, V.P., Ivanov, V.P. (2003) *Restoration of machine parts: Refer. Book*. Ed. by V.P. Ivanov. Moscow, Mashinostroenie [in Russian].
8. Ivanov, V.P., Lavrova, E.V. (2016) Controlling penetration zone formation in arc surfacing. *The Paton Welding J.*, **8**, 2–6. <https://doi.org/10.15407/as2016.11.04>
9. Ryabtsev, I.O., Babinets, A.A., Lentugov, I.P. (2018) Method of submerged-arc surfacing with flux-cored wire. Pat. 127598, Ukraine [in Ukrainian].
10. Babinets, A.A., Ryabtsev, I.A. (2017) Flux-cored wire for wear-resistant surfacing of thin-sheet structures. *The Paton Welding J.*, **1**, 54–57. <https://doi.org/10.15407/as2017.01.10>

Received 28.12.2018

WELDABILITY OF ELECTROSLAG REMELTED HIGH-CARBON STEEL AT FLASH-BUTT WELDING

A.A. POLISHKO, L.B. MEDOVAR, A.P. STOVPCHENKO,
E.V. ANTIPIN, A.V. DIDKOVSKY and A.Yu. TUNIK

E.O. Paton Electric Welding Institute of the NAS of Ukraine
11 Kazimir Malevich Str., 03150, Kyiv, Ukraine. E-mail: office@paton.kiev.ua

The paper presents the results of examination of the structure and properties of samples of rail metal produced by laboratory melting (in slightly deformed and cast state), which were obtained by electroslag remelting after flash-butt welding of rails. Examination showed that the microstructure of weld metal and heat-affected zone in both the cases features a homogeneous dense structure. Fracture of the samples took place mainly in the heat-affected zone. Strength of welded joints from metal in the cast state is lower, than that of slightly deformed one, which is apparently caused by coarse grains, the size of which can be reduced using heat treatment. Electroslag remelted rail steel in the cast and slightly deformed state has a level of mechanical properties in the range of requirements made to nonthermostrengthened rails K76 in GOST R 51045 and DSTU 4344 that reveals the prospects for application of electroslag remelting for manufacture of rails, including rail tongues, applied in as-cast state. 25 Ref., 3 Tables, 7 Figures.

Keywords: *flash-butt welding, rail steel, electroslag remelting, slightly deformed and cast metal, welded joint, metallographic studies, mechanical properties*

A current tendency in development of the railways is increasing the speed of the traffic, organizing which for passenger trains required making changes in technical equipment of the track and technologies of rail production and joining [1]. In the railways of Ukraine laying of new generation high-strength rails K76F (DSTU 4344:2004), 76F (GOST R 51045–97), and, not so long ago, R35HT (EN 13674-1:2011 + A1:2017) has been performed recently for the especially loaded sections of the railway track [2]. All these rails were produced in converters with subsequent ladle treatment and, furtheron, continuous casting and rolling of steel. In view of the absence of modern beam rail mill at PJSC MK «Azovstal» (Mariupol, «Metinvest») local rails do not quite meet the current requirements (small length and low resistance, which is practically two times lower than that of foreign samples) [3, 4]. Imported rails on average can stand passage of approximately 800–1000 million gross tons of cargo in the track before replacement, compared to 450–500 million gross tons for the domestic rails [5].

In order to reduce rail damage at their interaction with the rolling stock wheels, high hardness, wear resistance, contact fatigue strength of the head metal and at the same time, ductility, toughness, alternating load resistance of the rail web and foot should be ensured [6].

With this purpose, rail steels are subjected to ladle and vacuum treatment. However, despite the deep refining of steel, the nonmetallic inclusions (NMI) of

unfavourable morphology often are the cause for rail failure [7–9]. So, VNIIZhT [10, 11] investigations revealed that fracture toughness is influenced, primarily, by inclusion shape and size, their nature and distribution in steel.

PJSC MK «Azovstal» researchers showed that the most hazardous are sharp-angled inclusions of titanium nitrides and similar ones, as well as coarse inclusions of aluminium oxide and their clusters, which are the products of deoxidation and microalloying of rail steel, that led to a change of rail production technology [12, 13].

Electroslag remelting process is an effective method to remove NMI and change their morphology to a more favorable one [14, 15]. At present an extensive package of studies of NMI in ESR metal has been performed, which showed that at remelting under fluoride-oxide slags the quantity of NMI in the ingot metal is much lower, than that in the initial electrode, due to metal refining from sulphur and inclusion assimilation by slag [16–18].

It is known that modern rails are produced from continuously cast billets by subsequent rolling. The casting speed in CCMB depends on the billet section and may reach several meters per minute. A high speed of casting the continuously cast billet leads to formation of a deep liquid well, where feeding to replenish shrinkage is limited. This leads to segregation and porosity defects. However, it is not possible to significantly reduce the casting speed, as the menisk

Table 1. Comparison of rail welding processes [23]

Welding process	Welding time, min	Equipment		Operator skills	Weld quality
		Initial investment	Mobility		
FBW	2–4	Large	Low	Not required	Excellent
Gas pressure welding	5–7	Large	Medium	Required	Excellent
Thermit	30	Not large	High	Not required	Good
Electric arc	60	Not large	High	Required	Good

cools down and the billet surface quality deteriorates. Contrarily, at electroslag remelting (ESR) a very dense metal structure can be produced, but the ESR process efficiency is much lower and the process cost in this case is much higher, than that of continuous casting. Proceeding from world experience of ESR application, it can be anticipated that increase of rail cost at their production by ESR method using consumable electrodes, will not exceed \$ 100–300 per ton.

Works on producing sound rail metal by ESR were started at the E.O. Paton Electric Welding Institute of NASU together with PJSC MK «Azovstahl» as far back as in 1980s. Test batch of rails from ESR steel has passed full-scale testing in VNIIZhT experimental ring of 400 m radius along a curve, which is installed on wooden sleepers. Testing showed that fatigue life of rails from ESR steel is 3.4–4.7 times higher than that of the compared ones [19]. However, two times increase of the rail cost became the main obstacle to ESR application at that time. In order to assess the advantages of ESR metal for various critical applications, we conducted experimental melts [20, 21] and a package of studies of template metal quality in the cast state, after slight deformation and in butt welded joints.

The objective of the work is evaluation of applicability of ESR rail metal (in slightly deformed state and cast state) for a rail track joined by flash-butt welding, based on a complex of studies of the structure and properties of samples of a laboratory melt.

Rail welding. Kinds of processes. Rail joining into sections and then into the track is performed by welding, in order to reduce the number of butt joints and reach the maximum smooth running. Moreover, the impact of the wheel when rolling over the rail butt joint, leads to premature wear of their ends. The authors of work [22] showed that in the railroads with the predominant passenger train traffic (SNCF, HSPC, NS, DB, EJR) the number of defects in welded joints is equal from 5 up to 30 % of their total quantity, and in the railways for freight traffic (SPOORNET, HH1, HH2) and mixed traffic (BRANVERKET) a greater number of defects is observed exactly in welded joints (from 15 up to 60 %). Therefore, special attention should be given to weld quality.

Four main welding technologies, ensuring the safety and reliability of rail welded joints, are ap-

plied in the world for joining rails of high-speed and heavy-duty trunk railways. These are flash-butt (FBW), gas-pressure, thermit and electric arc welding [23] (Table 1).

Each of the considered processes of rail welding features its «pros» and «cons». In Ukraine, FBW is mainly used for welding rail steels, which is also widely applied abroad, as it meets the most stringent modern requirements to continuous rail tracks.

Procedure of producing electroslag metal samples, their flash-butt welding and metallographic studies. The metal for the experimental program was produced by the traditional electroslag process under laboratory conditions in a 3 t furnace with ingot drawing at drawing speeds of 20 and 40 mm/min. K76F rail (up to 0.82 % carbon content) from commercially produced steel (DSTU 4344:2004) was used as a consumable electrode. ANF-28M slag of the following composition, wt. %: 47 CaF₂; 3 Al₂O₃; 21 CaO; 11 MgO; 18 SiO₂ was applied. ESR ingots of 180 mm diameter were produced, from which templates were cut out in the cast state for welding. Part of metal of ESR rail steel ingots was rolled into a strip with blank heating up to 1050 °C temperature. Degree of deformation was 4:1, as the capacity of the laboratory mill used for rolling, was limited.

For comparative evaluation of the quality of welded joints of electroslag casting rail steel on samples (plates) with cross-sectional area of 1020 mm² from cast and slightly deformed metal, FBW was conducted by continuous flashing technology. The welding mode was selected in keeping with the parameters specified in TU U 24.1-40075815-002:2016 for R65 rails [24, 25]. Flashing duration, which is equal to 180 s for R65 rails, was taken as the main parameter, determining the energy input.

Metallographic studies were conducted in Neophot-32 microscope, fitted with QuickPhoto digital photography attachment. Obtained images were processed by «Atlas» program at 25–500 times magnification in the light field. To reveal the microstructure, the sections were etched in 5 % nitric acid solution.

Mechanical testing of cast and deformed metal of ESR rail steel, as well as their welded joints, was conducted by a standard procedure, in keeping with the requirements of GOST 1497–84 and GOST 6996–66,

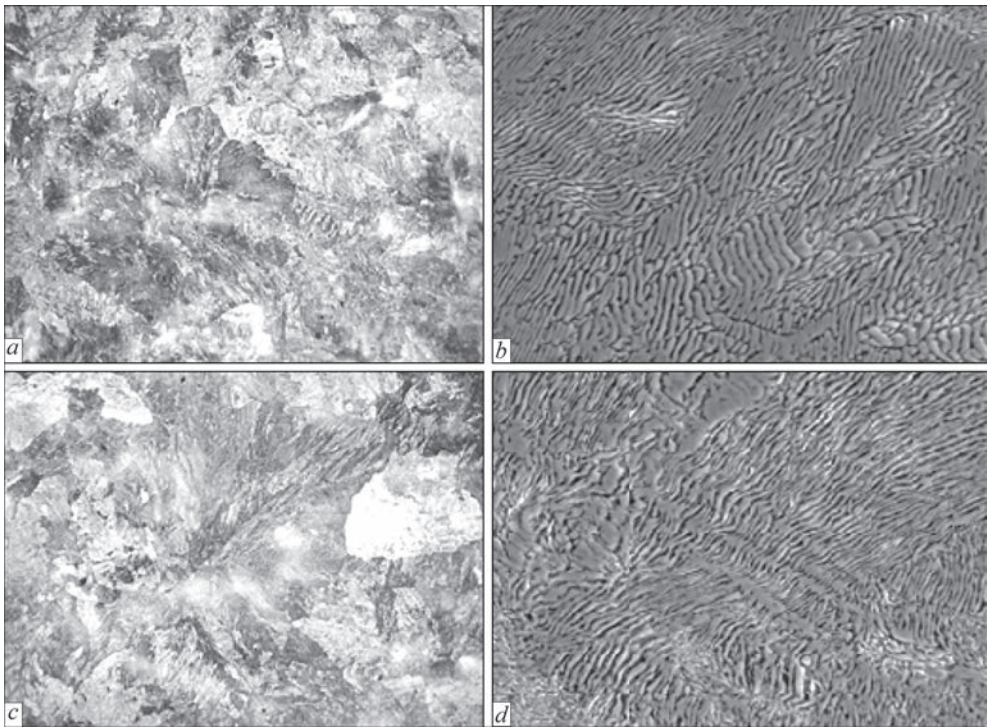


Figure 1. Microstructure ($\times 100$): optical (*a*, *b*) and SEM (*b*, *d*) of samples of metal of model ESR ingots formed with different drawing speed: *a*, *b* — 20 mm/min; *c*, *d* — 40 mm/min

for static (short-time) tension on samples of Mi3 and Mi18 type in MTS 318.25 machine (USA) with processing in TestWorks4 (MTS) software, providing a sufficient accuracy of the results ($\pm 0.5\%$)

Investigations of the structure and properties of cast and deformed metal of ESR ingot. Metal of ESR rail steel ingots has a homogeneous dense structure. No defects were found. The size of pearlite grains in ESR ingot at the drawing rate of 20 mm/min is equal to 100–120 μm , that of subgrains is 20–30 μm , whereas the size of pearlite grains in the ingot, produced at the drawing speed of 40 mm/min, is up to 80–100 μm , that of subgrains is 10–15 μm . Thus, even a small lowering of metal feed rate at gradual formation of the ingot has a positive influence on its structure. Density is also increased due to improvement of feeding to replenish shrinkage that promotes avoiding the central ingot heterogeneity.

Metal of both the ESR ingots has a typical homogeneous pearlite microstructure with thin cementite lamels (Figure 1). Measurements of interlamellar distance in pearlite showed close results for metal of both the ingots (0.74 and 0.56 μm for ingots with drawing speed of 20 and 40 mm/min, respectively). Pearlite

dispersity in the ingot metal after ESR is smaller than that usually observed in rail steel samples after deformation and heat treatment (about 0.2 μm). It should, however, be taken into account that this is cast metal without deformation or heat treatment.

Results of spectral chemical analysis of metal before and after electroslag remelting are given in Table 2. Analysis of element content shows correspondence to K76F steel grade composition, according to DSTU 4344:2004. Lowering of silicon and sulphur content is observed.

Welding of templates from cast and slightly deformed (further on — deformed) ESR rail steel was performed in K1000 stationary machine, developed by PWI, in the same modes. Butt welded joints of plates 350–400 mm long after flash removal were cut into samples for comprehensive metallographic studies and mechanical testing, in order to assess the produced joint quality.

Cast metal templates for welding were assembled so that FBW joints formed in the longitudinal section of model ESR ingots with two variants of crystal growth direction: in the direction of growth (butt welded joint connects the central parts of the longi-

Table 2. Chemical composition of rail steel K76F before and after ESR

Grade	Standard	Element content, wt. %						
		C	Mn	Si	V	Al	P	S
K76F	DSTU 4344:2004	0.71–0.82	0.8–1.3	0.25–0.45	0.03–0.07	0.025	0.035	0.04
	After ESR	0.76	0.93	0.11	0.05	0.020	0.035	0.020

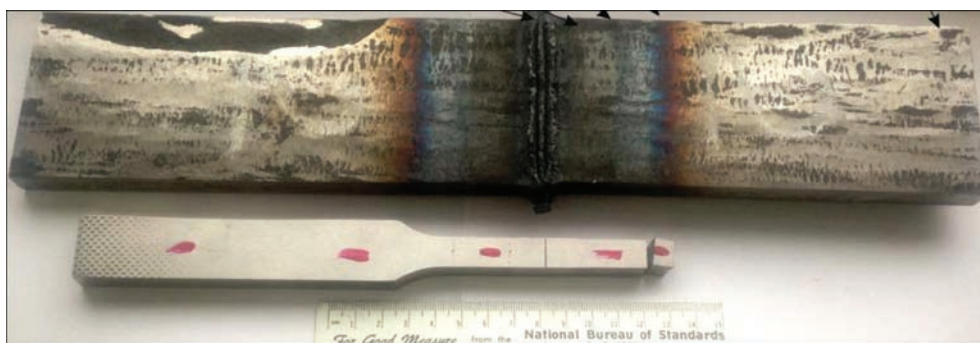


Figure 2. Welded butt joints of deformed ESR metal

tudinal templates) and with rotation through 180° so that the butt joint connected the worst zones of ESR ingot, namely the head and bottom parts. Deformed metal was welded along the rolling direction. Figure 2 shows the general view of the welded joint. Flash of 13–25 mm width, and 12–13 mm height formed on the surface of welded butt joints. The width of welded joint HAZ is up to 30 mm to each side.

Metal structure in all the ESR rail steel butt joints is ferrite-pearlite, with zones characteristic for welded joints (Figure 3). Microstructure of welds from cast and deformed metal is homogeneous and consists of equiaxed grains of approximately the same size.

Cementite precipitation is observed along the grain boundaries in weld metal (Figure 3, *a, d*), which is more pronounced for the cast metal welds. It is natural, as the characteristic pattern is found also in the structure of ESR metal — base metal of the welded joint (Figure 3, *c*). In the HAZ, the structure of both the cast and deformed metal is practically identical due to recrystallization under the impact of the temperature cycle of welding. In the HAZ region, cemen-

tite fringes are located not around the grain contour, but as fragments, as a result of grain refinement.

The grain size of cast ESR metal was evaluated in all the welded joint zones (using Tescan computer program). It is found that in the butt joints of cast templates the average grain size is equal to $87\ \mu\text{m}$, $60\ \mu\text{m}$ in the HAZ, $85\ \mu\text{m}$ in the weld, and in butt joints of deformed metal it is 54, 61 and $87\ \mu\text{m}$, respectively.

Results of mechanical testing of the cast and deformed ESR metal before welding and of FBW joints are given in Table 3.

Ultimate strength values for cast ESR metal after heat treatment are lower by 10 %, as are its ductile properties that is due to the stressed state of metal in the cast state, which can be relaxed by heat treatment. At the same time, in both the cases, these values are in the range of requirements made of nonthermostrengthened K76 rails, in keeping with GOST R 51045–97.

Evaluation of mechanical properties of metal in FBW joints of ESR rail steel showed no anisotropy of the ingot metal (head-bottom) (see Table 3). Sample

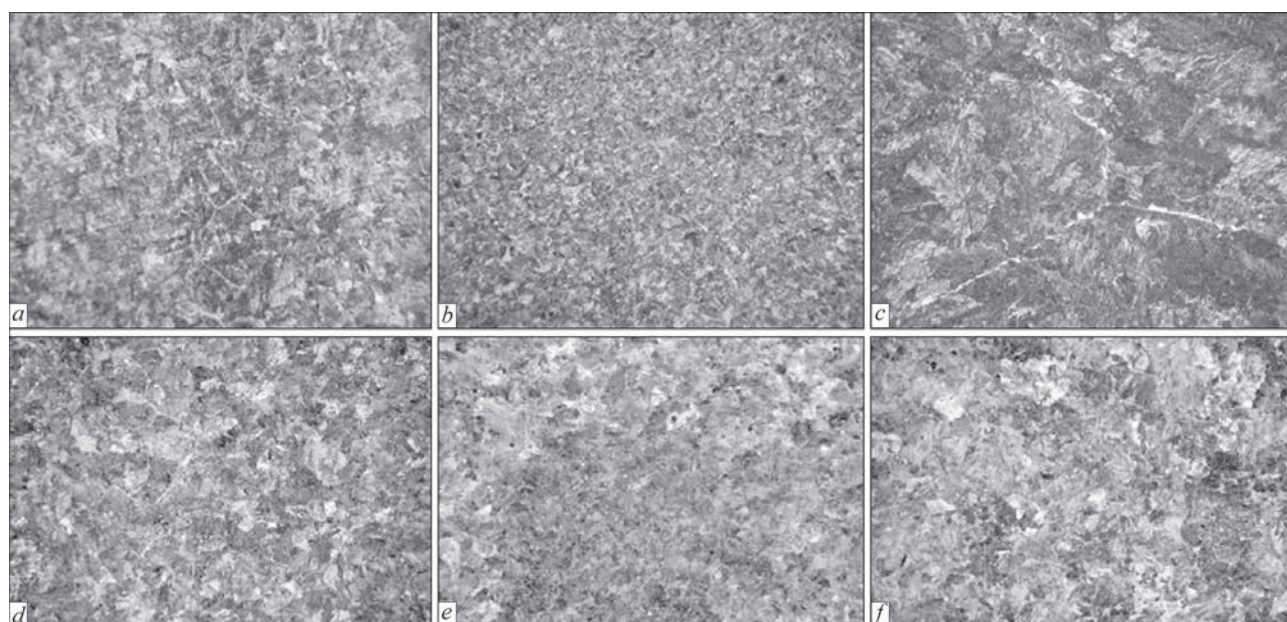


Figure 3. Microstructure ($\times 100$) of welded joint of cast (*a–c*) and deformed (*d–f*) metal of ESR rail steel: *a, d* — weld; *b, e* — HAZ; *c, f* — BM

Table 3. Mechanical properties of cast and deformed metal of ESR rail steel before welding and of FBW joints

Metal state		σ_p , MPa	δ , %
Before welding	Cast	871–887	2–3
	Deformed	954–959	4–5
After FBW	Cast	647–795	2–3
	Deformed	989–995	4–5
GOST R 51045–97		780 (for nonthermo-strengthened)	3

fracture occurred in the HAZ, and in some of the samples — in the base metal, that in our opinion is related to the hereditarily coarse grains in the cast ESR metal. The strength level of butt joints of cast ESR metal is, on average, 27 % lower than that of the wrought one, and its ductility is also lower. At the same time, a significant refining of the structure, observed in HAZ metal, confirms the need for application of heat treatment to improve the properties of cast ESR metal.

Fracture of butt joints of FWB templates of ESR metal after deformation occurred in the HAZ metal at 45–55 mm distance from the fusion line (see Figure 2). Strength and ductility index of the welded joint are somewhat higher than those for the initial deformed ESR metal (Table 3), that may be due to different size of samples and measurement accuracy.

Fractographic analysis of fracture surfaces showed the mixed nature of fracture in the cleavage and displacement modes for all the studied variants. Fracture initiated by the cracking mechanism, and ended by quick

development of complete fracture, that is indicated by presence of ductile component in the complete fracture section (Figure 4, *a, b*). The main part of the fracture surface is represented by the brittle component that is characteristic for the high-strength rail steels, the dimensions of cleavage being larger in cast steel samples that corresponds to larger size of the grains.

ImagePro computer program was used to evaluate the fraction of the ductile component on fracture surfaces of cast and deformed metal welded joints (Figure 5). Content of the ductile component in cast ESR metal is up to 18 %, in cast metal welded joint it is 16 %, and in the deformed metal it is 24 and 23 %, respectively. Higher content of the ductile component in the deformed metal is due to grain refinement.

At surface examination, the ductile component looks different by its darker gray colour and mat surface, but by its chemical composition it does not differ from the brittle component (Figures 6, 7).

Inclusions of manganese sulphide and aluminium oxide were found on the ductile component surface, and predominantly manganese sulphide inclusions were observed in the brittle component.

Metallographic studies of the cast and deformed ESR metal showed that heating before rolling and slight deformation of metal (degree of deformation of 4:1) provided 1.5 times refinement of the size of metal grains. This difference is leveled out in the HAZ and weld metal of butt joints. However, the large grain size in rail steel of the electros slag ingot (in the cast

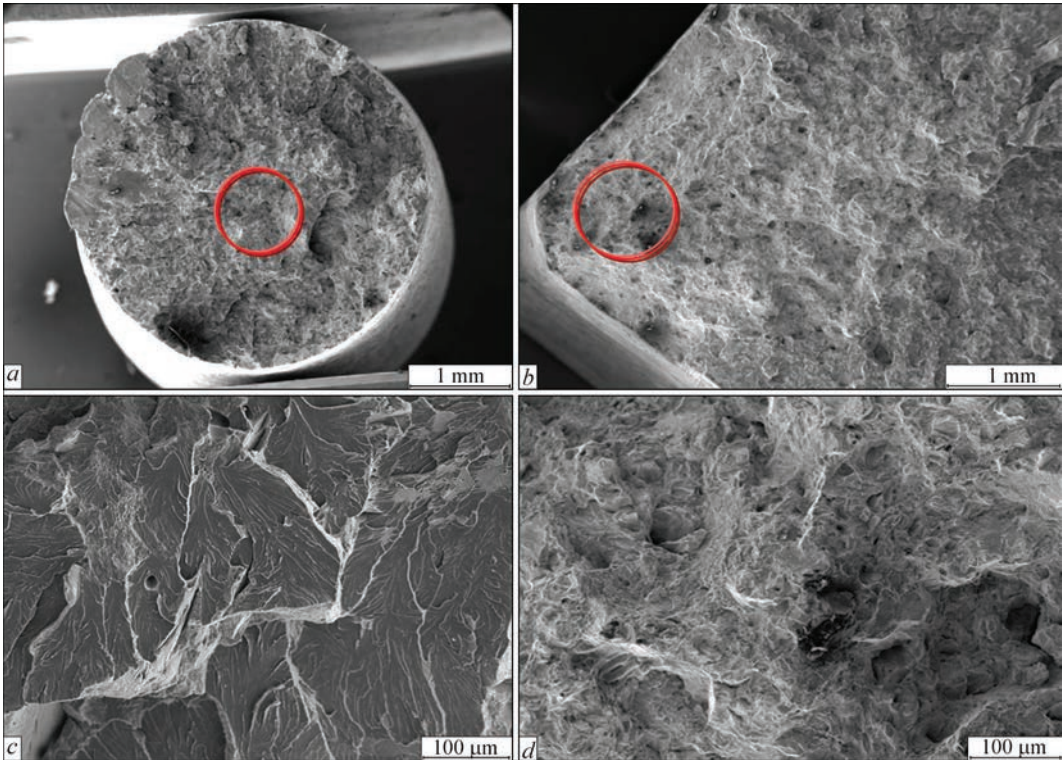


Figure 4. Macro- (*a, b*) and microfractograms (*c, d*) of welded joint fracture surfaces after mechanical tests of the cast (*a, c*) and deformed (*b, d*) ESR metal

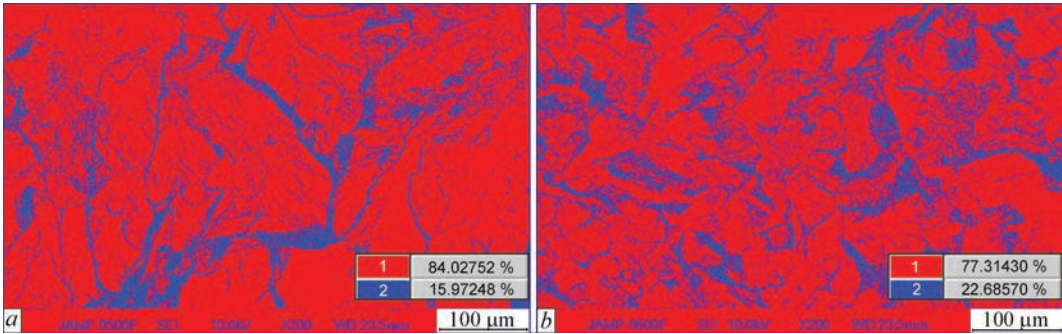


Figure 5. Ductile component of fracture surface of welded joint of cast (a) and deformed (b) metal of ESR rail steel: 1 — brittle component; 2 — ductile component

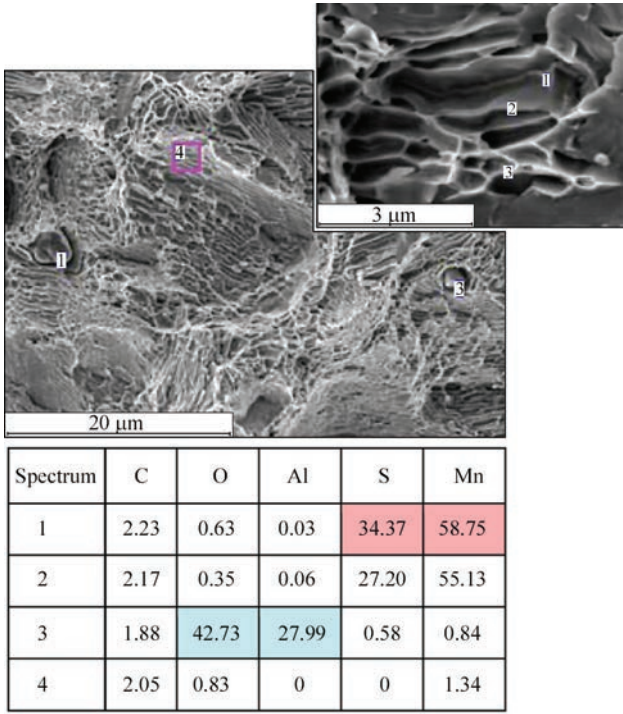


Figure 6. Microfractogram of ductile component of fracture surface of ESR rail steel metal

state) impairs the welded joint properties that can be changed by application of heat treatment. Development of heat treatment modes will be the subject of a separate study.

In conclusion it should be noted that ESR rail steel in the cast and deformed state has a dense and homogeneous structure with a set of properties within the range of requirements, made of non-thermostrengthened K76 rails by GOST R 51045 and DSTU 4344, that opens up the prospects for manufacture of rails, including rail tongues, applied in the as-cast state.

ESR rail steel in the cast and slightly deformed state can be welded by flash-butt welding. Testing of metal of flash-butt welded joints of rail steel, produced in the laboratory, showed that the microstructure of the metal of the weld and HAZ in both the cases features a homogeneous dense structure. Sample fracture occurred predominantly in the HAZ. Strength

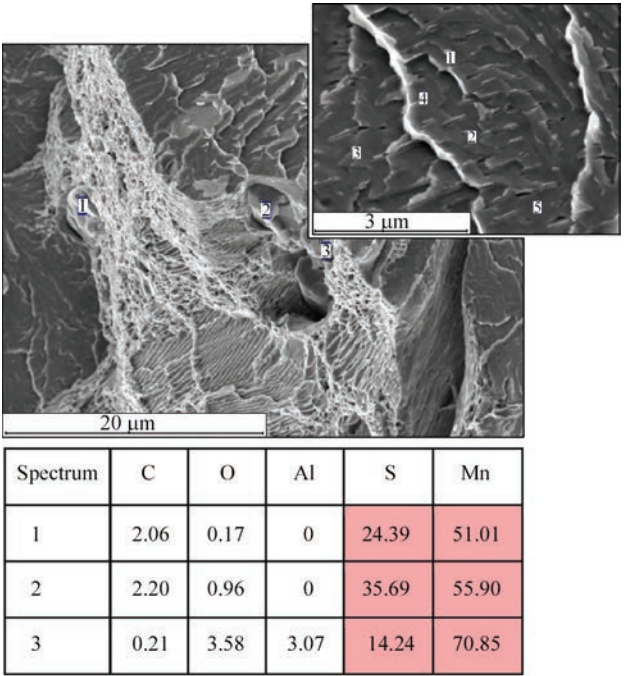


Figure 7. Microfractogram of brittle component of fracture surface of ESR rail steel metal

of welded joints of as-cast metal is lower than that of slightly deformed one that is, apparently, due to the coarse grains, the size of which can be refined by application of heat treatment.

1. Kuchuk-Yatsenko, S.I., Didkovsky, A.V., Shvets, V.I. et al. (2016) Flash-butt welding of high-strength rails of nowadays production. *The Paton Welding J.*, **5–6**, 4–12.
2. <https://mrpl.city/news/view/ukrzeliznytsya-perehodit-narelsy-vysshej-kategorii-kotorye-izgotovleny-azovstalyu>
3. Medovar, L.B., Stovpchenko, G.P., Polishko, G.O. et al. (2018) Modern rail steels and solutions ESR (Review). Information 1. Operating conditions and defects observed. *Sovrem. Elektrometall.*, **1**, 3–8 [in Russian].
4. Medovar, L.B., Stovpchenko, G.P., Polishko, G.O. et al. (2018) Modern rail steels, application of ESR (Review). Information 2. Requirements of standards to chemical composition of steel for railway rails of main-line tracks. *Ibid.*, **2**, 28–36 [in Russian].
5. Pykhtin, Ya., Levchenko, V., Ivanysenko, L. et al. (2009) Analysis of requirements of national standards on quality of railway rails and results of their service endurance. *Standarty-zatsiya, Sertyfikatsiya, Yakist*, **4**, 24–30 [in Ukrainian].

6. Rudyuk, A.S., Azarkevich, A.A., Voskovets, Yu.A. et al. (2011) Defectiveness of rails in Ukrainian railways. *Put i Putevye Khozyajstvo*, **7**, 28–32 [in Russian].
7. Simachev, A.S., Oskolkova, T.N., Temlyantsev, M.V. (2016) Effect of nonmetallic inclusions of rail steel on high-temperature plasticity. *Izv. Vuzov. Chyorn. Metallurgiya*, **59**(2), 134–137 [in Russian].
8. Kuchuk-Yatsenko, S.I., Shvets, V.I., Didkovsky, A.V., Antipin, E.V. (2016) Effect of non-metallic inclusions of rail steel on welded joint formation. *The Paton Welding J.*, **5–6**, 24–28.
9. Shur, E.A., Trushevsky, S.M. (2005) Effect of nonmetallic inclusions on fracture of rails and rail steel. Nonmetallic inclusions in rail steel. In: *Transact. Ekaterinburg, UIM*, 87–90 [in Russian].
10. Shur, E.A., Borz, A.I., Sukhov, A.V. et al. (2015) Evolution of rail damageability by contact fatigue defects. *Vestnik VNIIZhT*, **3**, 3–8 [in Russian].
11. Velikanov, A.V., Rejkhart, V.A., Baulin, I.S., Dyakonov, V.N. (1978) Statistical justification of permissible contamination level of rail steel by stringer nonmetallic inclusions. *Vestnik VNIIZhT*, **8**, 50–51 [in Russian].
12. <https://cyberleninka.ru/article/v/reservy-povysheniya-kachestva-relsov-sovershenstvovanie-tehnologiy-mikrolegirovaniya-relsovoj-stali>
13. Trotsan, A.I., Kaverinsky, V.V., Koshule, I.M., Nosochenko, A.O. (2013) On factors influencing the quality of rail steel and rails. *Metall i Litio Ukrainy*, **6**, 9–14 [in Russian].
14. (1981) *Electroslag metal*. Ed. by B.E.Paton, B.I. Medovar. Kiev, Naukova Dumka [in Russian].
15. Hoyle, G. (1983) *Electroslag processes: Principles and practice*. Elsevier Science Ltd.
16. Medovar, B.I., Emelyanenko, Yu.G., Tikhonov, V.A. (1975) *On mechanism of transformation and removal of nonmetallic inclusions in ESR process of large-section electrodes. Refining remeltings*. Issue 2. Kiev, Naukova Dumka, 73–81 [in Russian].
17. Zherebtsov, S.N. (2004) Peculiarities of metal refining from nonmetallic inclusions in electrosag remelting. *Omsky Naychny Vestnik*, **1**, 75–77 [in Russian].
18. Polishko, A.A., Saenko, V.Ya., Stepanyuk, S.N. et al. (2014) Behavior of non-metallic inclusions in structure of cast electrosag stainless steel of AISI of 316 type. *Sovrem. Elektrometall.*, **1**, 10–18 [in Russian].
19. Beshentsev, A.V., Galushka, A.A., Shur, E.A. (1992) On selection of technological scheme for manufacture of ESR rails in of Metallurgical Combine Azovstal. *Problemy Spets. Elektrometallurgii*, **2**, 22–28 [in Russian].
20. Kayda, P., Medovar, L., Polishko, G., Stovpchenko, G. (2015) ESR possibilities to improve railroad rail steel performance. In: *Proc. of 9th Int. Conf. on Clean Steel (8–10 Sept. 2015, Budapest, Hungary)*.
21. Medovar, L.B., Stovpchenko, A.P., Kaida, P.N. et al. (2016) New approach to the improvement of quality of billets for manufacture of high-strength rails. *Sovrem. Elektrometall.*, **1**, 7–15 [in Russian].
22. Sawley, K., Reiff, R. (2000) Rail failure assessment for the office of the rail regulator. An assessment of railtrack's methods for managing broken and defective rails. P-00-070.
23. Saita, K., Rarimine, K., Ueda, M. et al. (2013) Trends in rail welding technologies and our future approach. *Nippon Steel & Sumitomo Metal Technical Report*, 105.
24. Genkin, I.Z. (1951) Resistance welding of rails. Moscow, Transzheldorizdat. In: *Techn. Refer. Book of railwayman. Put i Putevye Khozyajstvo*, **5**, 378–390 [in Russian].
25. Kuchuk-Yatsenko, S.I., Lebedev, V.K. (1976) Continuous flash-butt welding. Kiev, Naukova Dumka [in Russian].

Received 13.12.2018

XVIII INTERNATIONAL INDUSTRIAL FORUM - 2019

INTERNATIONAL TRADE FAIRS

METAL WORKING
 UKR WELD
 HYDRAULICS PNEUMATICS
 BEARINGS
 UKRUSEC TECH
 UKR FOUNDRY
 UKR AUTOMATIZATION
 PATTERNS, STANDARDS AND INSTRUMENTS
 HOISTING AND TRANSPORTING STOREHOUSE EQUIPMENT
 INDUSTRIAL SAFETY

November
19-22

ORGANIZER:

International Exhibition Centre

General Information Partner:

Exclusive Media Partner:

Technical Partner:

International Exhibition Centre
15 Brovarskyi Ave., Kyiv, Ukraine
“Livoberezhna” underground station

☎ +38 044 201 11 65, 201 11 56, 201 11 58
e-mail: alexk@iec-expo.com.ua
www.iec-expo.com.ua
www.tech-expo.com.ua

APPLICATION OF FLUX-CORED WIRES AT SURFACING, REMELTING AND IN METALLURGY

Yu.M. KUSKOV

E.O. Paton Electric Welding Institute of the NAS of Ukraine
11 Kazimir Malevich Str., 03150, Kyiv, Ukraine. E-mail: office@paton.kiev.ua

The paper presents the history of flux-cored wires appearance and their application as remelted material, both in micro-metallurgy (surfacing), and in large-scale metallurgy (electroslag remelting and foundry). Features of technological processes with flux-cored wire application in each of the considered branches are shown. At present technologies ensuring improvement of metal quality in foundry are developing the most actively. Prospects for flux-cored wires application in surfacing from the viewpoint of improvement of their production technology and development of new compositions of deposited metal have largely been exhausted. Technologies of surfacing in a current-supplying mould have certain potential for a wider application, particularly in the field of producing composite layers. Electroslag remelting of metal, as in the years of its development, is mainly focused on producing ingots of a large mass and diameter with application of monolithic electrodes of a large cross-section. 37 Ref., 1 Table, 5 Figures.

Keywords: *flux-cored wire, arc surfacing, electroslag remelting, ladle treatment*

Flux-cored wire is a structure in form of hollow tube filled with charge of various dispersion and composition. Depending on determined tasks it can be of different diameter and length.

Applicable to welding the first mention of possibility of flux-cored wires use, apparently, shall be considered a proposal of N.N. Benardos on manufacture of electrodes of different design, including in form of «tubular electrodes with a core of various powders» [1]. Beginning of practical application of welding flux-cored wires refers to 1930th.

A series of reasons promoted distribution of arc welding and surfacing using flux-cored wires in comparison with seamless ones:

- need in performance of welding and surfacing of high-alloy and high-carbon steels and alloys, when corresponding doped wires cannot be manufactured in general or believed to be too expensive [1];
- application of self-shielded flux-cored wires allows performing welding without additional expenses for shielding gases and flux;
- surfacing, as well as welding, with self-shielded flux-cored wires is characterized by simplicity, manoeuvrability and low sensitivity to change of external welding conditions [2].

Nevertheless, today in Ukraine portion of flux-cored wires in the structure of production of welding consumables (electrodes, wires, fluxes) makes only 2 % [3].

Such low volumes of flux-cored wires refer particularly to wires designed for performance of welding operations. For arc surfacing, as type of welding technology, their application is more significant. Primary it is related with the need to get wear-resistant de-

posited metal, operation properties of which improve at its increased alloying. In this case, as it was mentioned above, in manufacture of seamless wire there are problems of technological as well as economical order. Some types of surfacing flux-cored wires are presented in Table [4].

Peculiarities of production and technical characteristics of flux-cored wire to a larger extent are determined by design of its cross-section [5]. Designs of tubular, with lap, edge bending, complex section types have found commercial application. The wires of complex section are mainly used as self-shielded. Tubular design with lap is oftenly used in manufacture of surfacing wires. A coefficient of filling (value of core portion in wire) is assumed to calculate in percent. The value of this coefficient for surfacing wires is in the 15–45 % limits.

Solid wire of 3 mm diameter is used as a rule in electroslag welding and surfacing as electrode metal. However, in some cases wire of other diameters (1–2 or 5–6 mm) [6] find application. Common welding equipment allows feeding electrode wires of 3–5 mm diameter. Nevertheless, in the beginning of active investigation and implementation of electroslag process in 1950th there were still different areas using surfacing flux-cored wires. This tendency of limited application of flux-cored wires was preserved in the next years, mainly, in 1970–1980th. Hardfacing with flux-cored wires was used in repair of steel rolls [7], strengthening of cams of pipe stripping machines [8], pressing tools of bearings production and different elements of stamps [9, 10], crushing hammers of aluminum production and grooves of pipe cold rolling mills [11], cutting edges of knives of hot cutting of metal

Flux-cored wires for hardfacing

Type of deposited metal	Typical composition of deposited metal, wt.%							Hardness after hardfacing <i>HRC</i>
	C	Mn	Si	Cr	W	Mo	Other elements	
Open arc hardfacing								
70Kh4M3G4FTR	0.7	3.5	0.5	4.0	—	3.0	1.0V; 0.7B; 0.1Ti	57–62
30Kh4V3M3FS	0.35	0.6	0.9	3.8	2.8	2.8	0.5V	47–50
30Kh5G2SM	0.3	1.6	0.8	5.0	—	0.6	0.2Ti	50–56
90G13N4	0.9	13.0	0.5	—	—	—	4.0Ni	≤ 20
200KhGSR	2.1	1.1	0.9	0.4	—	—	0.8B; 0.1T; 0.17Al	48–56
80Kh20RZT	0.8	—	—	20.0	—	—	3.0B; 0.6Ti	58–67
Submerged-arc hardfacing								
200Kh12M	1.8	0.6	0.6	12.0	—	0.8	—	40–44
10Kh17N9S6GT	0.1	1.8	5.5	17.6	—	—	9.2Ni; 0.15Ti	27–33
25Kh5FMS	0.25	0.6	1.0	5.0	—	1.1	0.4V	42–46
35V9Kh3SF	0.3	0.8	0.9	2.8	9.5	—	0.3V	44–50
30Kh2N2G	0.3	1.2	0.6	1.8	—	—	1.4Ni	42–48
100Kh4G2AR	1.0	2.2	1.3	4.0	—	—	0.2N	55
CO ₂ hardfacing								
80Kh12K4F3V2M2NR	0.8	—	—	12.0	2.0	2.0	4.0Co; 3.0V; 1.0Ni; 0.1B	57–60

and plug noses of pipe rolling plants [12], sealing surfaces of parts of shut-off valves.

Some technologies of electroslag surfacing (ESS) formally can also be considered as one using flux-cored wires of any design as electrodes. Thus, for example, for circumferential surfacing of mill rolls it is proposed to use flux-cored electrode of circular section, in which charge is located not in rolled from strip tube, but between two concentric steel casings [13]. In essence, such a design can be presented as continuous series of tightly mating between themselves separate flux-cored wires.

Regardless the presented above examples of application of flux-cored wires in electroslag surfacing of parts of different designation, it is necessary to note that currently application of seamless wires [14] is preferred. Apparently, it is mainly related with a fear to violate continuous feed of flux-cored wires, having less rigidity in comparison with seamless, through the feeding mechanism of welding apparatus, particularly during long in time surfacings, partial pouring out of charge at low grade manufacture of wires. To some extent it is because of the wish of surfacers to get wear-resistant layers with more uniform distribution of alloying elements in the deposited metal and, respectively, properties. This is particularly important for the cases when insignificant wear of metal of working layer have more effect on product working capacity (for example, in metal to metal friction). Such a concept appeared based on existing opinion that «arc welding and surfacing with solid alloyed electrode provides sufficiently high homogeneity». However, investigations of macroinhomogeneity of metal, deposited with flux-cored wire using electroslag method, showed, that in this case its «sufficient homogeneity» is provided.

New possibilities of application in surfacing of flux-cored wires appeared due to development at E.O. Paton Electric Welding Institute a device representing itself sectional nonconsumable electrode, titled by the developers as current-supplying mould (CSM) [15]. One of the advantages of this device is open slag pool surface and possibility of regulation of its heat state. This allows using in surfacing current-conducting as well as non-current-conducting wires. The perspectives of application of CSM in surfacing with flux-cored wires are proved by works of Volgograd State Technical University [16]. Moreover, currently the main direction in these works is technology of production of composite layers, at which hollow graphite electrode (electrodes) of special design is located in a CSM working zone. Non-current-conducting composite flux-cored wire is supplied in the slag pool through its cavity. From point of view of authors the presence of such electrode allows developing in under-electrode space a local zone of increased temperatures, that promotes uniform melting of metallic shell and filler being a part of flux-cored wire. The filler contains refractory and fusible components in form of metallic powders and wires.

The similar investigations are carried out at the E.O. Paton Electric Welding Institute for the purpose of production of deposited face working layers of high-wear products, for example, mandrels for pipe production. At that it is possible to provide minimum and uniform penetration of base metal. Figure 1 presents the macrosection of billet deposited in CSM of 85 mm diameter using non-current-conducting flux-cored wire PP-Np-25Kh5FMS of 3 mm diameter.*

*Cand. of Tech. Sci. Osin V.V. took part in surfacing.

In ESS with flux-cored wires (at any type of surfacing) the main technological parameter determining the stability of electroslag process and depth of base metal penetration is electrode feed rate [17]. The rate itself depends on many factors, namely diameter and composition of flux-cored wires, slag composition, slag pool temperature, electrical mode of surfacing. It is also necessary to note the effect of surfacing method on process of wire melting. In particular, at ESS using CSM the current-less as well as electrode wires can be fed in the slag pool and, respectively, conditions of their melting will be different. From practical point of view the rate of wire feed shall be selected such as to provide from one side melting in the slag of all its constituents, and on the other, eliminate coming of wire tip in the metallic pool.

A predecessor of method of electroslag melting (ESR) is so-called Kellogg process, proposed in the 1940 in USA by R.K. Hopkins (US patent No.2.191.479). The process was performed by means of arc remelting under layer of slag of tubular electrode, inside which dosed amounts of discrete filler were added in form of ferroalloys, foundry alloys and pure metals (Figure 2). In essence, a tubular electrode is an analogue of flux-cored wire. ESR directly was started from remelting of common welding wires with additional feed in the slag pool of charge materials. In the 1955–1956 works of D.A. Dudko, I.K. Pokhodnya and Yu.A. Sterenbogen showed the possibility of stable electroslag process using the electrodes of comparatively small sections (30–50 mm), later on larger and larger (more than 1000 mm). Remelting of flux-cored wires was used only in series of cases, for example, for evaluation of possibility in production of metal of different composition using electroslag process, in particular, cast irons for the purpose of further application of the results for manufacture of surfacing flux-cored wires [18].

With some assumption the technologies, in which seamless electrode strips (not folded in the tube) with additional feed to the surface of strip of discrete filler (charge) are melted in slag pool, can be referred to the processes of flux-cored wire remelting. At that the strip itself as well as filler shall be made of magnetic materials providing their magnetic adherence and simultaneous addition into the slag pool.

To such original technologies of ESR it is necessary to refer a technology proposed in 1960th by Belgian Cockerill S.A. and Electrotherm S.A. Companies (Figure 3). The main technical direction is the production of large round section ingots of low-alloy steels [19]. A strip of 75×2 mm section and powders with 0.5–3.0 mm particle size are used for surfacing. The

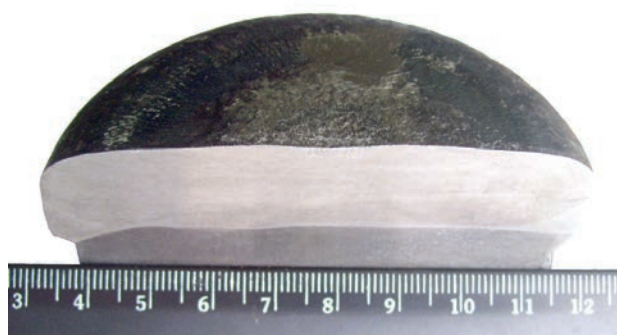


Figure 1. Macrosection of billet deposited with non-current-conducting wire PP-Np25Kh5FMS of 3 mm diameter in CSM of 85 mm diameter

powders can be produced by reduction of oxides of required metals or by means of spraying of a jet of liquid metal by air or water. Relationship of mass of remelted strips and powders makes 30 and 70 %, respectively.

Comparison of this remelting technology (process of CESR — continuous electroslag remelting of powders) with common ESR of electrodes of large section shows its next advantages:

- increase of remelting efficiency;

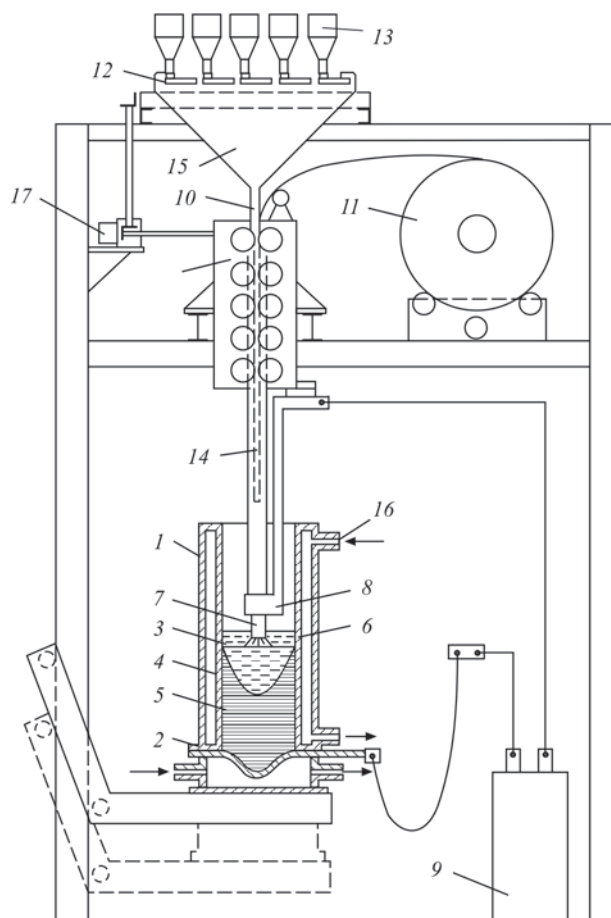


Figure 2. Scheme of Kellogg-process: 1 — mould; 2 — bottom plate; 3 — liquid slag; 4 — liquid metal; 5 — ingot; 6 — electric arc; 7 — consumable tubular electrode; 8 — current lead; 9 — heat source; 10 — tube forming device; 11 — strip coil; 12 — dosage unit; 13 — measuring hopper; 14 — pour out tube; 15 — hopper; 16 — cooling water input; 17 — motor drive

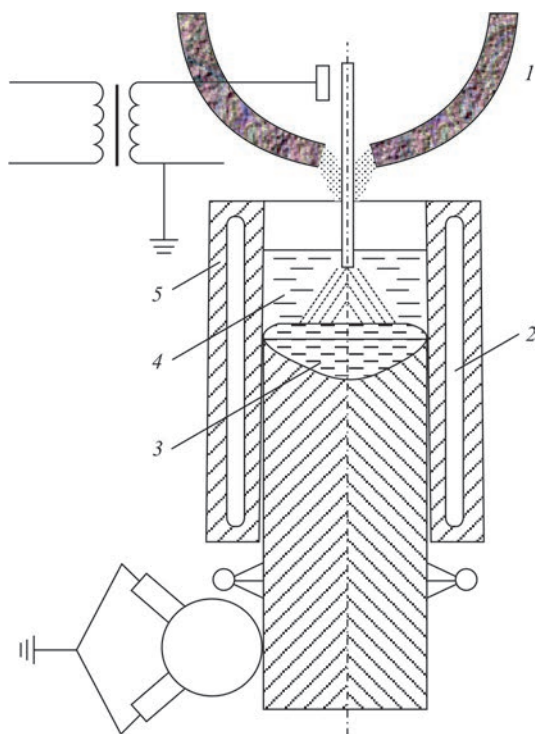


Figure 3. Scheme of CESR process: 1 — powder feeder; 2 — water cooling; 3 — liquid metal; 4 — slag pool; 5 — mould

- production of flatter metallic pool, that in many respects determines metal quality;
- reduction of expenses for production of materials being remelted;
- possibility of melting the ingots of virtually any length.

The perspectives of further application of this technology the authors connect also with the fact that, as practice of melting of 3 and 21 t ingots shows, economic efficiency of process rises with increase of mass of produced ingots [20]. Therefore, the real aim they consider achievement of melting of ingots of 40–50 t mass and more.

The similar technology of ESR with application of strips and powders is used by Electrotherm Corporation Company, USA [21]. The main product of remelting based on this technology is the small ingots of high-alloy steels, in particular, used in the USA tool steels. A scheme of remelting is presented on Figure 3.

This technology of remelting is characterized with some peculiarities. The process is started on a seed, transferring it from arc into electros slag due to strip melting and development of sufficient slag volume. After that, there is continuous feed into the slag pool of strip and powder. The particular requirements are made to strip electrodes and charge. The size of strip is selected taking into account its complete melting in the slag. Stick-out from current lead is of great importance, namely in the case of large stick-out the strip can be overheated (the same as powder) and lose its magnet-

ic properties that effects the melting stability and metal quality. If charge contains nonmagnetic metals, for example Cu, Cr, Ti or some weak-magnetic ferroalloys there can be difficulties in its proper fixing on the strip surface. In this case it is necessary to provide good stirring of components in the mixer, moreover, total amount of nonmagnetic fraction shall not exceed 7–10 %.

There are peculiarities of remelting procedure. Thus, in production of ingots of 100×100 mm size the strip during melting has reciprocating motion in the slag pool. Besides, it is subjected to oscillations in plane normal to its surface.

Modern technology of steel production develops in the direction of application of new metallurgical aggregates (arc furnace, converter) only for melting of solid constituent of the charge and oxidation of carbon, silicon, manganese, i.e. semi-finished product manufacture. Virtually all operations on bringing of melt in accordance with grade requirements on properties and in whole on metal quality are carried out by the processes of ladle refining.

One of the most state-of-the-art and perspective methods of ladle treatment is addition of flux-cored wire in the liquid steel. Based on data from [22] in the beginning of the 1990th around 200 machines for modification with flux-cored wire were operated in the world metallurgical industry. Due to higher technical and economic efficiency of treatment of steel and cast iron by flux-cored wires in comparison with other known methods of liquid metal treatment the tendency to application of this technology in metallurgy continuously rises [23].

Start of application of flux-cored wires in the metallurgy was related with wide application of calcium and calcium-containing materials in steelmaking. Their addition into the liquid metal in form of flux-cored wire showed high efficiency of metal refining from detrimental impurities and nonmetallic inclusions. The First International Symposium on treatment of liquid metal with calcium [24] was held on June 30, 1988 in Great Britain (Glasgow). It was sponsored by Affval Company (France), which entered mass production of flux-cored wires and devices for their addition into the melt.

In the recent years other companies in addition to Affval Company started to expand the possibilities of application of flux-cored wires as a method, which is technologically convenient and economically profitable. At that alloying, microalloying, deoxidizing, refining and modifying additives [25] served as charge of flux-cored wires. Such additives became the elements characterizing with high oxygen affinity (Ca, Mg, Al, Ba, Ti, Si, Zr, Ce and other REM), small den-

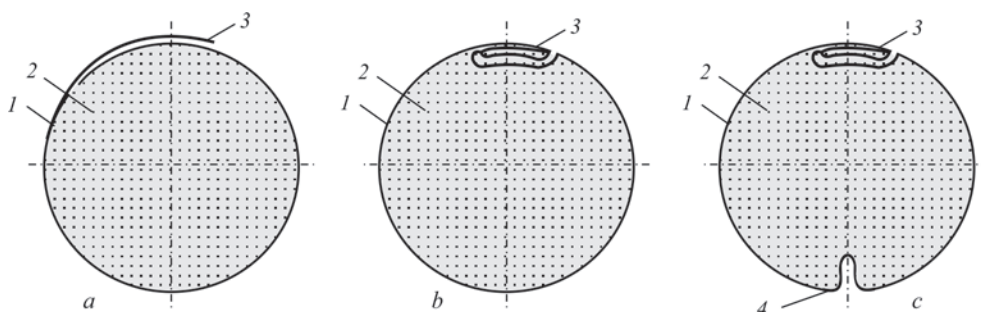


Figure 4. Types of using flux-cored wire joining: *a* — lap; *b, c* — finger (*1* — shell; *2* — filler; *3* — finger joint; *4* — compensator)

sity (C, B, S, Ca, Al, Mg etc.), relatively low melting and boiling temperatures (Ca, Mg, S, Se, etc.), high vapor pressure and small solubility in liquid metal (Ca, Mg, etc.). In a series of cases application of flux-cored wires is an alternative method for addition of calcium and other elements or compounds into liquid metal in comparison with method of injection in it of similar components in form of powders [26, 27].

In the former Soviet Union the most active work on improvement of elements of technology of wires production and methods of their addition to the melt were carried out by scientific institutes IPS, PWI, DonNII-CHERMET. For the period of 1986–1991 the development proceeded from issue of pilot batches of wires to their commercial production as well as special equipment for addition of wires into liquid metal at Donetsk production-implementation Company «Metall» (from 1989, OJSC «Zavod Universalnoe oborudovanie») [28]. Currently, flux-cored wire is manufactured by 20 more enterprises from former CIS countries [29].

The flux-cored wire used in this method of ladle treatment of liquid metal is a steel (steel 08Yu) shell of 0.2–0.5 mm thickness, filled with powder-like material, and reeled on coil. The length of wire in a coil is from 2000–4000 m and more. Wire diameter is 8–16 mm. At the first stage of mastering of wire production the ends of metallic shell were lap joined (overlapping 7–8 mm) with presence of longitudinal stiffening rib (compensator). Such a wire during its feed into liquid metal often opened that resulted in charge pouring out. In the future the flux-cored wires started to be manufactured using «finger» joint of the edges with or without compensator [29] (Figure 4). There are some requirements to powder-like chemical agents. They can be a metal, alloy or nonmetallic inclusions, milled to specific size. It was experimentally determined that the maximum fraction of powder particles shall not exceed 2.5 mm for 13 and 15 mm diameter and 2 mm for 10 mm diameter wire. From point of view of dense filling of section the pow-

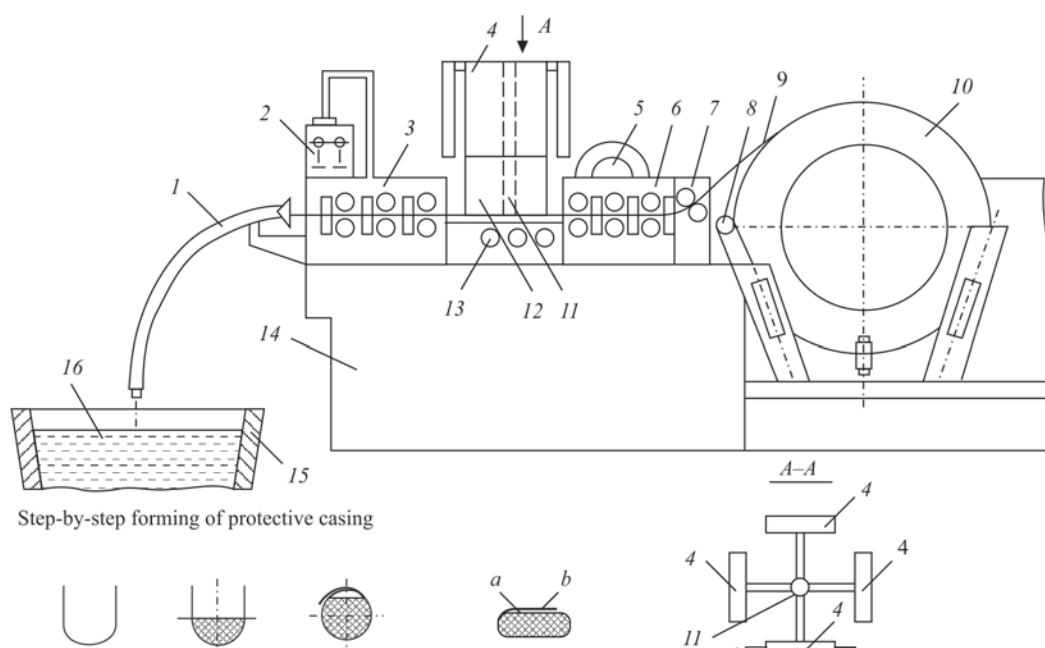


Figure 5. Technological complex of ladle treatment of melts using flux-cored wires: *1* — guide; *2* — control panel; *3* — forming-sizing stand; *4* — measuring hopper system; *5* — electromechanical group drive; *6* — forming stand; *7* — guide rollers; *8, 9* — tension device; *10* — decoiler with winded strip; *11* — rotating turret; *12* — protective casing; *13* — support rollers; *14* — frame; *15* — metallurgical capacity; *16* — melt; *a, c* — strip flanges overlapping

der-like material shall contain up to 25 % of dust-like fraction (particle size less than 0.2 mm) [29].

A technological line for production of flux-cored wire includes a series of devices, which provide uncoiling of strip, formation a channel in it, input of charge in it using the dosing machines, formation of closed profile, its calibration and row by row laying of wire in the coil.

The second main element of technology of secondary refinement of melt with flux-cored wires in ladle, tundish, mould is the presence in it of so-called pitch roll units. Their main task is to draw the wire with a set speed and create at the output a pushing force providing overcoming of wire friction forces on a guide pipe and at passing by it of metal melt as well as overcoming of friction forces in the pitch roll unit itself. The pitch roll units can be of single-, two- and multigroove design, i.e. for feeding into the melt of one, two or more types of wire [29, 30]. In a series of cases it is assumed to use technological complexes combining the processes of manufacture of flux-cored wire and its feeding into the liquid metal (Figure 5) [22]. Apparently, such technical solution still can not be recognized optimum one since any violation of wire manufacturing technology and its quality will have direct effect on quality of metal being treated. Besides, «lap» wire forming can result, as it was mentioned above, in its opening in the liquid metal.

Usually wire is fed vertically into the melt [29, 31], but some authors believe the wire feeding in the tundish at 40–70° is more reasonable, that significantly (1.5–3 times) increases the length of immersed part of wire and, respectively, allows varying its feed rate [32].

Thus, proposed at the end of the XIX century by N.N. Benardos welding consumable of special design, titled later on as a flux-cored wire, has found application not only in welding, but also in surfacing, remelting, and foundry. In each of these fields it was possible to show the main advantages, i.e. in surfacing it is a possibility of wide alloying of deposited metal; in remelting — continuous process of material melting; in foundry — improvement of quality of metal due to its refining, modifying and alloying.

1. Frumin, I.I. (1961) *Automatic electric arc surfacing*. Kharkov, Metallurgizdat [in Russian].
2. Pokhodnya, I.K., Suptel, M.A., Shlepakov, V.N. (1972) *Flux-cored wire welding*. Kiev, Naukova Dumka [in Russian].
3. Mazur, A.A., Lipodaev, V.N., Pustovojt, S.V., Petruk, V.S. (2017) State-of-the-art of welding equipment and consumables market in Ukraine. *The Paton Welding J.*, **11**, 31–37.
4. Gladky, P.V., Kondratiev, I.A., Yumatova, V.I., Zhudra, A.P. (1991) *Surfacing flux-cored strips and wires*: Refer. Book. Kiev, Tekhnika [in Russian].
5. Pokhodnya, I.K., Alter, V.F., Shlepakov, V.N. et al. (1980) *Manufacture of flux-cored wire*. In: *Manual for institutes of higher education*. Kiev, Vyshcha Shkola [in Russian].
6. (1980) *Electroslag welding and surfacing*. Ed. by B.E. Paton. Moscow, Mashinostroenie [in Russian].
7. Blaskovic, P., Peknitsa, P. (1979) Resistance of deposited by electroslag method rolls for hot rolling of sheet. In: *Information documents of CMEA*. Kiev, PWI, **1**, 49–50.
8. Sokolov, G.N., Filyushin, A.A. (1988) Influence of structure and type of deposited metal on wear resistance of cams of pipe turning machine. *Avtomatich. Svarka*, **8**, 47–49 [in Russian].
9. Sokolov, G.N. (1984) Investigation and development of materials for surfacing of extrusion toolage in production of bearings: *Syn. of Thesis for Cand. of Techn. Sci. Degree*. Kiev, PWI [in Russian].
10. Sokolov, G.N., Filyushin, A.A. (1982) Electroslag surfacing of volume ends of die parts. In: *Modern methods of surfacing and their application*. Kiev, PWI, 84–89 [in Russian].
11. Samsonov, I.G. (1981) Investigation of thermophysical processes in electroslag surfacing with flux-cored wires: *Syn. of Thesis for Cand. of Techn. Sci. Degree*. Sverdlovsk, UPI [in Russian].
12. Sokolov, G.N. (2004) Properties of deposited metal used for metallurgical tool hardening. *The Paton Welding J.*, **10**, 55–57.
13. Ramacciotti, A., Repetto, E., Sommovigo, P., Sondini, G. (1982) Production of bimetallic mill rolls by method of electroslag surfacing with metal-flux-cored electrodes. Electroslag remelting. In: *Proc. of 7th Int. Conf. on Vacuum Metallurgy, Special Types of Melting and Metallurgical Coatings (Japan, Tokyo, 26–30 November, 1982)*. Kiev, Naukova Dumka, Issue 8, 130–136.
14. Sushchuk-Slyusarenko, I.I., Lychko, I.I., Kozulin, M.G. et al. (1989) *Electroslag welding and surfacing in repair works*. Kiev, Naukova Dumka [in Russian].
15. Kuskov, Yu.M. (2003) A new approach to electroslag welding. *Welding J.*, **4**, 42–49.
16. Sokolov, G.N., Lysak, V.I. (2005) *Surfacing of wear-resistant alloys on pressing tools and tools for hot working of steels*. Volgograd, RPK Politekhnik [in Russian].
17. Korolyov, N.V., Platonov, A.G., Mukhin, D.V. (1992) Peculiarities of melting of wire electrodes in electroslag surfacing. *Svaroch. Proizvodstvo*, **3**, 26–28 [in Russian].
18. Daemen, R.A., Blaskovic, P. (1970) Pridavne materialy pre electroskove navaranie ocel'ovych valcov valcovacich stolic. *Zvaranie*, **8**, 234–239 [in Slovakian].
19. Leveau, J. (1973) Electroslag melting with addition of metal powders. Electroslag remelting. In: *Proc. of 3rd Int. Symp. on Technology of Electroslag Remelting (USA, Pittsburg, 8–10 June 1971)*. Kiev, Naukova Dumka, 26–33.
20. Descamp, J., Etienne, M. (1974) State-of-the art of the process of continuous electroslag remelting of powders. Electroslag remelting. In: *Proc. of Int. Conf. on Technology of Electroslag Remelting (Great Britain, Sheffield, 10–11 January 1973)*. Kiev, Naukova Dumka, Issue 2, 202–210.
21. Parsons, R.S. (1973) Production of tool steels by method of continuous electroslag remelting of powders. Electroslag remelting. In: *Proc. of 3rd Int. Symp. on Technology of Electroslag Remelting (USA, Pittsburg, 8–10 June 1971)*. Kiev, Naukova Dumka, 243–251.
22. Marchenko, I.K., Tsarev, A.V., Galentovsky, G.G., Khejfts, V.G. (1990) Resource-saving technology and equipment for ladle treatment of liquid steel. *Tyazholoe Mashinostroenie*, **5**, 28–29 [in Russian].
23. Dyudkin, D.A., Marintsev, S.N., Onishchuk, V.P., Grinberg, S.E. (2000) Technical and economic efficiency of cast iron

- and steel treatment with flux-cored wires. *Metall i Litio Ukrainy*, **1-2**, 41–42 [in Russian].
24. (1989) Calcium treatment of steel. Ed. by B.I. Medovar. In: *Proc. of Int. Symp. on Calcium Treatment of Steel (Great Britain, Glasgow, 30 June 1988)*. Kiev, PWI.
 25. Kablukowsky, A.F., Zinchenko, S.D., Nikulin, A.N. et al. (2006) *Ladle treatment of steel with flux-cored wire*. Moscow, Metallurgizdat [in Russian].
 26. Wissler, H.-J., Boom, R., Biglari, M. (2008) Simulation of the Ca-treatment of Al-killed liquid steel. *La Revue de Metallurgie, CIT*, **4**, 172–180.
 27. Wen Yang, Lifeng Zhang, Xinhua Wang et al. (2013) Characteristics of inclusions in low carbon Al-killed steel during ladle furnace refining and Ca treatment. *ISIJ Int.*, **53**(8), 1401–1410.
 28. Dyudkin, D.A., Bat, S.Yu., Grinberg, S.E. et al. (2002) *Ladle treatment of melt with flux-cored wires*. Donetsk, OOO Yu-go-Vostok [in Russian].
 29. Dyudkin, D.A., Kisilenko, V.V., Pavlyuchenkov, I.A., Bolo-tov, V.Yu. (2007) *Precision treatment of metallurgical melts*. Moscow, Teplotekhnika [in Russian].
 30. Titievsky, V.I., Bordyugov, V.N. (2000) Technological complex for introduction of flux-cored wire into liquid metal. *Metall i Litio Ukrainy*, **1-2**, 7–9 [in Russian].
 31. Dyudkin, D.A., Kisilenko, V.V., Matochnik, V.A. et al. (2006) Application of flux-cored wire with silicocalcium filling for ladle treatment of steel in Belarusian metallurgical plant. *Elektrometallurgiya*, **6**, 16–20 [in Russian].
 32. Nosochenko, O.V., Trotsan, A.I., Chichkarev, E.A. et al. (2003) Rational mode of steel treatment in cold hearth with flux-cored and solid wires. *Metall i Litio Ukrainy*, **7-8**, 28–30 [in Russian].

Received 12.11.2018

SAVE THE DATE

THE 72ND IIW ANNUAL
ASSEMBLY AND
INTERNATIONAL
CONFERENCE

Bratislava, Slovakia

7th – 12th July 2019

The annual event of the International
Institute of Welding IIW 2019

www.iw2019.com

The main topic of the International Conference:

New Progressive Materials and Welding
Methods in the Automotive Industry

Hosted by

Conference Secretariat

MODULAR DESIGN OF HIGH PRODUCTIVITY ELECTRON BEAM WELDING MACHINES

F. KOLENIC, L. KOVAC, R. SEKERKA and P. FARAGULA

FIRST WELDING COMPANY Inc., Bratislava, Slovak Republic

The paper presents the results achieved in the field of actual design and technical solution of modern high-tech electron beam welding equipments in THE FIRST WELDING COMPANY Inc. The fundamental conceptual approaches to solution of modern technological complexes with application of powerful electron beam generator systems are described. The electron beam technological welding equipments are constructed modularly with special attention paid to harmonisation of hardware and software compatibility. The individual modules of technological unit are periodically innovated with respect to the progressive world trends in the field of electrotechnics, drive systems, computer control, mechanical modules and advances in vacuum technology. The contribution presents both the development of principal modules which form the core of technological welding complex such as stationary and movable electron gun, beam generation systems, vacuum chambers as well as auxiliary modules, which are adapted to the needs of modern industrial production and quality management. Among the examples, remote diagnostics of electron beam machine by web applications, module for monitoring and editing the parameters of technological process can be found. Three examples of different design of electron beam equipments are documented and described. 5 Ref., 14 Figures.

Keywords: *electron beam, welding machines, modular design, modules of welding equipment, remote diagnostics, monitoring process parameters*

The electron beam technologies are finding their application in industrial production already for several decades. During their utilisation they have brought about an immense merit to progress in actually all industrial branches, participating thus in excellent results that have been achieved in development of scientific knowledge and technical progress for the past 50 years. These have played irreplaceable task in recognition of space, progress in aviation transport and aviation industry, power engineering and general machine building [1]. They meet the parameters for incorporation into the group of high-tech technologies. Design of welding complexes makes use of new scientific knowledge and methods, materials and modern computer technology. An important role in their further development is played by factors such as commercial availability, high reliability, application flexibility and the fact that they are immediately applicable to direct industrial applications.

In the field of development and supply of electron beam machines, a system of modular design was developed in the FIRST Welding Company (FWC). In this system, unified modules are used as the basic building blocks. Technical criteria for functional modules or units are set to meet a specified function with high reliability, hardware and software are fully compatible with other modules and allow for work in autonomous mode. According to the meaning and technical function, modules can be divided into principal and auxiliary. The principal modules form the

core of technological welding complex and assure the primary function of equipment, namely the fabrication of welded joints of metallic materials in vacuum. The main modules comprise the power generator of electron beam, which is briefly called as a power block, electron gun, vacuum welding chamber, modules for vacuum generation in the welding chamber and in the electron gun, modules for positioning of welded parts, CNC control modules, modules for monitoring and illumination of welding process. The software is an inseparable part of technological complex. The auxiliary modules are not necessary a part of the equipment, however they fulfil an essential function in setting and monitoring of process parameters, creation of process databases, protection of welded joints against defect formation, extension of technological capabilities of equipment, allowing the remote diagnostics, prophylactics and service of the equipment, with utilization of remote approach by the aid of web applications. FWC have at present completed design of several tens unified, mutually compatible functional modules for the delivery of electron beam welding equipment. The concept of modular design allows to satisfy actually nearly all technical and technological requirements of customers in the highest quality and in the desired time terms. Some specific requirements of customers, mainly in deliveries of high productive welding equipment are prevailingly solved by the adaptation of design of a selected module with application of its conceptual solution.

Selected modules of electron beam welding equipment. It is impossible to present all unified modules within the extent of this contribution. The following chapter will present the significant modules of welding complexes from the production of FWC.

Modules of beam generation system. The powerblock belongs to the main unified modules and serves for creating the conditions for generation of electron beam and its automatic control [2]. The electron beam itself is formed in the electron gun. FWC is offering three power grades of electron beam generators with type designation PZ EB 7.5, PZ EB 15 and PZ EB 30. All power blocks grades have the same external dimensions, they differ just in internal electrical connections. They are inserted into two unified 19" racks & electronics cabinets type Schroff (Figure 1).

The first cabinet comprises a controllable and stabilized HV source serving for acceleration of electrons of electron gun. This source provides the kinetic energy to electrons, which is transferred to thermal energy after impingement on welded joint and serves thus for formation of welded joint. The second cabinet comprises the auxiliary sources which serve for heating the thermo-emission cathode of electron gun, the source of control voltage which regulates and stabilises the welding current, the source of current for magnetic beam focusing, the source system for magnetic beam deflection and a logic PLC automat for the manual and/or automatic control of powerblock operation. The powerblock type PZ EB 7.5 generates the electron beam with maximum power of 7.5 kW. At acceleration voltage of 60 kV it provides the welding current within the range from 0 to 125 mA. The powerblock type PZ EB 15 generates the electron beam with maximum power of 15 kW and with welding current value adjustable from 0 to 250 mA at the voltage of 60 kV. Maximum current of electron beam at the acceleration voltage of 60 kV can attain 500 mA. Figure 1 shows the mechanical design of powerblocks. Three power grades of powerblocks are conceptually built on the identical basis, they differ just in electronic outfit.

The high-voltage source of acceleration voltage is of inverter type and it consists of the following main parts:

- HV transformer with rectifier, filtration capacitors and measuring circuits situated in a separate vessel insulates with transformer oil.
- Medium-frequency converter with a series-parallel resonance circuit with the frequency of 20 kHz.
- Control, regulating, safety and measuring circuits.

Excitation of high-voltage transformer is realised via a medium-frequency inverter (20 kHz). In the case of this solution, the exciting signal is formed by an alternating switching of power transistors T1, T4 and

T2, T3 connected in a bridge, what forms the alternating voltage with rectangular course of constant frequency in the bridge diagonal. This voltage is connected to the primary HV winding via the serial-parallel resonance LC circuit, which ensures almost ideal harmonic course of the excitation voltage and a more efficient energy transfer. Stabilization of voltage and power regulation of HV source is solved by altered range of transistor switching, what allows a regulation intervention at the level of several milliseconds. Advantage of such a connection consists in application of a constant switching frequency of the exciting current, what allows to achieve very low ripple of accelerating voltage at suitable selection of filtration capacity of the secondary circuit. The measured value of welding voltage ripple at the nominal source power output of 30 kW and the switching frequency of 20 kHz is at the level of $\pm 1.0\%$. The electronic anti-discharge protection is selectable by an auxiliary module to HV source. The electric scheme of HV source type PZ EB 30 kW is shown in Figure 2.

The auxiliary sources serve for generation of electron beam and the desired setting of welding parameters. These allow manual, automatic and/or program control of welding current, focusing current and electron beam deflection. The group of auxiliary sources includes the current source for filament heating, source of cathode bombarding current, voltage source for control electrode, the source of focusing current and the source for beam deflection.

The typical technical parameters of powerblock are as follows

Value of accelerating voltage, kV	controllable from 30 to 60
Maximum power of electron beam, depending on the type, kW	7.5, 15, 30
Stability and ripple of acceleration voltage, %	max ± 1.0
Stability and ripple of welding current, %	max ± 1.5
Stability of focusing current, %	max ± 0.5



Figure 1. The powerblock type PZ EB 30

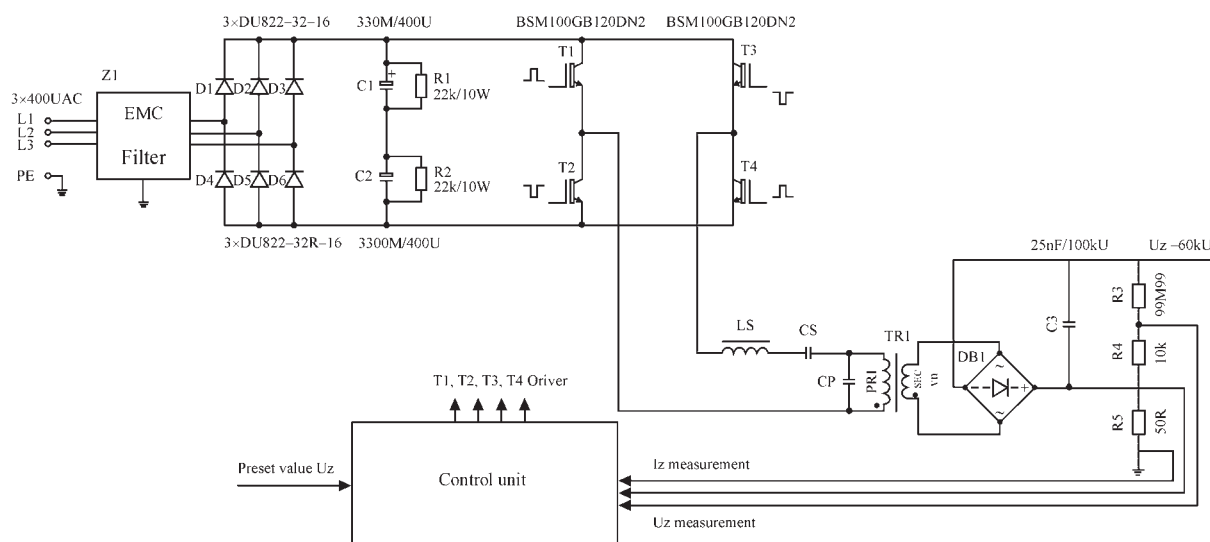


Figure 2. Electric scheme of HV source type PZ EB 30 kW

Electron gun module. The electron gun serves for generation, control and adjustment of power electron beam for the technological operations of welding and/or surface treatment of metallic materials [3]. It is the most important part of electron beam welding equipment. The power necessary for generation of electron beam is supplied from the powerblock. Therefore, the gun and powerblock must be mutually compatible. Modular concept recognizes the stationary electron gun working from outside at atmospheric pressure and the gun destined for applications in vacuum chamber — movable electron gun. The stationary guns are situated on the welding chamber wall to which they are tightly vacuum-proof attached. They are mostly attached to vacuum chamber statically and the welded joint is formed by programable positioning of weld joint against the electron beam. Stationary electron guns have the same design for all output power graders. An example of design of stationary gun is shown in Figure 3.

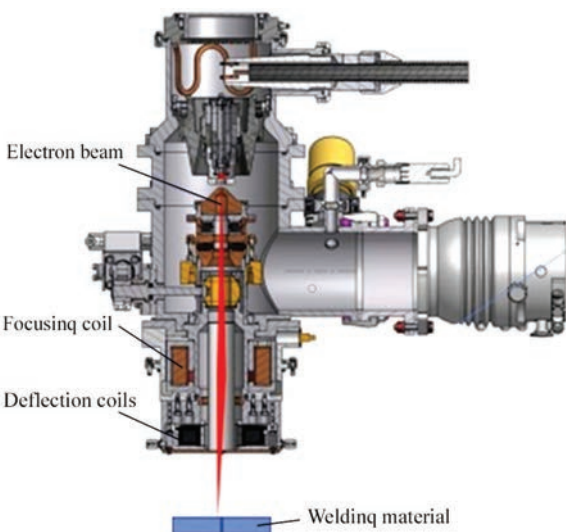


Figure 3. Design of a module of atmospheric gun

Such a gun cannot properly perform the welding operation unless it is equipped with the appropriate modules, permitting its basic functions and which enable an exact setting of electron beam on the welded joint. This is realised via auxiliary modules as the module of gun pumping to a high vacuum, module for monitoring of welding process and the module for process illumination. These modules together with the gun body are attached to a common base and create a separate unit. An example of placing the configuration of auxiliary modules on a common base with gun is shown in Figure 4.

Regarding the design viewpoint, the differences between stationary gun and movable gun for welding applications are minimum, consisting of a small deviation in sealing the inner space of the gun and the total weight. Greater differences may be observed only in the system of vacuum pumping of both guns. The atmospheric vacuum gun is pumped by a turbomolecular vacuum pump, which is additionally pumped also with a rotary vacuum pump. The movable electron gun is pumped only with a turbomolecular gun, whereas the rotary vacuum pump is unnecessary, since the vacuum is ensured by the vacuum system

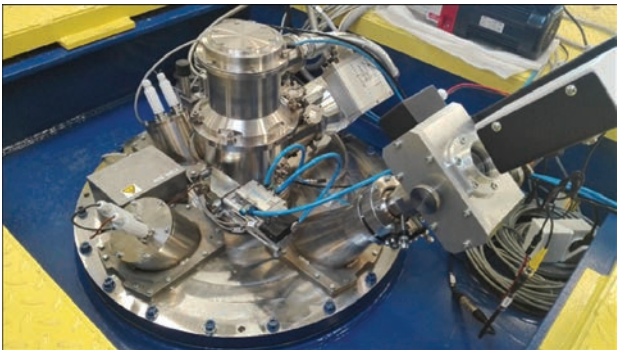


Figure 4. Configuration of auxiliary modules of the stationary electron gun

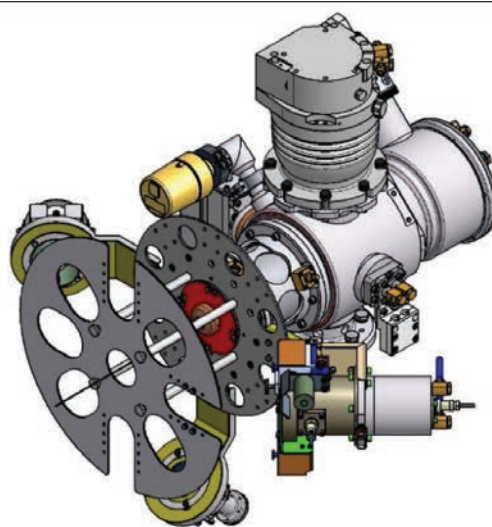
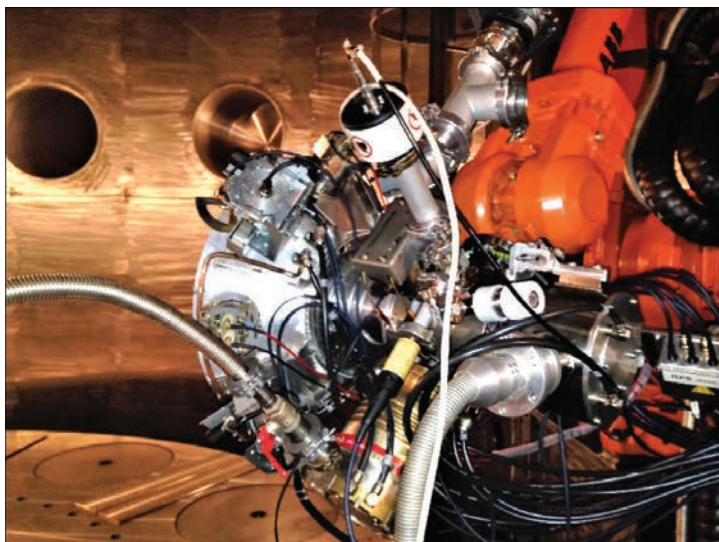


Figure 5. Design of movable electron gun

of the chamber. The design of vacuum electron gun is shown in Figure 5.

Another essential condition for correct operation of this electron gun consists in its positioning to welding trajectory in the vacuum welding chamber.

Module for positioning the vacuum electron gun. Two types of modules for positioning of movable electron gun in vacuum chamber are designed. These differ both conceptually and in the way of application. For the vacuum chambers of medium size, the module of two-axial positioning is designed in a Cartesian coordinate system with addition of a manual or fully automatically controlled rotary axis. Design of the two-axial module with a manual rotary axis is shown in Figure 6. The x and z axes are fully program-controlled axes ensuring the gun positioning in x - z plane. Gun tilting in rotary axis is performed manually. This system serves for fabrication of linear welds and in combination with an additional rotary positioner also for fabrication of the face and circumferential rotary welds. The presented concept allows the location of a

feed mechanism for the additive manufacturing with application of a filler in the form of wire. Practical application of this type of positioning system is shown in Figure 7.

Another way of electron gun positioning in vacuum is solved with application of an adapted robotic system, modified for the operation in vacuum environment. This way of electron gun positioning is suitable for application in large vacuum chambers. Positioning of electron gun is assisted by an industrial robot type IRB 4600 in special adaptation for the work in high vacuum (Figure 8). The ABB IRB 4600 represents industrial robot with 6 axes, 45 kg carrying capacity and 2200 mm working radius. It is provided with control unit type IRC5 and RobotWare software. The robot is situated on a carriage of vertical support, which in the function of fully controlled axis allows the robot positioning in its vertical Z axis. The additional « Z » axis has extended the working range of robot in Z axis to value of 8.5 m. Next additional axes ω_1 — rotation of the main positioner and ω_2 — rotation of rotation-

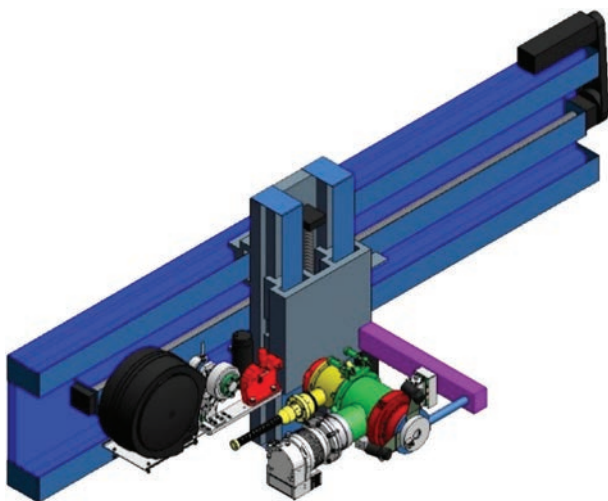


Figure 6. Design of a positioning module of electron gun

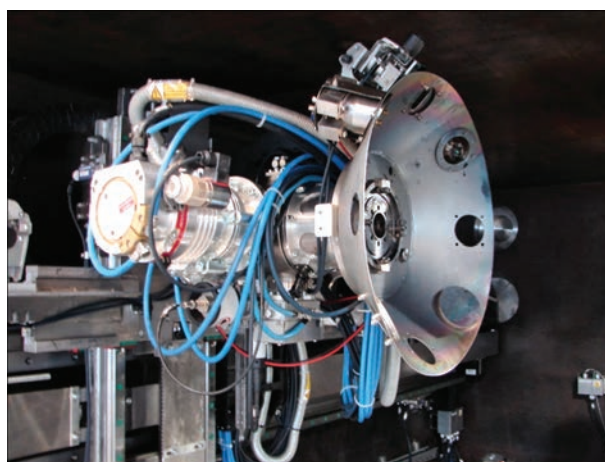


Figure 7. Practical application of a module for vacuum gun positioning

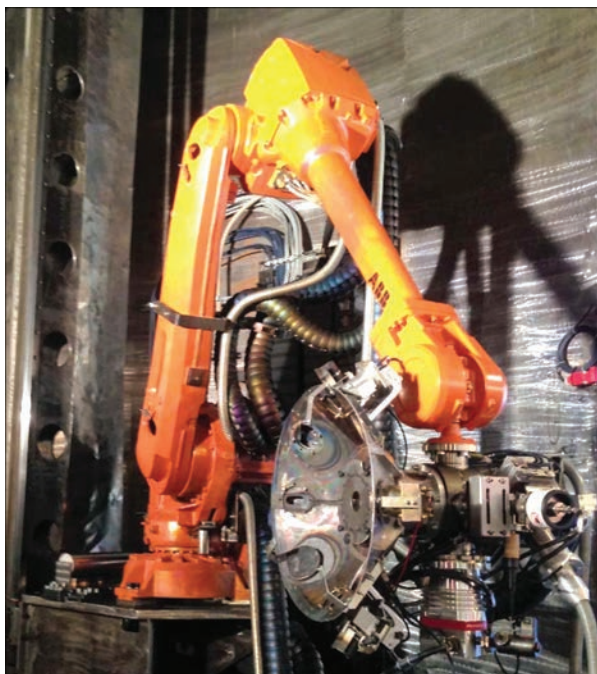


Figure 8. Module for vacuum electron gun positioning

al nests serves for positioning of weldments. All nine axes of positioning system e.g. six robot axes and the additional three axes ω_1 , ω_2 and Z represents fully controlled axes and can be controlled by FlexPendant unit on selecting the «technology» option from the main menu and/or by a program from the technological computer. The electron gun with monitoring is defined as the working tool EB_GUN_Ti. This tool has a defined mass centre of gravity and has determined the tool coordinates TCP (Tool Centre Point). RobotWare software supports all aspects of robot system, as robot motion, development and implementation of applica-

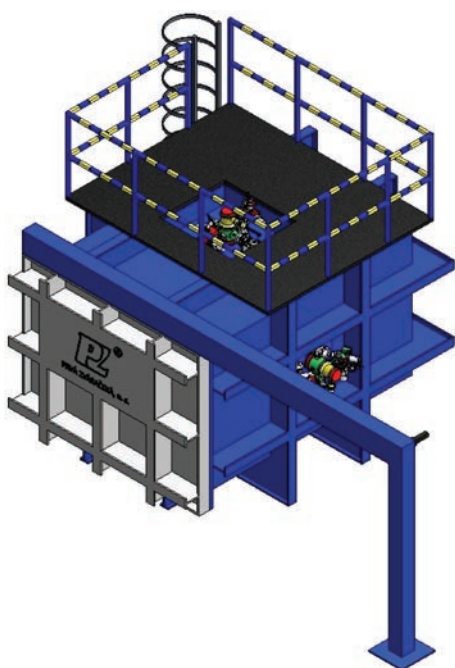


Figure 9. Module of a versatile chamber with the volume of 16 m³

tion programs system, as robot motion, development and implementation of application programs and communication. Communication between the control unit IRC5 and technological computer is realized through Ethernet interface. The FlexPendant controller is a portable operation unit with graphical touch screen. The RAPID programming language contains the instructions allowing the application to perform robot motions, to set the outputs and/or to read the inputs.

Modules of vacuum chambers. The vacuum chambers are in most cases designed by the «fitness for purpose» approach, i. e. tailored for the needs of an actual customer. The size and shape of vacuum chamber is given by the dimensions of parts to-be-welded, desired time for pumping to working vacuum and the electron gun employed. The technological preparation and manufacturing technology comprise the unifying element of modules for welding chamber design. The welding chamber must be vacuum proof, resistant against distortions and must comprise an advanced and unified system for sealing of static flanges and door systems and also for sealing of movable parts.

A versatile medium-size vacuum chamber with the volume of 16 m³ may be shown as an example in Figure 9.

The welding chambers for high-productive welding must meet the condition of high efficiency. These are destined for welding of a great number of parts with identical shape and with a slight dimensional diversity. They are mostly composed of a vacuum welding chamber and one or more auxiliary chambers. Such a design makes possible that the welding chamber could be permanently pumped to the working vacuum. The auxiliary chambers ensure the operation of loading and unloading of weldments and also the operation of air intake and vacuum pumping

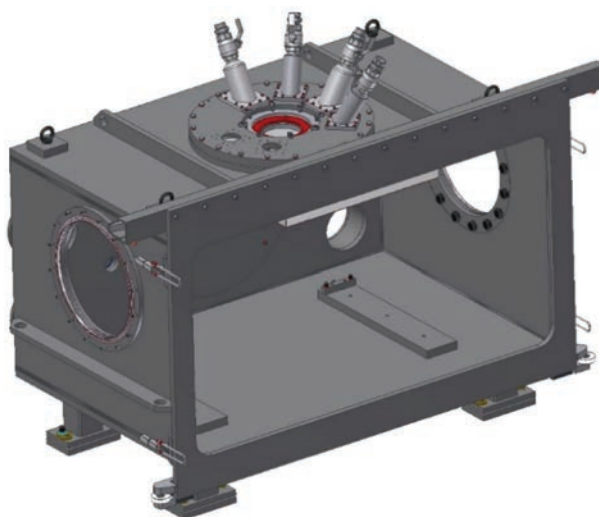


Figure 10. An example of design of welding chamber module for high-productive welding machine

of the auxiliary chamber. The proportion of net welding time during one shift against the manipulation and preparatory times is at the level of 80 %. An example of modular concept of welding chambers for the high-productive welding is shown in Figure 10 and Figure 11.

The presented examples of design of principal modules of electron beam welding equipments elucidate the concept of modular design which is applied by the FWC Inc. in design, construction and manufacture of electron beam equipment for diverse applications destined for external customers. This concept has proved as sufficiently flexible, economical and it thus creates the conditions for deliveries of equipments for the external customers in the shortest possible terms and in high quality.

Modul for processing data collection. This module belongs to the auxiliary modules. It can be integrated into the device upon customer request. Main function of the module is to collect all decisive welding process parameters, as the value of accelerating voltage, welding current, focusing current, welding speed, electron beam position related to welded joint etc. These and other selected parameters are recorded during the entire welding cycle. They are used for the retrospective diagnostics. The recorded process parameters are gained from the sensors of the control system and it allows simultaneous recording of more than 15 process parameter with the sampling period from 1 to 10 ms. The elaborated program allows to alter the sampling period and it also allows the collection and storage of data coming from several sources. The recorded data from individual sensors are sent in a special binary format through the communication line to the archiving computer, which assigns them the identification signs and stores them on memory media. Moreover, the program records also all binary states of the drives. The developed program for data analysis represents a browser for a huge quantity of binary data in graphical and tabular form.

Remote diagnostics of electron beam machine by web applications. Solution of remote diagnostics, which belongs to the next auxiliary module of electron beam welding machine, is based on special hardware and software configuration. For connecting equipment to the remote access, the industrial router from eWON company was selected and for creating a communication for data transfer between the equipment and remote user the internet service Talk2M (from the English «Talk to Machines») was utilised. These circuits are then integrated into a control system of electron beam welding machine at the customer workplace. The present state of technological solution of equipment provides the remote access to equipment



Figure 11. An example of design of auxiliary chamber module for high-productive welding machine

by utilising the internet and it offers the following options: Sending an alarm message in case of failure occurrence, connection of a remote visualisation, work of programmer directly in the development environment of PLC, access to archive of records of welding parameters created via a special software module for collection and analysis of processing data. The created communication channel meets all relevant safety standards, what provides a high level of protection for the transferred data against abuse.

Examples of design of electron beam equipments. As an example, three designs of welding equipments are shown, representing different field of industrial application of high-tech technologies from the production portfolio of FWP company, making use of electron beam technologies.

The first example is a welding technological complex with type designation PZ EZ 30 JUMBO.

This equipment is destined for welding sizable parts in general engineering and power industry [4]. The new design of equipment employing the electron gun attached on the robot arm with integrated other two rotary and one liner axes makes possible to fabricate the rotary and linear welded joints as follows:

Rotary circumferential joints of sizable weldments on a central rotary positioner in side position as follows:

- range of weldment diameter from 500–5000 mm;
- range of weldment weight from 200 kg to 100 t;
- range of weldment height from 500–8000 mm;
- range of weld depth from 1–90 mm on austenitic steel in PC position.

Rotary circumferential welds on medium size weldments fabricated on auxiliary rotary positioners as follows:

- range of weldment diameter from 100–500 mm;
- range of weldment weight from 1–200 kg;
- range of weldment height up to 5000 mm;

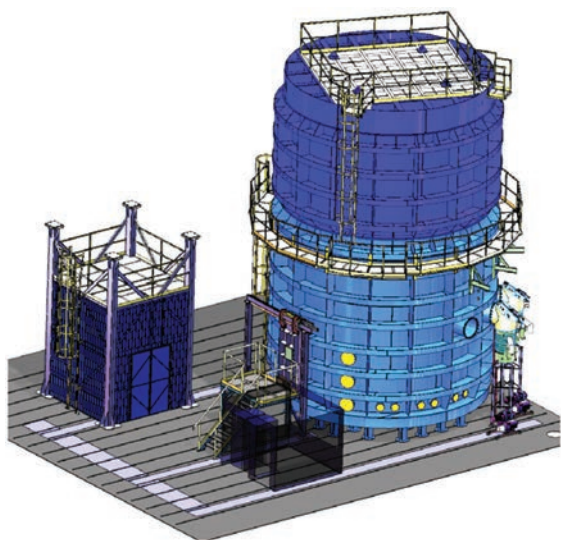


Figure 12. The welding workplace type PZ EZ30 JUMBO

- maximum number of weldments placed in welding chamber and welded under one vacuum pumping makes 10 pieces.

Linear welds on sizable weldments fabricated on a central positioner as follows:

- range of weld length from 10–5000 mm;
- range of distance from the axis of central positioner varies within 500–2500 mm;
- range of weldment weight from 100 t to 200 kg;
- range of weld depth (penetration depth) from 1–100 mm on austenitic steel.

Linear weld of slim weldments in weight up to 200 kg fabricated on the auxiliary rotary positioners as follows:

- range of weld length from 10–5000 mm;
- range of distance from the axis of auxiliary positioner varies within 50–400 mm;
- range of weld depth (penetration depth) from 1–100 mm on austenitic steel.

The electron gun of triode type with maximum power of 30 kW is made of titanium and allows to weld the CrNi steels in thickness of 90 mm on one pass [5]. The system is provided with an electronic anti-discharge protection, monitoring module with three video cameras and laser space navigator. For

the needs of surface heat treatment and fabrication of surface layers the equipment is provided with a module for programmable beam scanning. The volume of welding chamber is 265 m³ (Figure 12). The time of pumping to working vacuum of $5 \cdot 10^{-2}$ Pa is 85 min.

The welding workplace type PZ EZ 30 TWIN-BEAM is a versatile workplace with the volume of welding chamber of 16 m³. It is destined for welding thin-walled and heavy-walled (up to 80 mm) parts in medium vacuum. Besides welding it also allows the heat treatment of surfaces of metallic materials and additive manufacturing with application of filler in the form of wire. The complex electron beam workplace is equipped with two guns, whereas it is possible to weld just with one gun or both guns simultaneously. The time of vacuum pumping to working vacuum is maximum 25 min. The vacuum chamber is equipped with the X–Y positioning table for positioning during welding, which is integrated with the system for loading and unloading of weldments to and from the vacuum chamber, a rotary positioning system and also with a wire feed unit. The overall view on the workplace is shown in Figure 13.

The welding equipment type PZ EZ ZPH may be shown as an example of a single-purpose high-productive workplace. This workplace is destined for series welding of hydromotor pistons in vacuum. The pistons of hydro-converters represent an example of extremely loaded part made of hardenable low-alloyed Cr–Mo steel. Since the steel type 42CrMo4 (1.5124) is susceptible to cold cracking, it is necessary to alter the steep thermal cycle of welding by application of preheat eventually postheat. The purpose of application of preheat/postheat is to suppress the formation of martensite in the weld metal and to ensure the formation of a tougher structure which is not susceptible to cold cracking. Possible notch effect of unsuitable geometry is eliminated by the relieving recesses under the weld root. This mechanical adaptation has allowed to dissipate the stress flow from welding, what resulted in reduced concentration of stresses in the



Figure 13. The welding workplace type PZ EZ 30 TWINBEAM



Figure 14. The welding equipment type PZ EZ ZPH

root of welded joint. Welding of hydromotor pistons in vacuum represents an ideal application of electron beam welding technology, regarding their dimensions and desired productivity, which by its nature allows to realize a controlled preheat and postheat by the same heat source which is used also for welding.

Welded joints are fabricated at the acceleration voltage of 40 kV, while the nominal power of welding equipment is 6 kW. Maximum annual production of equipment is 500 000 weldments per one shift. This welding equipment is shown in Figure 14.

Conclusions

The aim of this contribution is to present a unified concept of design and realisation of deliveries of sophisticated technological equipments and complexes with a high degree of automation. Based on the presented results the system of modular design can be characterized as flexible and economically efficient. As the main constructional elements this system makes use of unified modules, which represent a separate functional unit which are hardware and software fully compatible with the other modules of technolog-

ical complex. This system offers a great potential of a broader application in design and construction of versatile and single-purpose equipments in the segment of general engineering.

Acknowledgement. This work was supported Slovak Research and Development Agency under the contract No.APVV-17-0432.

1. Schultz, H. (2004) *Electron beam welding*. Cambridge, Abington Publishing, England.
2. Kolenič, F., Faragula, P., Maštalír, P. (2016) Modernizácia modulov elektrónového dela umiestneného vo vnútri vákuovej komory (Modernisation of electron gun modules situated inside the vacuum chamber) *Zvárač-profesionál, (Welder-professional)*, **XIII**, 16–19.
3. Kolenič, F., Fodrek, P. (2012) New generation of EB welding machines, IIW DOC XII-2063–12, *Joint Intermediate meeting Com. IV, Com. XII and SG 212, Berlin, April, 2012*.
4. Kolenič, F. (2014) Large chamber EBW machine using 9 axes robotic system for positioning of electron gun and weldment in vacuum. In: *Proc. of 67th IIW Int. Conf., 13th–18th July, 2014, Seoul, Korea*.
5. Kolenič, F., Kováč, L. (2011) Nová generácia elektrónovo-lúčových zariadení s výkonom do 30 kW (New generation of electron beam welding equipment with the power up to 30 kW). *Zvárač-profesionál, (Welder-professional)*, **VIII**, 22–24.

Received 13.11.2018



E.O. Paton Electric Welding Institute of the NAS of Ukraine
National Technical University of Ukraine
«Ihor Sikorsky Kyiv Polytechnic Institute»
International Association «Welding»

The Ninth International Conference BEAM TECHNOLOGIES in WELDING and MATERIALS PROCESSING

9 – 13 September 2019

Ukraine, Odessa

Conference Chairmen
Prof. I. Krivtsun

Conference topics

- Laser and electron-beam welding, cutting, surfacing, heat treatment, coating deposition
- Electron-beam melting and refining
- Hybrid processes
- 3D-technologies
- Modelling and materials science of laser and electron-beam technologies

EQUIPMENT ♦ TECHNOLOGIES ♦ MODELLING



LTWMP 2019 Organizing Committee
03150, 11, Kazimir Malevich str., Kyiv, Ukraine
E.O. Paton Electric Welding Institute of the NAS of Ukraine
Tel./fax: (38044) 200-82-77, 200-81-45
E-mail: journal@paton.kiev.ua
www.pwi-scientists.com/eng/ltwmp2019



METHODS FOR DETERMINATION OF LOCAL STRESSES IN WELDED PIPE JOINTS (Review)

P.N. TKACH, A.V. MOLTASOV, I.G. TKACH and S.N. PROKOPCHUK

E.O. Paton Electric Welding Institute of the NAS of Ukraine
11 Kazimir Malevich Str., 03150, Kyiv, Ukraine. E-mail: office@paton.kiev.ua

For welded joints of pipelines and elements of welded structures, including tubular ones, changes of section in weld zone are typical. The local rise of stresses or their concentration appears in the places of shape change. The level of concentration often plays a decisive role in determination of stress-strain state of structure in whole, has an effect on life at cyclic loads as well as influences the process of nucleation and propagation of cracks. This paper provides a review of works dedicated to the procedures for determination of maximum local stresses acting in the zone of stress concentration caused by geometry of welded joints of pipelines and tubular structures. 49 Ref., 1 Table, 4 Figures.

Keywords: *pipeline welded joints, tubular structures, weld geometry, local stresses, stress concentration factor*

Stress concentration, caused by weld geometry, is one of the main factors determining the characteristics of fatigue resistance of welded joints [1].

The experience shows that the stress concentration shall be taken into account not only at effect of vibration load, but also at static load and impact, when there is a possibility of brittle fracture [2], that is particularly relevant for pipelines operated at low climatic temperatures, for example, under conditions of the Extreme North or transpolar regions [3, 4].

Traditionally, the maximum stresses in elastic deformation are obtained by multiplication of nominal stresses on value of theoretical stress concentration factor (SCF), which is a quantitative evaluation of stress concentration.

An approach according to which the theoretical stress concentration factor is presented as a product of two factors is very wide spread in the recent years in engineering practice. The first takes into account macrogeometry, i.e. welded assembly structure, therefore it was titled as structural SCF. The second considers presence of weld and its microgeometry. Such an approach provides sufficiently trustworthy result that was also proved by domestic researchers [5]. Presence of linear (pipes misalignment) or angular (pipe distortion) displacements of edges in the welded assembly promote additional external loads, which are considered by corresponding factors, to which first two are multiplied [6].

Stress concentration related with dimensions of reinforcement and geometry of transition zone from weld to base metal, first of all depends on relationship of a radius of this transition to thickness of base metal [7] and in our case to pipe wall thickness [8].

Investigation of SCF effect on fatigue strength is described in many works of domestic and foreign

authors [9, 10] that indicates significant scientific interest in this issue, in particular, applicable to welded joints of pipelines and tubular structures [11].

Analytical, experimental and numerical methods are used as a rule for evaluation of stressed state of loaded parts and structure elements, and modern procedures are based on their combination with the maximum application of the advantages of each of them. Therefore, aim of the present review is tracing the modern tendencies and determination of priority directions of further development of procedures for calculation of the maximum local stresses in pipe welded joints.

Majority of the works, published in the recent decades, are based on application of a finite element method (FEM) for deriving the formulae allowing determining hot spot stresses (HSS), which are the maximum local stresses. Use of the indicated approach allows determining structural SCF applying shell members at axial load as well as bending moments in various planes of investigated welded assembly. For example, in work [12] in a such a way there were determined the values of structural SCF along the whole weld length in the case of application of axial load along the branch pipe F_a , bending moment across the pipe section and branch pipe M_{IPB} and in pipe section plane M_{OPB} (Figure 1) for T-joints.

SCF values (Figure 1) satisfactorily match with the results of works provided in [12]. It should be noted that the authors [12] were limited by graphic interpretation of the results, and did not derive the equations allowing determining SCF depending on geometry parameters.

Formulae for determination of structural SCF in the joints of square and circular pipes of DT/X tubular structures were obtained in work [13] using FEM. Comparative evaluation of the SCF calculation val-

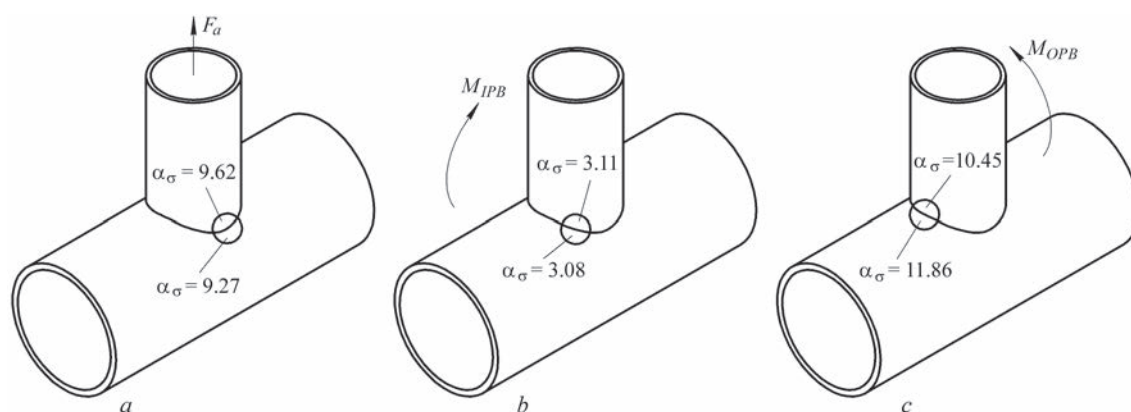


Figure 1. Maximum values of SCF on data of [12] under effect of axial force (a), moment across pipe section and connecting pipe (b) and moment in pipe section plane (c)

ues of indicated joints with corresponding value for similar joints of circular pipes, obtained by known at that moment formulae, was carried out. It was determined that «square–circle» joints at applied axial load and bending moment out of plane have SCF less than «circle–circle» joints. At bending moment the picture is opposite in the structure plane.

The authors of [14] analyzed using FEM around 2 thou variants of structures with different intersection angles and six schemes of loading (tension and bending in different directions and planes) for welded joints of X- and cruciform tubular structures. As a result, new parametric equations for determination of structural SCF were derived based on regression analysis. The results of calculation on obtained dependencies were compared by authors with the experimental results performed with steel and acrylic models. The coincidence was satisfactory, therefore, obtained formulae were recommended for calculation of tubular frames.

Work [15] in many respects is similar to work [14], but dedicated to K-tubular structures. They based on solution using FEM of 254 problems, corresponding to different variants of structures, and further regression analysis of obtained results, provided the dependencies for determination of structural SCF. Verification of obtained results was also carried out on steel and acrylic models.

A procedure for prediction of values of structural SCF and deflection angle of K-tubular structures was developed in work [16] by the same authors based on [15] and data base of other their works.

Authors of [17] for K-tubular structures based on a displacement method in the effective concentrator determined the local stresses considering weld geometry parameters. The authors of this work studied the stress concentration in the welded joints with fillet welds having corrected profile. Minimizing the SCF (here weld shape SCF) was reached by means of removal of defects in a transition zone from weld to base metal and providing the profile with necessary radius.

Data base of SCF was obtained in work [18] based on FEM for welded joint of XX-spatial tubular structures. Using it a simple and efficient procedure for prediction of SCF values at different types of loads was developed. The equations and diagrams recommended for engineering practice were obtained for SCF determination.

The approach used in works [12–15] is extended to T-, X- and Y-tubular structures for twelve schemes of load application in work [19].

Paper [20] specifies the values of structural SCF for welded joint of connecting pipe and spherical reservoir in a wide range of variation of their parameters (diameters and thicknesses of walls) and presented in form of tables and diagrams.

The authors used FEM and theory of thin shells under internal pressure. Both methods showed good reproducibility of the results even with consideration of reinforcement, present in the joint. Therefore, in authors' opinion, the results obtained in this work can be used for branch to cylinder shells welds.

The results of experimental investigations of fatigue life of DT-joints of pipes are presented in work [21]. The authors using TIG welding made two types of samples of steel S31803. The first type of the samples simulated tubular structure, i.e. welding of smaller diameter pipe to pipe of larger diameter. The second type of the samples presented itself the elements of pipelines, i.e. pipe with welded to it connecting pipes. In course of investigations the authors determined structural SCF for both types of the samples. Based on the results of in-situ measurements as well as by means of calculation using formulae recommended by IIW (IIW Doc. XV-E-98-236), it was determined that SCF of the samples of second type is 35 % lower than that in the first.

Paper [22] presents the method for determination of structural SCF of welded joints of pipelines based on FEM, where SCF is outlined as a main factor effecting life of girth welds. According to ASME Section II and B31 codes for pressure vessels and

pipelines, respectively, their life is determined by such important index as fatigue strength degradation factor (ASME Section III) and stress intensity factor (ASME B31). Both are the analogues of efficient concentration factor and related with SCF, therefore, the problem of more accurate and reliable determination of SCF is relevant. The authors of this work outline that generally accepted approach to its determination using FEM is not effective enough for welds of pipelines due to sensitivity of the results to mesh size, and proposed method provides SCF values which do not depend on it. An important result of this work is determination of functional relationship between the fatigue strength degradation factor and SCF.

Developed and presented in work [22] approach was successfully realized by its authors in work [23] by the example of T-tubular structure working in bending in plane, the proposed method was used for HSS determination. Similar to work [21], [23] studies tubular structures as well as joints of pipelines. In order to obtain the latter the model eliminated part of the pipe corresponding to intersection. The results indicate the following, namely structural SCF acquires the highest value on the larger diameter pipe. The nature of SCF distribution along the weld is different for tubular structure and pipeline joining. In a zone of maximum SCF of pipeline joining its value is 33 % lower than that in the tubular structure. The latter result coincides with the results of work [21] obtained on full-scale specimens and using analytical dependencies.

Work [24] in many aspects is similar to [22], moreover, authors note the excessive conservatism of ASME codes, which provide oversetimated values. Authors of work [24] obtained using FEM the diagrams of dependence of structural SCF on relationship of pipe diameter D and welded to it branch of diameter d with alternating wall thickness. The data were obtained for wide range $d/D = 0.05-1.0$. The values of structural SCF in loading by inner pressure are within 1.8–3.5 limits.

A new method for determination of structural SCF [22] presented in 2003 was validated till 2007. In

work [25] the authors successfully used their method in updating 2007 ASME Div 2 codes. Issue of new edition became possible also due to new, more accurate method of SCF determination.

Authors of [26] investigated the effect on structural SCF of local wall thinning in area of T-joint of pipe and branch (Figure 2).

The investigation was carried out in two stages. At the first stage the model was validated using known dependencies for structural SCF, which were obtained by such researchers as:

- Lind

$$\alpha_{\sigma} = \min\{K_1; K_2\},$$

where

$$K_1 = \frac{[1 + 1.77(d/D)\sqrt{D/T} + (d/D)^2\sqrt{s/S}][1 + (T/D)/\sqrt{s/S}]}{1 + (d/D)^2\sqrt{s/S}/(s/S)},$$

$$K_2 = \frac{[1.67\sqrt{s/S}\sqrt{D/T} + 0.565(d/D)][1 + (T/D)/\sqrt{s/S}]}{0.67\sqrt{s/S}\sqrt{D/T} + 0.565(d/D)^2/(s/S)},$$

$$S = d/(2t), \quad s = t/(2T);$$

- Money

$$\alpha_{\sigma} = 2.5 \left[(r/t)^2 (T/R) \right]^{-0.2042} \text{ for } r/R < 0.7;$$

$$\alpha_{\sigma} = 2.5 \left[(r/t)^2 (T/R) \right]^{-0.24145} \text{ for } r/R > 0.7. \quad (2)$$

- Decock

$$\alpha_{\sigma} = \frac{[2 + 2(d/D)\sqrt{(d/D)(t/T)} + 1.25(d/D)\sqrt{D/T}]}{1 + (t/T)\sqrt{(d/D)(t/T)}}; \quad (3)$$

- Gurumurthy

$$\alpha_{\sigma} = 1.75(T/t)^{0.4}(d/D)^{-0.08}(\lambda)^{0.6}, \quad (4)$$

where $\lambda = d/(DT)^{0.5}$;

- Moffat

$$\alpha_{\sigma} = [2.5 + 2.2715(d/D) + 8.125(d/D)^2 - 6.877(d/D)^3] +$$

$$+ [-0.5 - 1.193(d/D) - 5.416(d/D)^2 + 5.2(d/D)^3](t/T) +$$

$$+ [0.078(d/D) - 0.195(d/D)^2 + 0.11(d/D)^3](D/T)^{1.2} +$$

$$+ [-0.043(d/D) + 0.152(d/D)^2 - 0.097(d/D)^3](t/T)(D/T)^{1.2}. \quad (5)$$

The models in wide range of parameters of joint were constructed and effect of wall thinning on structural SCF was evaluated after validation. As a result it was determined that it rises with decrease of wall thickness. For relatively thin-walled pipes at $d/D < 0.2$ effect of thinning of SCF becomes not as significant up to opposite picture, when reduction of thickness can promote decrease of SCF. For relatively thick-walled pipes at $d/D > 0.3$ SCF considerably rises with thickness reduction. For joints with thinning as well as without it the maximum local stresses appear on a line of intersection of inner surfaces.

Distribution of SCF along the weld and zone of maximum SCF in the tubular welded structures have

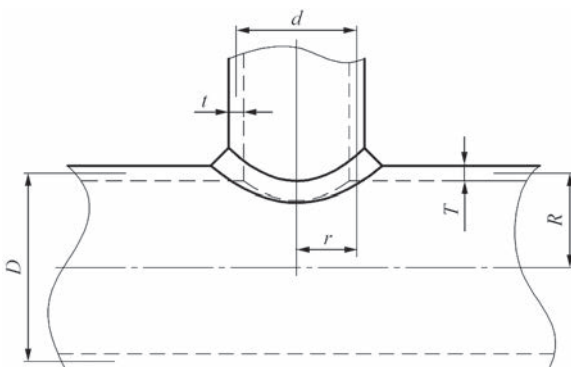


Figure 2. Parameters of T-joint of pipe and branch

significant effect on structure life. Particularly, it is important to know the nature of SCF distribution for spatial tubular structures. Authors of [27] investigated the distribution of structural SCF for DKT-structures under effect of axial loads. Using parametric modelling and FEM the effect of structure geometry on SCF distribution along the welds was evaluated. The evaluation included also comparison of SCF values of flat structures (KT) with spatial (DKT). It is stated that structural SCF of DKT structure is 1.1–1.6 times higher than SCF of KT structure. The parametric equations were derived connecting the structural SCF with dimensions of tubular structure, correlation coefficient made 0.993–0.999. Data on distribution of SCF in T-shaped element of KT-structure are similar to the results in [12].

It should be noted that generation of reliable analytical dependencies is a relevant problem by now. An illustrative example of convenience of application of SCF formulae, similar to [27], in combination with other factors, is the papers [28, 29], which investigate the effect on structure life of residual stresses and impact treatment of welds. Very often in the literature SCF definition goes in combination with other factors determining life of welded joints.

Work [30] clearly demonstrated how a value of structural SCF affects the accumulation of fatigue damage of butt welded piles made by single weld at their piling in sea ground. Structural SCF in the considered case is related with bending due to eccentricity because of difference of thicknesses of joined pipes, and is introduced together with classification factor, depending on method of welding, i.e. presenting itself the theoretical SCF of weld shape. Increase of the latter from 1.34 to 1.52, i.e. by 13 %, results in rise of accumulated fatigue damage (that was determined on Palmgren-Miner hypothesis) by 46 %. It was determined by authors of mentioned above work in calculation way using GRLWEAP software.

In contrast to work [30], which considers only axial load in piling, the authors of [31] evaluated SCF under effect on the pile of axial load as well as bending moment (separately and together). Effect on accumulated fatigue damage was not estimated, however, a great work was carried out on determination of general SCF depending on diameter and thickness of pile wall t with the next weld parameters, namely convexity height makes 5 % of wall thickness plus 2 mm, and radius of transition from weld to base metal ρ is 1 mm. Width and height of reinforcement was determined constructively, radial displacement of pipes e was taken as fixed and made 2 mm. Obtained values were graphically presented and compared with known formulae for flat parts ($K_{dis} = 1 + 3e/t$) [32] and with

specified formulae derived for pipes [33, 34]. It is determined that all results are in satisfactory agreement. Dependence of SCF on wall thickness obtained by the formulae and using FEM have similar nature. SCF has virtually no dependence on pipe diameter.

Separately it is necessary to outline the works of Inge Løtsberg. He made a great contribution in the development of methods of determination of local stresses in welded joints of pipelines and tubular structures. The peculiarity of his work is accurate analytical expressions for SCF based on classical shell theory. Thus, for example, Løtsberg formulae presented in work [35] allow determining the structural SCF depending on structure manufacturing errors. The formulae can be used for butt joints of pipes, strengthening and stiffening ribs, conical pipe crossings. His further works were directed on expansion of area of formulae application and evaluation of SCF effect on fatigue life of tubular structures [33, 36]; consideration of wider spectrum of loads, for example, under effect of internal pressure [34]; specification of empirical dependencies for SCF determination obtained by other authors [37]. The result of more than 40 years activity of the scientist became a book [38] accumulating virtually all aspects of fatigue life of tubular structures.

Expansion of field of application of the formulae for SCF determination is the typical feature for investigations of the recent years [39–43]. Works [39, 40] complement each other and are directed on investigation of the problem of SCF distribution in T-welded joints of square pipes (Figure 3).

In work [39] there were determined the zones of the largest SCF along the weld as well as its maximum values at bending moment loading in pipe plane (Figure 3, *a*). The evaluation was carried out experimentally on the pipe samples of different size (9 samples) by means of change of displacements taking into account nonlinear nature of their distribution along the hot line. It is known that the method of HSS determination allows the possibility of linear and quadratic extrapolation. The authors [39] determined that for the joints presented on Figure 3 it is necessary to use quadratic extrapolation. Particularly in this case SCF determination is more accurate, thus, it is possible to use fatigue curves, recommended by IIW. The authors note that application of formulae for SCF calculation is very convenient, therefore, derivation of such formulae they presented as the aim of their further investigations.

The same authors in work [40] have considered the similar joints under effect of axial loads where FEM was used for SCF determination. In other aspects the obtained set of data is similar to [39], the maximum SCF were obtained for the sample with the same relationship of dimensions that in [39]. It is determined that the largest SCF values are present in the joint at

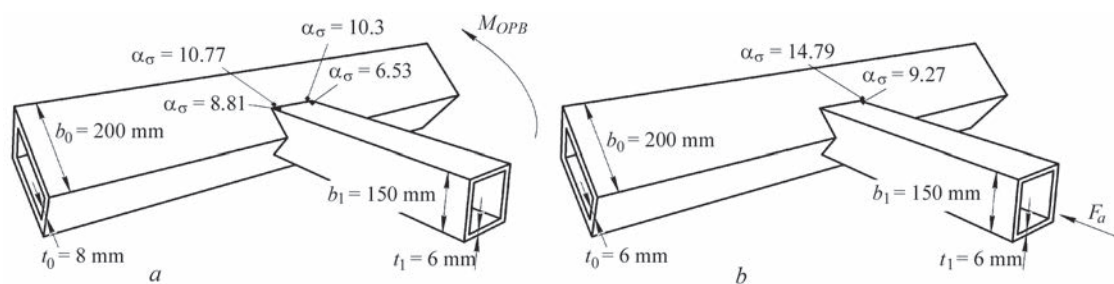


Figure 3. Maximum SCF on data of [39, 40] under effect of moment in pipe plane (a) and axial force along connecting pipe (b)

application of axial force to the smaller diameter pipe (Figure 3, b). Besides, the authors have compared the obtained results with SCF values of traditional T-joints (Figure 4) and circular pipes (Figure 2). The critical values of pipe size, at which the joints (Figure 3) have advantages over the rest, are provided.

The authors of [41] also researched T-joints of square pipes, in which smaller section pipe is turned to 45° relatively to position shown on Figure 3. FEM was used for the investigations, model was validated using full-scale measurements of displacements. In total four types of loads were considered, namely axial loads, applied to pipes of larger and smaller diameter, bending in the plane and out of it. The work proves the conclusion [39] that the quadratic extrapolation shall be used for of square pipe joints for HSS determination. Trustworthy formulae for determination of SFC at variants of loads mentioned above were derived based on determination of SCF using FEM on multiple models in the considered work.

Since formulae (1)–(5) for calculation of structural SCF of fillet T-welds of tubular structures (Figure 2) have comparatively low accuracy, the authors of [42] using FEM and based on solution of 1526 problems have derived simpler and more reliable formulae for determination of its value under effect of internal pressure.

The formulae for determination of SCF of K-tubular structures were derived in work [43] using FEM based on regression analysis of data obtained from multiple models. The structure considered by the authors was welded from larger pipe of circular and two smaller pipes of square sections. The formulae can be used for determination of SCF at each pipe under effect of axial loads.

Work [44] in methodological concept is related to work [26], but dedicated to estimation of effect of volumetric surface defects on life of tubing tees, including welded ones. At the first stage of investigation the author constructed the models of tees and using FEM determined the values of structural SCF. From all types of tees the maximum values were obtained for the tees with welded branch. They made $\alpha_\sigma = 4.5$ for tee with $D = 426$ mm, $T = 20$ mm, $d = 168$ mm, $t = 9$ mm. The zones of maximum concentration have become the place of further consideration of postulated defects. It should be noted that these zones matched with the zones marked by authors of [26]. A comparison of the results of SCF calculation on formulae (1)–(5) with the results obtained in [44] and experimental data is given in the Table. Numerical values of SCF agree with experimental data as well as calculation values. At that there is a difference in the results of calculations on formulae. Obviously, that formula (2) provides underestimated and formula (4) overestimated value for this dimension type of the tee.

Since most of the works considered above [6, 8, 11–31, 33–45] are limited by determination of only structural SCF using FEM, moreover, not all the researchers derive formulae for its determination, the experimental methods of SCF determination of weld shape is still relevant. Thus, authors of work [46] using polarization-optical method and models constructed by real dimensions of T- and Y-tubular structures, obtained the SCF value taking into account structural parameters and weld geometry. The constructed models consider weld shape instability and its effect on stressed state of tubular assemblies. HSS values de-

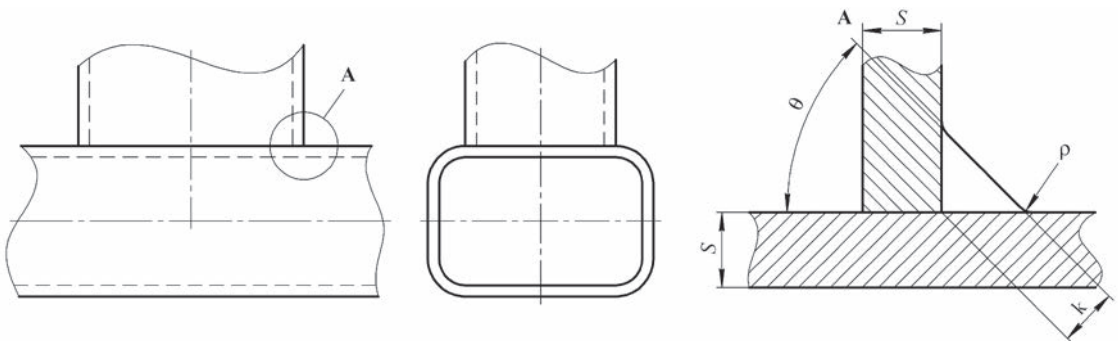


Figure 4. Scheme of T-welded joint of rectangular pipes

SCF of welded joints of tees under effect of internal pressure

Method of determination	Experimental [45]	FEM		Formula				
		[44]	[26]	(1)	(2)	(3)	(4)	(5)
Value	4.23	4.5	4.08*	4.47	3.57	4.11	6.14	4.18

*Value was obtained on data of [26] by method of interpolation of tee parameters, the closest to [44]; calculation on formulae (1)–(5) made for parameters obtained by interpolation. Experimental value corresponds to the same parameters.

terminated taking into account actual geometry of weld by estimations of authors rise 2.5–3.0 times. Conclusions made in [46] indicate the need of consideration of weld geometry, otherwise it can result in formation of cracks in a weld to base metal transition zone in tubular assemblies. In work [47] the SCF values of butt welded joints of pipes were also obtained using polarization-optical method. The range of values depending on geometry parameters of weld made 1.1–1.7.

The authors of [48] in course of modeling of non-stationary processes in butt welded joint of pipeline using FEM obtained the value of theoretical SCF, which made 1.8. Thus result agrees with the results of [46] and SCF values of butt welded joints of flat parts given in reviews [9, 10].

The polarization-optical method was also used for determination of SCF of welded joints used in repair of main pipelines without interruption of product transporting [49]. SCF values depending on type of load made 1.6–3.0 for fillet and 1.2–2.0 for lap-butt welded joints.

Conclusions

1. During the last decades a significant progress was made in the problem of determination of SCF of pipelines and tubular structures. Today the procedures based on application of FEM are most wide spread for evaluation of stressed state. The procedures based on experimental methods of acquiring of local stresses and analytical methods have considerably lower amount.

2. The limitations of FEM application for calculation of SCF of pipelines and tubular structures in each separate case are related with high labor intensity in construction of accurate 3D model and its approximation by 3D finite elements. Therefore, most of the researchers tend to use parametric modeling based on shell elements and derive regression equations allowing calculation of SCF in wide range of parameters.

3. Formulae for SCF determination using FEM presented in the literature for indicated period are of private concernment. They can be used only for specific structure in a set range of parameters. The second peculiarity of existing dependencies is the fact that they allow determining only structural SCF, i.e. do not consider presence and geometry of weld. At that, the experimental investigations show that the stresses in the local zones of transition from weld to base metal noticeably rise, and elimination in calculations of

weld presence can result in premature failure of welded tubular assembly.

4. In the modern engineering practice the local constituent of SCF, related with presence of weld, is recommended to calculate using the approximation formulae, however, such formulae for welded joints of pipes have not been yet derived today. Therefore, determination of a fatigue resistance characteristics of tubular welded structures is carried out using different methodological means, for example, a method of displacement in effective concentrator. It should be noted that application of fictional radius of weld to base metal transition does not allow determining the places with the maximum value of local SCF along girth or fillet weld in tubular structures and pipeline joints that plays an important role for reliable evaluation of their life.

1. Trufyakov, V.I., Dvoretzky, V.I., Mikheev, P.P. et al. (1990) *Strength of welded joints under alternating loads*. Kiev, Naukova Dumka [in Russian].
2. Navrotsky, D.I. (1968) *Calculation of welded structures taking into account stress concentration*. Leningrad, Mashinostroenie [in Russian].
3. Kuchuk-Yatsenko, S.I., Kirian, V.I., Kazymov, B.I., Khomenko, V.I. (2006) Methodology for control of fitness for purpose of flash butt welded joints in pipelines. *The Paton Welding J.*, **10**, 2–6.
4. Paton, B.E. (2013) Research and developments of the E.O. Paton Electric Welding Institute for nowadays power engineering. *Ibid.*, **10-11**, 14–22.
5. Korostylyov, L.I., Litvinenko, D.Yu. (2015) Evaluation of stress concentration factor in welded assemblies of thin-walled structures using calculation of macro- and microconcentration. *Nauk. Visnyk Khersonsk. Derzh. Morskoi Akademii*, **2(13)**, 184–194 [in Russian].
6. Ostsemin A.A., Dil'man V.L. (2003) Effect of stress concentration in a welded seam on the low-cycle fatigue of large-diameter pipes. *Chemical and Petroleum Engineering*, **39(5-6)**, 259–264.
7. Rybin, Yu.I., Stakanov, V.I., Kostylyov, V.I. et al. (1982) Investigation by finite element method of geometric parameters influence of T- and cruciform welded joints on stress concentration. *Avtomatich. Svarka*, **5**, 16–20 [in Russian].
8. Macdonald, K.A., Haagenzen, P.J. (1999) Fatigue design of welded aluminum rectangular hollow section joints. *Engineering Failure Analysis*, **6**, 113–130.
9. Tkacz, P.N., Moltasow, A.W. (2017) Rozwój metod oceny stanu naprężenia w elementach konstrukcji spawanych. Część 1. Metody tradycyjne. *Biuletyn Instytutu Spawalnictwa*, **4**, 52–56 [in Polish].
10. Tkacz, P.N. Moltasow, A.W. (2017) Rozwój metod oceny stanu naprężenia w elementach konstrukcji spawanych. Część 2 Metody najnowsze. *Ibid.*, **5**, 98–103 [in Polish].

11. Wood, J. (2008) A review of literature for the structural assessment of mitred bends. *Int. J. of Pressure Vessels and Piping*, **85**, 275–294.
12. N'Diaye, A., Hariri, S., Pluvinage, G., Azari, Z. (2007) Stress concentration factor analysis for notched welded tubular T-joints. *Int. J. Fatigue*, **29**, 1554–1570.
13. Ai-Kah Soh, Chee-Kiong Soh (1991) SCF equations for DT/X square-to-round tubular joints. *J. Construct. Steel Research*, **19**, 81–95.
14. Chang, E., Dover, W.D. (1996) Stress concentration factor parametric equations for tubular X and DT joints. *Int. J. Fatigue*, **18**, 6, 363–387.
15. Morgan, M.R., Lee, M.M.K. (1997) New parametric equations for stress concentration factors in tubular K-joints under balanced axial loading. *Ibid.*, **19**(4), 309–317.
16. Morgan, M.R., Lee, M.M.K. (1998) Prediction of stress concentrations and degrees of bending in axially loaded tubular K-joints. *J. Construct. Steel Res.*, **45**(1), 67–97.
17. Rodriguez, J.E., Brennan, F.P., Dover, W.D. (1998) Minimization of stress concentration factors in fatigue crack repairs. *Int. J. Fatigue*, **20**(10), 719–725.
18. Karamanos, S.A., Romeijn, A., Wardenier, J. (1999) Stress concentrations in multi-planar welded CHS XX-connections. *J. Construct. Steel Res.*, **50**, 259–282.
19. Lee, M.M.K. (1999) Estimation of stress concentrations in single-sided welds in offshore tubular joints. *Int. J. Fatigue*, **21**, 895–908.
20. Dekker, C.J., Brink, H.J. (2000) Nozzles on spheres with outward weld area under internal pressure analysed by FEM and thin shell theory. *Int. J. of Pressure Vessels and Piping*, **77**, 399–415.
21. Maddox, S.J., Manteghi, S. (2002) Fatigue tests on duplex stainless steel tubular T-joints. *Welding in the World*, **46**(3–4), 12–19.
22. Dong, P., Hong, J.K., Osage, D., Prager, M. (2003) Assessment of ASME's FSRF rules for vessel and piping welds using a new structural stress method. *Ibid.*, **47**(1–2), 31–43.
23. Dong, P., Hong, J.K. (2004) The master S–N curve approach to fatigue of piping and vessel welds. *Ibid.*, **48**(1–2), 28–36.
24. Finlay, J.P., Rothwell, G., English, R., Montgomery, R.K. (2003) Effective stress factors for reinforced butt-welded branch outlets subjected to internal pressure or external moment loads. *Intern. J. of Pressure Vessels and Piping*, **80**, 311–331.
25. Dong, P., Prager, M., Osage, D. (2007) The design master S–N curve in ASME Div 2 rewrite and its validations. *Welding in the World*, **51**(5–6), 53–63.
26. Qadir, M., Redekop, D. (2009) SCF analysis of a pressurized vessel–nozzle intersection with wall thinning damage. *Int. J. of Pressure Vessels and Piping*, **86**, 541–549.
27. Ahmadi, H., Lotfollahi-Yaghin, M.A., Aminfar, M.H. (2011) Distribution of weld toe stress concentration factors on the central brace in two-planar CHS DKT-connections of steel offshore structures. *Thin-Walled Structures*, **49**, 1225–1236.
28. Acevedo, C., Nussbaumer, A. (2012) Effect of tensile residual stresses on fatigue crack growth and S–N curves in tubular joints loaded in compression. *Intern. J. of Fatigue*, **36**, 171–180.
29. Habibi, N., H-Gangaraj, S.M., Farrahi, G.H. et al. (2012) The effect of shot peening on fatigue life of welded tubular joint in offshore structure. *Materials and Design*, **36**, 250–257.
30. Chung, J., Wallerand, R., Hélias-Brault, M. (2013) Pile fatigue assessment during driving. In: *Proc. of 5th Fatigue Design Conf., Fatigue Design 2013. Procedia Engineering*, **66**, 451–463.
31. Li, Y., Zhou, X.P., Qic, Z.M., Zhang, Y.B. (2014) Numerical study on girth weld of marine steel tubular piles. *Applied Ocean Research*, **44**, 112–118.
32. Vershinsky, S.B., Vinokurov, V.A., Kurkin, S.A. et al. (1975) *Design of welded structures in machine building*. Moscow, Mashinostroenie [in Russian].
33. Lotsberg, I. (1998) Stress concentration factors at circumferential welds in tubulars. *Marine Structures*, **11**, 207–230.
34. Lotsberg, I. (2004) Fatigue design of welded pipe penetrations in plated structures. *Ibid.*, **17**, 29–51.
35. Lotsberg, I. (2009) Stress concentrations due to misalignment at butt welds in plated structures and at girth welds in tubulars. *Intern. J. of Fatigue*, **31**, 1337–1345.
36. Lotsberg, I. (2008) Stress concentration factors at welds in pipelines and tanks subjected to internal pressure and axial force. *Marine Structures*, **21**, 138–159.
37. Lotsberg, I. (2011) On stress concentration factors for tubular Y- and T-joints in frame structures. *Ibid.*, **24**, 60–69.
38. Lotsberg, I. (2016) *Fatigue design of marine structures*. Cambridge University Press.
39. Cheng, B., Qian, Q., Zhao, X.L. (2015) Stress concentration factors and fatigue behavior of square bird-beak SHS T-joints under out-of-plane bending. *Engineering Structures*, **99**, 677–684.
40. Cheng, B., Qian, Q., Zhao, X.L. (2015) Numerical investigation on stress concentration factors of square bird-beak SHS T-joints subject to axial forces. *Thin-Walled Structures*, **94**, 435–445.
41. Tong, L., Xu, G., Liu, Y. et al. (2015) Finite element analysis and formulae for stress concentration factors of diamond bird-beak SHS T-joints. *Ibid.*, **86**, 108–120.
42. Mukhtar, F.M., Al-Gahtani, H.J. (2016) Finite element analysis and development of design charts for cylindrical vessel-nozzle junctures under internal pressure. *Arabian J. for Science and Engineering*, **41**, **10**, 4195–4206.
43. Chen, Y., Wan, J., Hu, K. et al. (2017) Stress concentration factors of circular chord and square braces K-joints under axial loading. *Ibid.*, **113**, 287–298.
44. Yukhimets, P.S. (2015) Evaluation of residual life of a damaged T-joint. *Tekh. Diagnost. i Nerazrush. Kontrol*, **3**, 26–31 [in Russian].
45. Moffat, D.G., Mistry, J., Moore, S.E. (1999) Effective stress factor correlation equations for piping branch junctions under internal pressure loading. *J. Press. Vessel Technol.*, **121**(2), 121–126.
46. Gubajdulin, R.G., Tingaev, A.K., Lupin, V.A. (2012) Investigation of stressed state of welded joints of non-faceted tubular assemblies. *Vestnik YuUrGU, Seriya Metallurgiya*, **18**(15), 31–36 [in Russian].
47. Makovetskaya-Abramova, O.V., Khlopova, A.V., Makovetsky, V.A. (2014) Examination of stress concentration in welding of pipelines. *Tekhn.-Tekhnol. Problemy Servisa*, **2**(28), 25–27 [in Russian].
48. Fedoseeva, E.M., Olshanskaya, T.V., Ignatov, M.N. (2011) Modeling of nonstationary processes in welded joint of pipelines. *Neftegazovoe Delo: Elektronny Nauchny Zhurnal*, **5**, 376–382 [in Russian].
49. But, V.S., Olejnik, O.I. (2014) Development of technologies of repair by arc welding of operating main pipelines in Ukraine. *The Paton Welding J.*, **5**, 40–47.

Received 29.10.2018

NEW EQUIPMENT FOR PREPARATION OF POSITION BUTTS
OF NPP PIPELINES FOR WELDING*

L.M. LOBANOV¹, N.M. MAKHLIN², V.E. VODOLAZSKY², V.E. POPOV² and L.P. MUTSENKO²

¹E.O. Paton Electric Welding Institute of the NAS of Ukraine

11 Kazimir Malevich Str., 03150, Kyiv, Ukraine. E-mail: office@paton.kiev.ua

²SE «Scientific and Engineering Center of Welding and Control in the Field of Nuclear Energy of Ukraine
of the E.O. Paton Electric Welding Institute of the NAS of Ukraine»

11 Kazimir Malevich Str., 03150, Kyiv, Ukraine. E-mail: electro@paton.kiev.ua

Investigations and practical experience showed that the quality of welded joints of pipelines, meeting the modern requirements largely depends on the quality of treatment of the end faces of groove edges of their butts prior to welding and on the quality of assembly of pipeline parts directly before welding. The paper presents the results of experimental, technological and design works carried out at the Engineering Center for Welding and Control in the Field of Nuclear Energy, on development of a facing tool for metal pipes of 76 to 108 mm diameter. It is shown that, in comparison with the best foreign analogs, the designed facing tool has a number of significant technological and operational advantages. 7 Ref., 2 Tables, 1 Figure.

Keywords: nuclear power engineering, position butt joints of pipelines, machining, pneumatic drive, facing tools, carriages, cutters

During performance of investigations and experimental and technological works the effect of the accuracy of edge preparation of parts of metal pipelines with nominal outer diameter of 76, 89 and 108 mm, the geometrical elements of which meet the requirements of PN AE G-7-009–89 and OST 24.125.02–89 was studied, and the range of optimum modes for treatment of these edges by cutting were established.

Investigations were performed on samples of parts of pipelines from steel 08Kh18N10T and steel 20 of nominal diameters of 76; 89 and 108 mm, and nominal wall thickness of 7.0; 8.0 and 12.0 mm, respectively. The edges of pipeline part samples used for investigations and experimental-technological works were

treated using screw-cutting lathe 1M61 and milling machine 6R82Sh.

Treatment of groove edges of butts of the tested samples of pipeline parts for simulation of deviations of the linear and angular dimensions, specified by PN AE G-7-009–89 and OST 24.125.02–89 for welded joints of C-42 type, was performed in keeping with Table 1. Here, the asymmetry of beveling angles of groove edges of pipeline part samples for simulation of deviations from the normative values was equal to 4 and 8° for pipes with nominal dimensions of 76×7.0; 89×8.0 and 108×12.0 mm.

During treatment of the tested samples of parts of pipelines from steel 08Kh18N10T and steel 20, their

Table 1. Linear dimensions of edge preparation of samples of pipeline parts for simulation of deviations from specified values

Nominal dimensions of pipe ($D \times S$), mm	Edge preparation						
	Bore diameter d_b , mm		Wall thickness in boring location, not less than	Blunting ($S-M$) at $S_1 = S_2$, mm			
	Nominal value	Largest allowable deviation		S_1-M_1	S_2-M_2		
					$M_2 = M_1$	$M_2 = M_1 + 1$	$M_2 = M_1 + 1.5$
76×7.0	63	+0.23	5.6	2.3 ^{+0.4}	3.3 ^{+0.4}	3.8 ^{+0.4}	4.2 ^{+0.4}
89×8.0	74		6.5	2.7 ^{+0.3}	2.7 ^{+0.3}	3.7 ^{+0.3}	4.2 ^{+0.3}
108×12.0	88		8.8	3.0 ^{-0.3}	3.0 ^{-0.3}	4.0 ^{-0.3}	4.5 ^{-0.3}

Note. Explanation of designations of dimensions S_1 , S_2 , M_1 and M_2 is given in [1].

*The following engineers participated in the work: D.S. Oliyanenko (SE «SEC WCNE of PWI of NASU»): S.I. Lavrov, A.A. Kirilenko, V.G. Prityka, and A.V. Kovalyuk (SE «Atomenergomash of SC «NNEGC «Energoatom»).

linear and angular dimensions were controlled with application of standard measuring devices, in particular, calipers ShTs-P-160 and ShTs-P-250 to GOST 166 (greatest measurement error of ± 0.07 and ± 0.08 mm, respectively), indicator wall meters S-10A and S-25 to GOST 11358 (greatest measurement error of ± 0.02 and ± 0.10 mm, respectively), goniometer with nonius UT mod. 127, with measurement range from 0 to 18° and greatest measurement error of $\pm 2'$ [2].

The main part of the treated in keeping with Table 1 test samples of parts of pipelines from steel 08Kh18N10T and steel 20 were joined by multipass automatic orbital nonconsumable electrode argon-arc welding (GTAW) with filler wire feed and nonconsumable electrode oscillations. Here, a prototype of orbital automatic welding machine ADTs 628 UKhL4 developed at SEC WCNE was used [3], and a certain part of these test samples were joined by multipass manual arc welding (GTAW) with filler wire feeding and nonconsumable electrode argon-arc welding (TIG) with filler wire feeding. TIG welding was performed with application of earlier developed by SEC WCNE prototypes of power source ITs 617 U3.1 for TIG and GTAW welding, power supply module MPS-101 and electronic regulator of welding current RDG-201 U3.1 [4], as well as ABITIG GRIPP 26 torch (ABICOR BINZEL Company) with tungsten electrode of WT20 grade of 3.15 mm diameter. At test welding of butt joints of parts of pipelines from steel 08Kh18N10T, wire Sv-04Kh19N11M3 was used as filler, and for those from steel 20 wire Sv-08G2S was applied, the diameter of these wires being 1.6 mm.

The quality of welded joints of the tested samples of parts of pipelines of nominal diameter from 76 to 108 mm, was controlled by visual, radiographic and penetrant techniques [5].

As a result of performance of several series of test welds it was established that:

- asymmetry of bevel angles of edges on parts of metal pipelines of 76 to 108 mm diameter during performance of welded joints of C-42 type should not be higher than 4° , as at larger values of bevel asymmetry characteristic are such continuity defects as inadmissible violation of weld formation, lacks-of-penetration of the edges and individual beads, lacks-of-penetration of filling passes, «sagging» of part of the weld near the edge with a greater bevel, undercuts in the facing weld;
- deviations of internal diameter boring from the normative values during performance of welded joints of C-42 type should not exceed $+0.23$ mm for

pipes with nominal outer diameter from 76 to 108 mm inclusive, and the difference between blunting of both the edges should not exceed 0.5 mm, as the welded joints of pipeline parts, where blunting of one of the edges differs from blunting of the other one by more than 0.5 mm, are prone to such weld root defects as violation of its specified shape, lacks-of-penetration, weld «sagging» from one of its sides, and «shrinkage cavities» or lacks-of-fusion from the other. Here, it should be noted that in the case of application of the modes of modulated current welding when joining parts of metal pipelines of 76 to 108 mm diameter, even at up to 0.75 mm difference between edges blunting, weld root defects are very rare, and in most of the cases they were not detected at all, and at up to 0.60 mm difference between edges blunting these defects are practically completely absent;

- based on the recommendations, arising from many years of research on machining parts from steels of austenitic class and available production experience of such treatment [6], in the case of thin external longitudinal turning and cross-cutting of parts from steels of austenitic class (for instance, 08Kh18N10T) the region of optimum values of cutting speed is limited by the range from 10 to 40 m/min, values of correction factors K_m and K_{nv} (first of which takes into account the influence of physico-mechanical properties of the billet from corrosion-resistant steel on cutting speed, and the second — the influence of the state of this billet surface on cutting speed) are equal to 0.8 and 0.9, respectively, and the feed values for finish turning of parts from heat-resistant and stainless steels — from 0.04 to 0.12 mm/rev., respectively.

When facing tool TRTs 108 U3.1 was developed, results of analyzing the information on the parameters, characteristics and design of the available in the market best foreign samples of equipment for treating the end faces and edges of pipeline parts to be welded and main disadvantages inherent in these analogs were taken into consideration [1]. The desire to standardize the main components of domestic equipment for machining the end faces and edges of pipeline parts before welding was also taken into account.

We used the kinematic scheme, similar to that of facing tool TRTs 76 U3.1 [1], and also performed calculations of transmissions and faceplate mechanisms of this facing tool, calculation of strength and fatigue life of elements of such transmissions and mechanisms and calculations of cutting forces. This enabled selection of the required materials of the main parts of facing tool TRTs 108 U3.1 and allowed taking

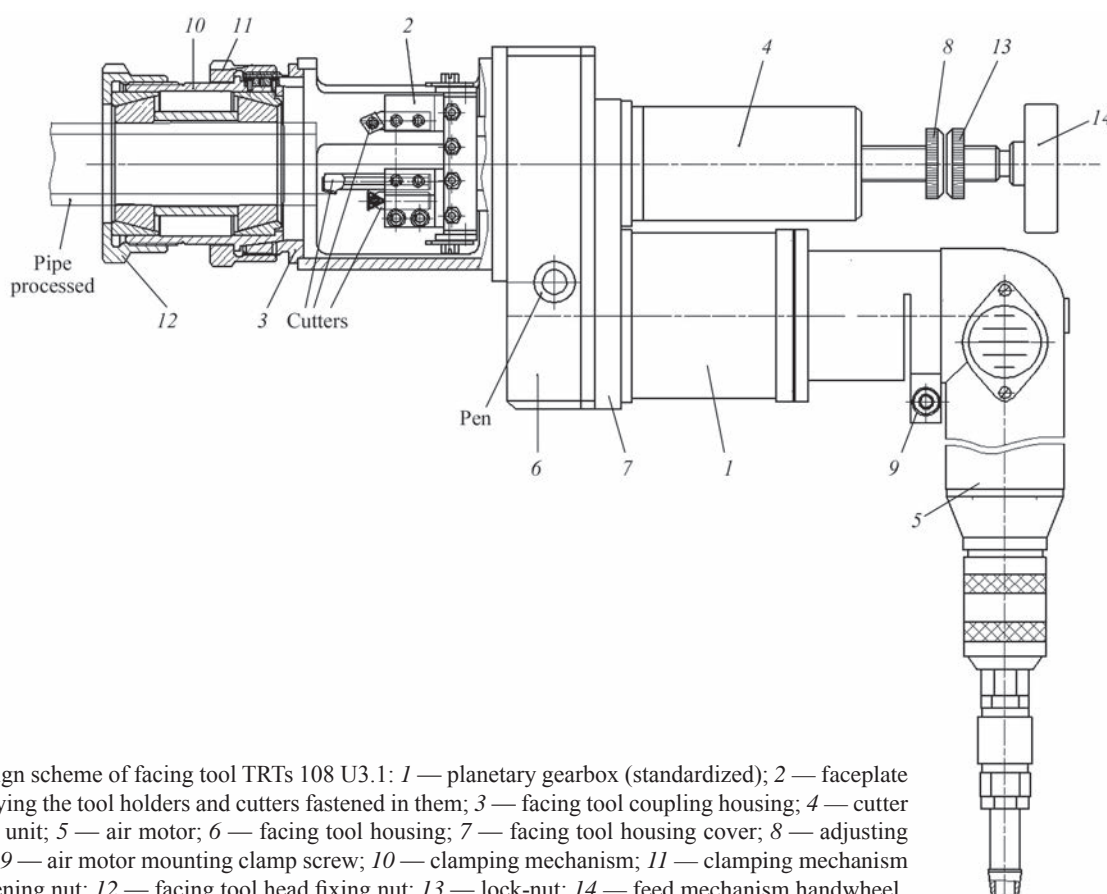
Table 2. Main parameters and characteristics of test samples of facing tools TRTs 76 U3.1 and TRTs 108 U3.1 and some of their foreign analogs

Name of parameter or characteristic	Model			
	TRTs 76 U3.1	TRTs 108 U3.1	Mangust-2T (Russia)	PROTEM PUS40 (France)
Smallest outer diameter of treated pipe, mm	38	76	45	43
Largest outer diameter of treated pipe, mm	76	108	120	219
Maximum wall thickness of treated pipe, mm	7.0	12.0	5.0	16.0
Depth of bore of internal diameter of treated pipe, mm, not more than	15	20	Boring option is not available	
Basing	On outer surface of treated pipe		Internal basing	
Maximum possible number of cutters in tool holders, pcs	4		1	1
Method of feeding the cutters	Manually			
Cutter feeding, mm/rev., not more than	0.15		0.20	
Frequency of faceplate revolution nominal, rpms	100	70	70	25
Compressed air consumption during idle running, m ³ /min, not more than	1.5		1.7	1.6
Weight with drive, kg; not more than	12.6	13.4	9.5	16.0

design solutions for its main components, similar to those which were taken during design of facing tool TRTs 76 U3.1 [1, 7], in particular as regards one-time external basing, faceplate design, self-centering coaxially with longitudinal axes of the treated pipe and basing mechanism. To provide feeding of air-oil mix-

ture to facing tool TRTs 108 U3.1, a unified block of air preparation, applied in facing tools TRTs 38 U3.1, TRTs 76 U3.1 and split pipe cutter TRTs 660 U3.1, was used.

Table 2 gives the main parameters and characteristics of test samples of facing tools TRTs 76 U3.1



Design scheme of facing tool TRTs 108 U3.1: 1 — planetary gearbox (standardized); 2 — faceplate carrying the tool holders and cutters fastened in them; 3 — facing tool coupling housing; 4 — cutter feed unit; 5 — air motor; 6 — facing tool housing; 7 — facing tool housing cover; 8 — adjusting nut; 9 — air motor mounting clamp screw; 10 — clamping mechanism; 11 — clamping mechanism fastening nut; 12 — facing tool head fixing nut; 13 — lock-nut; 14 — feed mechanism handwheel

and TRTs 108 U3.1, as well as some of their foreign analogs from among the best foreign samples.

Design scheme of facing tool TRTs 108 U3.1 constructed using the engineering solution given in [7], is shown in the Figure.

Conclusions

1. New import-substituting facing tool TRTs 108 U3.1 for preparation in welding of position butts of pipelines of 76 to 108 mm diameter of NPP power units and facilities of other sectors of Ukrainian economy was developed.

2. The following was achieved as a result of development of facing tool TRTs 108 U3.1:

- expansion of technological capabilities of domestic equipment for preparation for welding of parts of position butts of metal pipelines and increase of the efficiency of the processes of machining the end faces and edges;
- improvement of the quality and accuracy of preparation of these end faces and edges for manual or automatic welding;

• simplifying and lowering the cost of maintenance of facing tools, lowering the cost to manufacture such items by not less than 1.5 to 2.0 times.

1. Lobanov, L.M., Makhlin, N.M., Smolyakov, V.K. et al. (2015) Equipment for preparation of pipe ends to welding of position butt joints of pipeline. *The Paton Welding J.*, **9**, 36–44.
2. Troitsky, V.A. (2012) *Visual and measuring testing of metal structures and constructions*. Kiev, Fenix [in Russian].
3. Makhlin, N.M., Korotynsky, O.E., Svyrydenko, A.O. (2013) Hardware-software complexes for automatic welding of position butt joints of nuclear power plant pipelines. *Nauka ta Innovatsii*, **9(6)**, 31–45 [in Ukrainian].
4. Makhlin, N.M., Korotynsky, A.E., Bogdanovsky, V.A. et al. (2011) Single- and multioperator systems for automatic welding of position butt joints of nuclear power plant piping. *The Paton Welding J.*, **11**, 28–36.
5. Troitsky, V.A. (2006) *Concise manual on testing of welded joint quality*. Kiev, Fenix [in Russian].
6. (2001) *Handbook of technologist-mechanical engineer*. Vol. 2. Ed. by A.M. Dalsky et al. Moscow, Mashinostroenie [in Russian].
7. Lobanov, L.M., Smolyakov, V.K., Vodolazsky, V.E., Makhlin, N.M. (2015) *Portable device for treatment of ends and edges of pipes in their preparation for welding*. Pat. 102582, Ukraine [in Ukrainian].

Received 21.01.2019

E.O. PATON ELECTRIC WELDING INSTITUTE OF THE NAS OF UKRAINE
INTERNATIONAL ASSOCIATION «WELDING»
ASSOCIATION «ELECTRODE»
SOCIETY OF WELDERS' OF UKRAINE

International conference

«Consumables for welding, surfacing, coating deposition and 3D-technologies»

4–5 June, 2019 ♦ Kyiv ♦ E.O. Paton Electric Welding Institute

Topics of the Conference:

- ☒ relevant problems of metallurgy and technology of arc processes in welding and surfacing;
- ☒ consumables for mechanized and robotized processes for permanent joints production;
- ☒ consumables for manual arc welding;
- ☒ consumables for 3D-technologies;
- ☒ technology, equipment and analytical control during production of welding consumables.

The working languages of the Conference: **Ukrainian, Russian and English.**

For participation in the Conference, please, fill the registration form and send it to the Organizing Committee. The Proceedings of Conference plenary papers will be published in special issue of «Avtomaticheskaya Svarka» Journal and «The Paton Welding Journal» No.6, 2019.

Mailing of the second call for papers with conference program – before 20.04.2019.

Organizing committee:

International Association «Welding»

- 📍 11, Kazimira Malevicha (Bozhenko) st., Kyiv, 03150, Ukraine
- ☎ tel.: (38044) 200-82-77, 200-63-02
- @ e-mail: journal@paton.kiev.ua
- 🌐 http://pwi-scientists.com/eng/welding-consumables_2019

*Calendar of March**

MARCH 1, 1936



Birthday of V.R. Ryabov (1936–2002) — representative of the Paton school, famous scientist and experimenter in the field of welding dissimilar materials. Principles and procedural approaches to studying the problem of weldability of metal composites were presented, and processes, promoting formation of high-strength joints, were investigated in his works. Results of studying the weldability of dissimilar and multilayer metals and aluminium composites became a significant contribution to development of their welding technologies, promoted wide introduction of the above-mentioned materials in structures of aviation and aerospace industry. He is author of more than 310 scientific works, including 20 monographs.



MARCH 2, 1927 Construction of Tuapse section of Grozny–Tuapse oil pipeline began. This was the first large Russian trunk oil pipeline from medium-diameter pipes. Construction was conducted from 1927 till 1928. Electric arc welding was applied for the first time in the world for joining pipes in the oil pipeline. This welding method turned out to be highly successful and found wide application further on.

MARCH 3, 1953 One of Castolin Electric Company patents was issued. This Company made a substantial contribution into development of welding technologies. The enterprise was established by Jean-Pierre Wasserman in 1906 in Lausanne, Switzerland. He discovered the method of brazing cast iron by braze alloys. In the following years, machines for spraying, coating, and welding and proprietary consumable materials have been developed. The company is present with its own subsidiaries in over 100 countries on all five continents and has a high international image.



MARCH 4, 1918



Birthday of N.G. Ostapenko (1918–1965) — representative of the Paton school. He was the first to apply carbon dioxide gas as shielding medium for carbon-electrode arc welding. N.G. Ostapenko also made a significant contribution into substantiation of wider application of flash-butt welding in the main oil pipelines due to use of special transformers and solving the problem of butt welding of casing pipes at their lowering into the well.

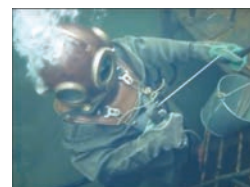


MARCH 5, 1870 Birthday of E.O. Paton (1870–1953) — outstanding scientist in the field of bridge building and electric welding, founder of the world-renowned Paton scientific-engineering school, Hero of Socialist Labour, winner of Stalin Award, founder of the Electric Welding Institute, which bears his name since 1953. His activity in bridge construction, structural mechanics, electric welding and electro-metallurgy will forever remain in the history of world science and technology.

MARCH 6, 1906 Birthday of David Roland Smith (1906–1965) — US artist, famous for his large abstract geometric sculptures from steel, representative of abstract impressionism, who created his works from metal. He gained his first experience of manufacturing metal products when he was still a student in 1925, working as a welder at Studebaker factory. Impressed by metal artwork of Pablo Picasso (1881–1973) and Julio Gonzalez (1876–1942), David Smith created his first sculpture using welding in 1933.



MARCH 7, 1942 K.K. Khrenov (1894–1984) was head of the laboratory of underwater welding and cutting at the Moscow Electromechanical Institute of Railway Engineers. The technology of underwater welding and cutting was studied and developed in detail, and appropriate personnel were trained over a short period. By the end of 1943 hundreds of underwater welders and cutters were performing work under the water. Underwater welding enabled conducting repair of underwater part of ships without placing them into the docks, sometimes directly in the open sea.



MARCH 8, 1924



Birthday of Antony Caro (1924–2013) — famous British sculptor. Beginning from 1960s, Caro's individual manner is characterized by abstract compositions, created using welding. In addition to steel beams and pipes, he uses in his work the forms resembling «found objects».

*The material was prepared by the Steel Work Company (Krivoy Rog, Ukraine) with the participation of the editorial board of the Journal. The Calendar is published every month, starting from the issue of «The Paton Welding Journal» No.1, 2019.

MARCH 9, 1943 Testing of US Army tank of M6 modification began. The initial concept of the new heavy tank was defined already on May 22, 1940. In December 1941, the first sample of heavy 60 ton tank was manufactured in a locomotive plant in Baldwin. The tank hull was welded manually. In 1944 they switched to automatic submerged-arc welding. Welding of armored hulls of combat vehicles was performed both at alternating and at direct currents. Butt joints were assembled with edge preparation and 2 mm root face, then welded manually in several passes. Just 40 T1/M6 tanks of various modifications were manufactured all together, which were never used in combat.



MARCH 10, 1986 G.Z. Voloshkevich (1911–1986), a representative of the Paton school, died. He created the theoretical foundations of a number of new welding processes, directly participated in organizing a wide introduction of electroslag welding processes in production in heavy machine-building plants. In 1957 B.E. Paton and G.Z. Voloshkevich, together with the staff of Novokramatorsk Machine-Building Plant and Krasny Kotelnshchik Plant (Taganrog) were awarded the Lenin Prize for development of the process of electroslag welding and production of large-sized critical items on its base. In 1958 this work received a Grand Prix at the Brussel's World Fair. A number of companies in industrialized countries bought licenses for application of this high-performance welding process.



MARCH 11, 1818 Birthday of Henry Saint-Claire Deville (1818–1851) — French chemist. In 1850 he developed a torch, in which hydrogen and oxygen were mixed in a special chamber, even before going out (a similar scheme is also used in modern welding torches). Introduction of a mixing chamber enabled regulation of the gas flame composition and temperature, by changing the ratio of combustible gas and oxidizer.



MARCH 12, 1683 Birthday of John Theophilus Desaguliers (1683–1744), British naturalist. He demonstrated the first outstanding example of cold pressure welding (without heating) at the Royal Society. Two lead spheres (the first of which weighed 1 pound, and the 2nd – two pounds), from which spherical segments were cut off, were pressed together by hand with simultaneous twisting. It turned out that as a result they were bonded. The spheres bonded to each other with such strength, that the supported by hand upper one pound sphere separated from the lower one only at more than 16 pound load. Examination of the contacting surfaces revealed that their bonding area did not exceed that of a circle of 1/10 inch diameter, although this surface could not be measured accurately, because of its irregular shape.



MARCH 13, 1903 Bouchayer, French scientist developed the design of «duplex-electrodes» (French Patent No.330200 of 13.03.1903) to make two spot welds at once. The upper and lower electrode assemblies had their own transformers. At parallel connection of the transformer windings just one spot can be made, and at serial connection — two spots at once. This invention essentially improved the productivity of spot welding process.



MARCH 14, 1692 Birthday of Pieter van Musschenbroek (1692–1761), Dutch physicist. Musschenbroek's most well-known achievements include development of the Leyden jar — the first capacitor, invented by Musschenbroek and his student, Cunaeus in 1746 in Leyden. Irrespective of Musschenbroek and a little earlier, the capacitor principle was discovered by Ewald von Kleist, Pomeranian Catholic Dean, on October 11, 1745. The capacitor is widely used in modern welding engineering, for instance in capacitor-type welding.



MARCH 15, 1906 Rolls-Royce Company was registered. At that time businessmen treated welding with distrust. However, if welded joints could not be avoided, it was allowed to make them by gas welding under the mandatory condition that the weld was located in non-critical part areas. They tried not to apply welding for heavy-duty parts. Still, with the advance of technology, entrepreneurs began applying welding more and more often. And now the full range of welding technologies is used in manufacture of new Rolls-Royce models.



MARCH 16, 1942 First trial launch of Fau-2 rocket. Fau-2 was exactly the first ever artificial object, making a suborbital space flight. Later on, it gave an impetus to creation and development of rocket science. Specimens of Fau-2 rocket were manufactured by the Germans at the end of the war, under the conditions of deficit of strategic raw materials. Therefore, a large number of inexpensive substitutes were used in production. For the same reason the rockets were mostly made of steel. Such an important component as the tail part of the rocket was made from a steel sheet by spot welding. The machine for spot welding of rocket body sections, in which welding was performed in several points simultaneously, was interesting from the engineering viewpoint.



MARCH 17, 1890 N.G. Slavyanov (1854–1897) — Russian engineer, inventor of electric arc welding, filed a petition for issuance of privileges of Russia for the invented by him «method of electric casting of metals». The first generator ensuring «direct» power supply for this welding process was made by N.G. Slavyanov in 1888. The machine for welding using this generator, worked at the Perm factories up to 1895. It was used to perform more than 1500 practical welding operations.



MARCH 18, 1917 Birthday of V.E. Paton — Honoured Inventor of the Ukrainian SSR, talented engineer, brilliant designer. In 1948, he developed an all-purpose automatic welding machine-tractor TS-17, which had no analogs in domestic and foreign technology. He made a significant contribution to development of specialized machines for welding and spraying in space, for conducting astrophysical experiments. V.E. Paton is the winner of three state awards, and author of 90 inventions.



MARCH 19, 1894 P.N. Yablochkov (1847–1894) died. He was Russian electrical engineer, military engineer, inventor and entrepreneur. He is famous for development of the arc lamp (which went down in history under the name of «Jablochkov candle») and other inventions in the field of electrical engineering. In 1875 during one of the numerous experiments, P. Jablochkov came up with an idea of a more perfect design of the arc lamp (without the interelectrode space regulator) — future «Yablochkov candle». He often cooperated with N.N. Benardos, founder of carbon electrode arc welding, giving him the opportunity to do work in the enterprises and develop electric welding.



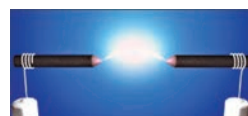
MARCH 20, 1831 Chevalier Paul ship was commissioned: the first French vessel of 2750 t displacement with an all-welded hull. By the advice of Alfred Kruppe (1907–1967), electrodes with a chromium-molybdenum steel core and coating developed by A. Stromenger, English chemist, began to be applied for welding armour plates in the ship construction. Arc welding was widely used in France also at construction of cruisers of Duplex class and battleships of Dunkerk class.



MARCH 21, 1800 In 1800 Alesandro Volta, Italian scientist (1745–1827), informed the Royal Society in London about development of an energy source, better known as «Voltaic pile». Alesandro Volta lowered two plates (zinc and copper) into a jar with acid and connected them by wire. After that, the zinc plate began to dissolve, and gas bubbles began to appear on the copper plate. Volta suggested and proved that electric current flows through the wire. This is how the Voltaic cell — the first galvanic cell was invented. But at the dawn of electrical engineering this is exactly the device which became the first source for the electric arc.



MARCH 22, 1892 August de Meritens, French electrical engineer, was born in 1834. He published French Patent No.123766 (improved magneto-electric generator). Experiments with magneto-generators became his most famous work. A. Meritens also produced the first torch for carbon electrode arc welding and patented in 1881. It was successfully used for welding in manufacture of acid cells. August de Meritens also invented a special device for welding operations — enclosed hoods and hazardous fume extraction pipe. These were the first means of welder's protection.



MARCH 23, 1942 Birthday of Abbott Lawrence Pattison (1916–1999) — US abstract painter. His sculpture «Kneeling Women» won the Medal of the Arts in 1942. The master used autogenous welding in his work. He was one of the most famous artists working in this field.



MARCH 24, 1988 M.G. Belfor (1920–1988), a representative of Paton school, died. He made a significant contribution to establishing the fundamentals for design of welding equipment. His developments of automatic machines for electroslog and arc welding, which were classical examples of modern welding equipment, received international recognition. Alongside introduction of design developments of mechanization and automation means, he promoted advanced welding methods and equipment, gave a lot of his energy to education of young designers and researchers. He is author of 8 monographs and 62 foreign patents.



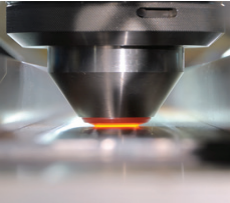
MARCH 25, 1958 RL-201 (Avro CF-105 Arrow) made its first flight. It was a delta-winged interceptor aircraft, developed by Avro Aircraft Limited (Canada) in 1953–1959. The aircraft design was in many ways advanced for its time. Inert-gas tungsten electrode welding in equipment supplied by Lincoln Electric Company was used for joining the aircraft components. The aircraft inner structure was a spatial frame from butt-welded tubes. The weapon bays were also made from stainless steel tubes, welded frames and beams.



MARCH 26, 1953 One of Sarazin's patents for welding electrode is issued. R. Sarazin and O. Moneiron, French inventors, developed a method of applying a thick layer of coating on metal rods, which included compounds of alkali and alkali-earth metals (fluorspar, marble, chalk and soda). They have low ionization potential. Therefore, the arc was more readily excited and maintained at application of such electrodes. It is known that N.N. Benardos also applied carbon electrodes with a «wick», i.e. electrodes, the core of which was filled by sodium and potassium salts.



MARCH 27, 1968 The British Welding Institute (TWI) was formed through merging of a number of organizations. TWI works across all the industry sectors and in all aspects of production. The institution also offers training and examination services on NDT, welding and inspection all over the world. Employing over 900 staff, TWI cooperates with welding organizations from 80 countries of the world. The history of the organization starts in 1923. Later on, in 1946, the British Welding Research Association (BWRA) was established. One of the outstanding achievements of the Institute was invention of friction stir welding.



MARCH 28, 1945 Polish Institute of Welding was established in Gliwice. It is the largest and most important research center in Poland, which performs work on investigation, development and introduction of welding technologies. The number of staff is 170 people. An important direction of the Institute activity is education and training of specialists in the field of welding and nondestructive testing. The Institute publishes its own welding scientific and technical journal «Biuletyn Instytutu Spawalnictwa».



MARCH 29, 1853 Birthday of Elihu Thompson (1893–1937) — one of the founders of electricity industry in the USA, outstanding engineer, inventor and pioneer, whose discoveries in the field of alternating current led to invention of alternating current motor by him. This is exactly the scientist, who is believed to be the «father of resistance welding», who managed to introduce it into industry. Elihu Thompson had his own vision of the future of electricity. In the course of his career, which lasted five decades, he received 696 US patents for inventions of arc lamps and generators, which were the base for development of welding equipment.



MARCH 30, 1929 Irving Langmuir (1881–1957) called the ionized gas in gas-discharge lamp «plasma». The matter, which became the fourth state of substance, was discovered exactly when studying the electric discharge in a tube with rarefied air. He was awarded the Nobel Prize in Chemistry (1932) for studies in the field of surface chemistry. In 1962 the industrial technology of plasma cutting was realized by K.K. Khrenov and E.M. Esibyan, PWI scientists. Today this technology surpasses all the other cutting methods in popularity.



MARCH 31, 1948 Academician E.O. Paton initiated establishment of «Avtomaticeskaya Svarka», scientific-technical and production journal (called «Trudy po Avtomaticheskoy Svarke pod Flusom» collection during the first two years). By the breadth and depth of coverage of published materials the journal filings over the 70 years of its existence are often called the welding encyclopedia. It helped in the formation of already several generations of welders.

